Modelling Primary Production

by Žarko Kovač & Shubha Satyhendranath

CONTENTS

FOREWORD

The published text is a second, out of three planned parts, which together will comprise a textbook on marine primary production. This textbook is intended to be used as educational material for students and early careers researchers in the oceanographic community. The aimed audience are students of physics that wish to learn a bit of ocean biology, as well as students of biology that wish to learn a bit of mathematical modelling, based on the approaches used in physics. It is implied that the interested reader possess basic knowledge of calculus and ocean optics, as well as rudimentary understanding of photosynthesis. The textbook is an integral part of dissemination and outreach activities within the project Fragility of Marine Photosynthesis Under Climate Change, funded by the Croatian Science Foundation. In this project we try to collect as much data as we can on marine primary production and develop new mathematical models to explain what we see in the data. If you notice any errors in the text please write to the author. Also, if you find this textbook useful, write as well!

Žarko Kovač
Department of Physics, Faculty of Science
University of Split, Croatia
zkovac@pmfst.hr

Part I

THEORY

1

PHOTOSYNTHESIS IRRADIANCE FUNCTIONS

1.1 BASIC QUANTITIES

Consider a plane parallel ocean with light impinging directly overhead. Take into account the fate of photons in this ocean: some get scattered, some absorbed. Portion of the photons that get absorbed by phytoplankton pigments are used to drive photosynthesis. It is the fate of these photons we are interested in. To be more precise, our goal is to formulate a mathematical relation between the photons that find themselves below the sea surface at any time, the so called available light, and the rate of photosynthesis in the water column. Complementary to the available light, the rate of photosynthesis will undoubtedly be set by the sheer number of phytoplankton present in the water column.

Before we can even begin to quantify the rate of photosynthesis we need a measure of available light. For this we take **irradiance** I ($\mathrm{W\,m^{-2}}$), defined as light energy that in unit time passes through a unit surface [30], for now omitting the wavelength dependence. In our case this corresponds to the total energy per unit surface carried by the photons that pass a horizontal plane in our simple plane parallel ocean. Since the ocean water scatters and absorbs photons, light gets attenuated with depth and becomes a function of depth. Therefore, at any given depth z (m) we can state the following:

$$I = I(z). \tag{1.1}$$

In order to actually calculate $I(z)$ we need a light penetration model. For now, we assume $I(z)$ as given.

Knowing the underwater light filed, albeit in a rather simple form, makes our second step possible: relating light and the rate of photosynthesis. Prior to that we need to be more precise as to what is meant by the rate of photosynthesis. We define **primary production** P ($\mathrm{mg\,C\,m^{-3}\,h^{-1}}$) as the rate of inorganic carbon assimilation by phytoplankton in photosynthesis [41].

Having defined irradiance and primary production we are now in a position to formulate a relation between the two. We state this in the following form:

$$P = P(I). \tag{1.2}$$

Considering that irradiance is a function of depth (1.1), production is also a function of depth:

$$P(z) = P(I(z)). \tag{1.3}$$

This relation implicitly holds information about the physiology and the number of phytoplankton in the water column at any time. In order to model primary production we would like to have the physiological status and the concentration of phytoplankton decoupled and stated explicitly. In other words, the relation we have just stated is diagnostic, whereas we would like to have a prognostic relation.

With this goal we take Chlorophyll *a* concentration as a measure of phytoplankton **biomass** B ($\mathrm{mg\,Chl\,m^{-3}}$). This further enables us to eliminate the effect of biomass variability from (1.2) by defining **normalized production** P^B ($\mathrm{mg\,C\,(mg\,Chl)^{-1}\,h^{-1}}$) as:

$$P^B = \frac{P}{B}. \tag{1.4}$$

We now acknowledge that normalized production is a function of irradiance, dictated by the physiological status of the phytoplankton and write:

$$P^B = p^B(I). \tag{1.5}$$

The simplest of such photosynthesis light relations would be a linear one:

$$p^B(I) = \alpha^B I, \tag{1.6}$$

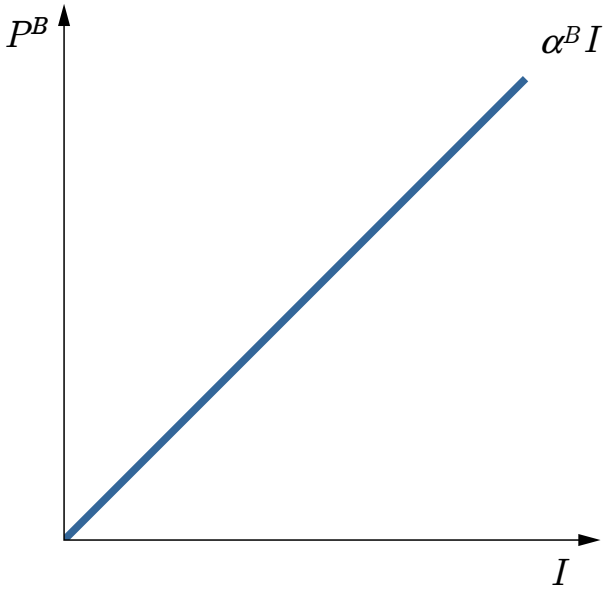

Figure 1: A linear photosynthesis irradiance function relating normalized production P^B to irradiance I. The coefficient of proportionality is the initial slope α^B.

as shown in Figure 1 [5]. The coefficient of proportionality in this relation is called the **initial slope** $(\mathrm{mg\,C\,(mg\,Chl)^{-1}\,(W\,m^{-2})^{-1}\,h^{-1}})$ and is the first physiological parameter in our model. Also, the function just presented (1.6) is our first example of a **photosynthesis irradiance function** (typically written with a lower case p^B to differentiate it from P^B).

Knowing a photosynthesis irradiance function and taking into account (1.4) we can now state our simple production model as:

$$P(z) = \alpha^B I(z) B(z), \tag{1.7}$$

where we have assumed that biomass and irradiance are depth dependent, whereas the initial slope is constant. We have therefore implicitly assumed a physiologically uniform population with vertically variable concentration. On the left hand side we have instantaneous production, whereas on the right hand side we have biomass as a state variable, initial slope as a parameter and irradiance as an argument of the photosynthesis irradiance function.

1.2 BEYOND LINEARITY

In the ocean a linear production light relation seldom holds for naturally occurring phytoplankton populations, as they are typically exposed to irradiance levels well beyond the range in which photosynthesis responds linearly to an increase in irradiance. At low irradiance a change in irradiance causes a linear response in production, which can be stated as:

$$\frac{\mathrm{d}P^B}{\mathrm{d}I} = \alpha^B, \tag{1.8}$$

and is in fact a differential form of expression (1.6). Following [7], a more realistic assumption would be to treat the rate of change in P^B with respect to I as a power series in P^B, stated mathematically as:

$$\frac{\mathrm{d}P^B}{\mathrm{d}I} = a_0 + a_1 P^B + a_2 (P^B)^2 + ..., \tag{1.9}$$

where a_i $(i = 1, 2, ...)$ are the coefficients to be determined. In this manner the linear photosynthesis irradiance function (1.6) is the solution to the previous equation with only the first parameter a_0 detained, such that (1.9) reduces to (1.8), making $a_0 = \alpha^B$.

A logical step forward would be to take into account the next factor in the power series, so that we have:

$$\frac{\mathrm{d}P^B}{\mathrm{d}I} = \alpha^B + a_1 P^B, \tag{1.10}$$

now with a_1 to be determined. This would allow the $p^B(I)$ function to have curvature (Figure 2), since the second derivative would not equal zero for $a_1 \neq 0$.

To derive the exact solution to equation (1.10) we make use of an observational fact that production saturates at high irradiance, which mathematically translates to:

$$\lim_{I \to \infty} p^B(I) = P_m^B, \tag{1.11}$$

and here we encounter a second physiological parameter called the **assimilation number** P_m^B $(\mathrm{mg\,C\,(mg\,Chl)^{-1}\,h^{-1}})$ [41, 4]. In our current

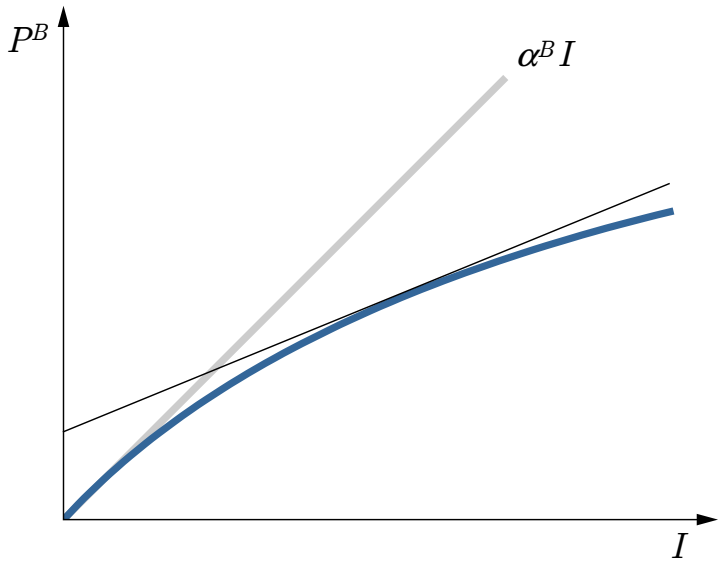

Figure 2: Curvature in the photosynthesis irradiance function exhibited with increasing irradiance.

context this condition translates to a boundary condition for equation (1.10) of the following form:

$$\lim_{I \to \infty} \frac{\mathrm{d}P^B}{\mathrm{d}I} = 0. \tag{1.12}$$

Using the previous two facts in equation (1.10) gives:

$$a_1 = -\frac{\alpha^B}{P_m^B}, \tag{1.13}$$

turning (1.10) into:

$$\frac{\mathrm{d}P^B}{\mathrm{d}I} = \alpha^B \left(1 - \frac{P^B}{P_m^B}\right). \tag{1.14}$$

Therefore, at low P^B, which occurs at low I, the response of production to a change in irradiance is highest and equals α^B. With an increase in P^B, which occurs at higher irradiance, the response declines, manifested mathematically by the decrease in $\mathrm{d}P^B/\mathrm{d}I$ (Figure 2).

Having derived equation (1.14) we now wish to solve it to obtain another photosynthesis irradiance function as its solution. By separation of variables and integration we obtain:

$$-\ln\left(P_m^B - P^B\right) = \frac{\alpha^B}{P_m^B} I + C, \tag{1.15}$$

where C is a constant of integration. Acknowledging that production ceases with no light, such that $P^B = 0$ at $I = 0$, we get:

$$C = -\ln\left(P_m^B\right), \tag{1.16}$$

transforming (1.15) into:

$$\ln\left(\frac{P_m^B - P^B}{P_m^B}\right) = -\frac{\alpha^B}{P_m^B} I. \tag{1.17}$$

After a little algebra and reintroducing the notation $P^B = p^B(I)$, yields:

$$p^B(I) = P_m^B \left(1 - \exp\left(-\alpha^B I \Big/ P_m^B\right)\right). \tag{1.18}$$

and we recognize this as the **exponential photosynthesis irradiance function** [60, 42].

The presented procedure can be extended still further [7]. For example, retaining the third term in the power series (1.9) the hyperbolic tangent photosynthesis irradiance function can be obtained:

$$p^B(I) = P_m^B \tanh\left(\alpha^B I \Big/ P_m^B\right). \tag{1.19}$$

These are but a few examples of a number of photosynthesis irradiance functions in the literature. Commonly used functions can be traced back to the following papers [5, 1, 55, 28, 42]. Extensive reviews on photosynthesis irradiance functions can for example be found in [28, 41, 16, 29]. In the literature the photosynthesis irradiance functions are also referred to as the light saturation functions, or simply as $P - I$ curves. All functions share some common properties which we now state explicitly.

1.3 PROPERTIES

The shape of the photosynthesis irradiance function expresses biophysical, biochemical and metabolic processes which regulate photosynthesis [12, 13]. Fortunately, just two parameters uniquely determine the photosynthesis irradiance function: the initial slope α^B and the assimilation number P_m^B [41, 4]. The initial slope is also referred to as photosynthetic efficiency and the assimilation number as the photosynthetic capacity [37]. Both parameters are referred to as the **photosynthesis parameters**.

Without explicitly stating the parameter values, the photosynthesis irradiance function can be written as a function of irradiance, in the following form [43]:

$$p^B(I) = p^B\left(I \mid \alpha^B, P_m^B\right), \tag{1.20}$$

highlighting the role photosynthesis parameters have. Having defining the photosynthesis irradiance function with two parameters, α^B and P_m^B, a whole family of photosynthesis irradiance functions is set. It is worth noting that the parameters are strictly positive.

The photosynthesis irradiance function itself is also positive and defined only for positive values of irradiance $I \geq 0$ [41]:

$$p^B(I) > 0. \tag{1.21}$$

For low irradiance normalized production is a linear function of irradiance with a coefficient of proportionality given by α^B, and we write:

$$\lim_{I \to 0} p^B(I) = \alpha^B I. \tag{1.22}$$

With increasing irradiance the slope of the curve drops. Finally, at high enough irradiance the slope flattens, and we have:

$$\lim_{I \to \infty} p^B(I) = P_m^B. \tag{1.23}$$

In that case light saturation takes place and normalized production stops being dependent on irradiance (Figure 3).

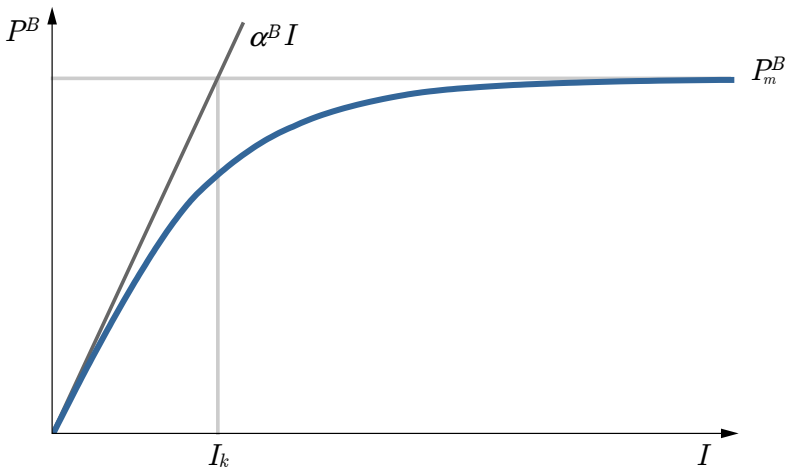

Figure 3: A typical photosynthesis irradiance function: at low light production is proportional to irradiance, as irradiance increases the response becomes nonlinear and finally for high irradiance production saturates.

Mathematically, for $I > 0$, the photosynthesis irradiance function is a strictly increasing function:

$$\frac{\mathrm{d}p^B(I)}{\mathrm{d}I} > 0, \tag{1.24}$$

with a negative second derivative:

$$\frac{\mathrm{d}^2 p^B(I)}{\mathrm{d}I^2} < 0. \tag{1.25}$$

The ratio of photosynthesis parameters is called the **photoadaptation parameter**:

$$I_k = \frac{P_m^B}{\alpha^B}, \tag{1.26}$$

which is expressed in the same unit as irradiance, namely $\mathrm{W\,m^{-2}}$. In the vicinity of I_k normalized production depends on both parameters: α^B and P_m^B. With values of irradiance lower than I_k, α^B dominates, while at values higher than I_k, P_m^B dominates.

1.4 PROBLEMS

1. Derive the hyperbolic tangent photosynthesis irradiance function (1.19) by retaining the third term in the power series (1.9) and following the same procedure as used to derive the exponential photosynthesis irradiance function (1.18).

2. Below are listed some of the typical photosnthesis irradiance functions, of which some were already given in the text:

$$p^B(I) = \frac{I + P_m^B \Big/ \alpha^B - \left| I - P_m^B / \alpha^B \right|}{2 \Big/ \alpha^B}, \tag{1.27}$$

$$p^B(I) = P_m^B \frac{I}{P_m^B \Big/ \alpha^B + I}, \tag{1.28}$$

$$p^B(I) = P_m^B \frac{I}{\sqrt{I^2 + (P_m^B \Big/ \alpha^B)^2}}, \tag{1.29}$$

$$p^B(I) = P_m^B \tanh\left(\alpha^B I \Big/ P_m^B\right), \tag{1.30}$$

$$p^B(I) = P_m^B \left(1 - \exp\left(-\alpha^B I \Big/ P_m^B\right)\right). \tag{1.31}$$

By order of appearance the authors are: [5], [1], [55], [28], and finally [42]. Express all the functions using the following notation for dimensionless irradiance:

$$I^* = \frac{\alpha^B I}{P_m^B} = \frac{I}{I_k}. \tag{1.32}$$

Plot all the functions on the same graph as a function of I^*.

3. A more general form of the exponential photosynthesis irradiance function takes into account photoinhibition, a process whereby photosynthesis gets reduced at high irradiance. The mathematical expression for this function is:

$$p^B(I) = P_m^B \left(1 - \exp\left(-\alpha^B I \Big/ P_m^B\right)\right) \exp\left(-\beta^B I / P_m^B\right), \tag{1.33}$$

where β^B is the photoinhibiton parameter. Plot this function for various values of β^B starting from zero (no photoinhibiton) and gradually increasing, whilst observing the change in the shape of the function.

4. Assume that irradiance is a function of time $I = I(t)$, given by:

$$I(t) = \langle I \rangle + \delta I, \tag{1.34}$$

where $\langle I \rangle$ is the average irradiance and δI is the perturbation. Make a numerical model in which the perturbation is taken as a normally disubstituted random variable with zero mean. Set the standard deviation of the perturbation arbitrarily. Calculate production by applying (1.18) with $I(t)$ as the argument. Study the effect of light variability under low light and under high light, relative to I_k. Compare this result to the one obtained by using only average irradiance $\langle I \rangle$.

2

PRIMARY PRODUCTION PROFILE

In the sea, phytoplankton biomass and production typically have a pronounced vertical structure [35]. The structure in biomass is caused by the combined action of biological and physical processes on time scales longer than that of a day [17] while the structure of normalized production is primarily caused by available light at a given time and the physiological status of the phytoplankton population [59, 43]. The available light is determined by the optical properties of the water column and surface light, which is primarily determined by day of the year, latitude and cloud cover [30].

Having established the production-light relation in the previous chapter, we now turn our attention to the problem of modelling the vertical structure of primary production. We have already touched upon this in the previous section, namely equation (1.7), where all the basic ingredients for solving such a problem were laid out. To model the vertical profile of production, information on the following is required: biomass profile, irradiance profile and the photosynthesis irradiance function, along with the values of photosynthesis parameters. At any given time production at depth can be easily calculated by simply plugging the irradiance value at that depth into the photosynthesis irradiance function and multiplying it by biomass at the given depth. By subsequently integrating over time one can calculate daily production, taking into account that irradiance is a function of time, as well as depth. We now proceed to do just that, but first state the problem in a slightly more formal manner.

2.1 PROBLEM FORMULATION

Let the z axis, oriented downward with the origin at the surface, mark depth and let t mark time, with $t = 0$ corresponding to the timing of sunrise. Acknowledging that irradiance has both a depth and a time dependence:

$$I = I\left(z, t\right), \tag{2.1}$$

the same holds for **instantaneous normalized production at depth**:

$$P^B\left(z, t\right) = p^B\big(I\left(z, t\right)\big), \tag{2.2}$$

measured in $(\mathrm{mg\,C\,(mg\,Chl)^{-1}\,h^{-1}})$. For generality, the explicit form of the photosynthesis irradiance function and the dependence of irradiance on depth and time will for now remain undefined. To calculate production at depth z and time t we multiply (2.2) by biomass $B\left(z, t\right)$ and obtain $P(z, t)$:

$$P\left(z, t\right) = B\left(z, t\right) p^B\big(I\left(z, t\right)\big), \tag{2.3}$$

referred to as the **instantaneous production at depth** $(\mathrm{mg\,C\,m^{-3}h^{-1}})$. To calculate **daily production at depth** $P_T\left(z\right)$ $(\mathrm{mg\,C\,m^{-3}})$, previous expression is integrated over time:

$$P_T\left(z\right) = \int_0^D B\left(z, t\right) p^B\big(I\left(z, t\right)\big)\,\mathrm{d}t, \tag{2.4}$$

with D being the time from sunrise till sunset, referred to as **daylength**. $P_T(z)$ viewed as a function of depth is the **daily production profile**.

To analytically solve the previous integral we assume that biomass does not change significantly during the course of one day, allowing it to come out the integral:

$$P_T\left(z\right) = B\left(z\right) \int_0^D p^B\big(I\left(z, t\right)\big)\,\mathrm{d}t, \tag{2.5}$$

which significantly simplifies the problem. In the remainder of this chapter we will continue considering biomass as time independent:

$$B(z, t) = B(z). \tag{2.6}$$

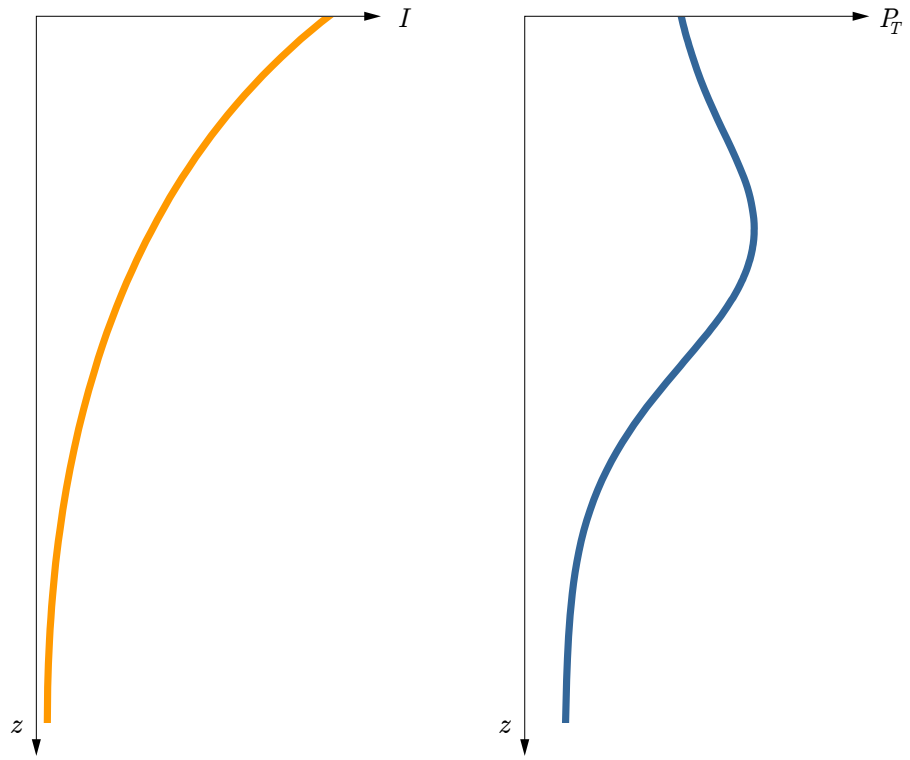

Figure 4: Sketch of the irradiance profile $I(z)$ (orange) and the daily production profile $P_T(z)$ (blue). The shape of the production profile is determined by the product of the biomass profile $B(z)$ (not shown) and the $p^B(I)$ function.

Subsequently, with biomass out of the integral, the **normalized production profile** $\left(\mathrm{mg\,C(mg\,Chl)^{-1}}\right)$ is obtained from (2.5) by dividing with biomass:

$$P_T^B(z) = \int_0^D p^B\left(I(z,t)\right) \mathrm{d}t, \tag{2.7}$$

which could have also been obtained by direct integration of (2.2). To solve the stated integral we need to specify irradiance as a function of depth and time, pick a photosynthesis irradiance function, and integrate over daylength. We now proceed to do just that.

2.2 UNDERWATER LIGHT FIELD

We begin by first considering a simple model for the irradiance profile. In the sea, irradiance has a pronounced vertical dependence, which is determined by the optical properties of seawater and surface radiation. The surface irradiance is simply given as a boundary condition:

$$I(0,t) = I_0(t). \tag{2.8}$$

A sine function is assumed for time dependence of surface irradiance:

$$I\left(0,t\right) = I_0^m \sin\left(\pi t/D\right), \tag{2.9}$$

where I_0^m is noon irradiance [27, 36, 30] (Figure 5). Optical properties of seawater are described by means of the **attenuation coefficient** of downward irradiance which is denoted by K (m^{-1}). It is defined as the rate of reduction of irradiance in an infinitesimally thin layer of seawater per unit depth, per unit irradiance: [30]:

$$K = -\frac{1}{I}\frac{\mathrm{d}I}{\mathrm{d}z}, \tag{2.10}$$

where the negative sign comes from the orientation of the z axis (Figure 6). As an optical medium, sea water both scatters and absorbs light, and the attenuation coefficient is the result of any combination of these two optical processes. The attenuation coefficient depends, among other things, on biomass concentration. The simplest and often used dependence of the attenuation coefficient on biomass reads:

$$K = K_w + k_B B, \tag{2.11}$$

where K_w is the seawater attenuation coefficient, which represents light attenuation processes due to scattering and absorption by pure seawater, particles and dissolved organic matter. The specific attenuation coefficient of phytoplankton k_b represents the processes of light attenuation due to absorption and scattering caused by phytoplankton [51]. The mentioned model is simple because it describes only the vertical structure of irradiance and reduces all the optical properties of sea water to the

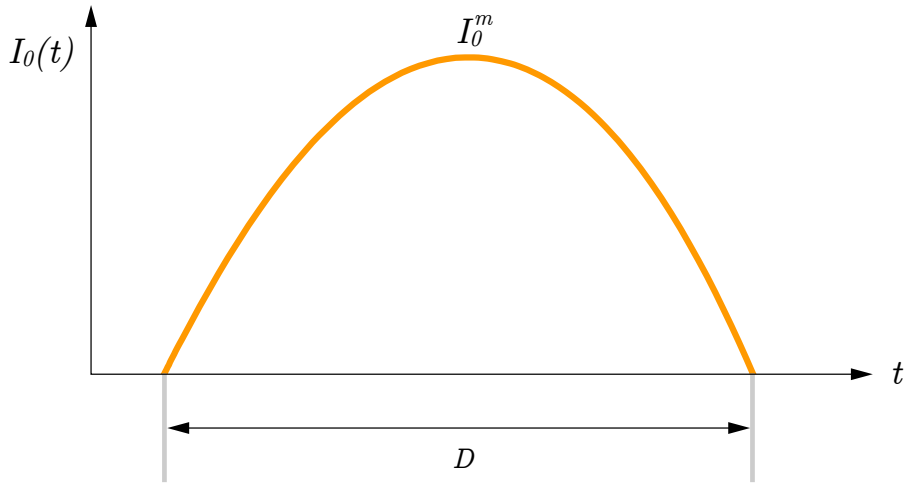

Figure 5: Idealized surface irradiance given as a sine function (2.9). Sunrise equals $t = 0$ and sunset $t = D$. Noon irradiance is given as I_0^m.

attenuation coefficient. More complex models that take into account the spatial, temporal, angular and spectral dependence of light were established [53, 11], but for pedagogical reasons for now we restrict to this model.

In case of an optically inhomogeneous water column $K = K(z)$, vertical integration of (2.10), along with the boundary condition (2.8), yields:

$$I(z,t) = I_0(t) \exp\left(- \int_0^z K(z')\, \mathrm{d}z' \right), \tag{2.12}$$

where z' is a dummy variable for integration. According to the solution (2.12) irradiance at the depth z is determined by the optical properties of the water column from the surface to that depth and the surface irradiance $I_0(t)$.

In case of an optically homogeneous water column $K \neq K(z)$, vertical integration of (2.10), along with the boundary condition (2.8), yields:

$$I(z,t) = I_0(t) \exp\left(-Kz\right). \tag{2.13}$$

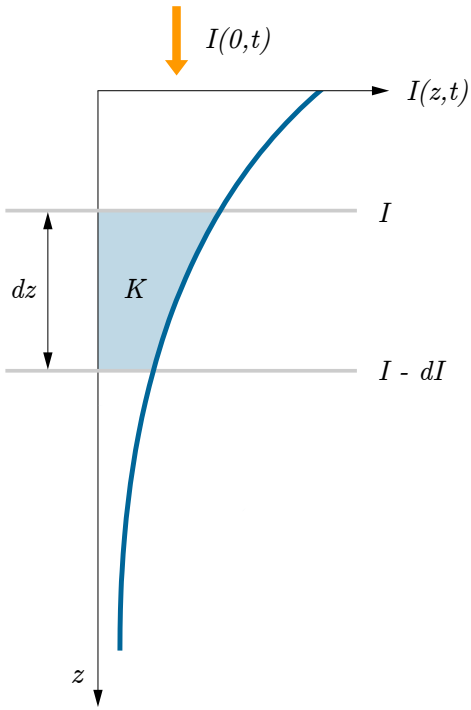

Figure 6: Water column forced by surface irradiance $I(0,t)$ and the resulting irradiance profile $I(z,t)$ (blue curve). A layer of thickness dz attenuates irradiance I by the amount dI. The attenuation coefficient K is a measure of the reduction in irradiance per unit depth per unit irradiance.

Although simple, the specified irradiance model is a commonly used model of the underwater light field when modelling primary production. The central element of the model is the attenuation coefficient, which determines the penetration depth of irradiance in the model. Taking into account the temporal dependence of surface irradiance (2.9), yields the underwater light field in our model:

$$I(z,t) = I_0^m \sin(\pi t/D) \exp(-Kz). \tag{2.14}$$

Next step in modelling the daily production profile is to use this expression in a photosynthesis irradiance function.

2.3 ANALYTICAL SOLUTION FOR THE DAILY PRODUCTION PROFILE

By taking the previous expression for irradiance (2.14) as the argument of the exponential photosynthesis irradiance function (1.18) the defining integral for daily normalized production (2.7) becomes:

$$P_T^B(z) = \int_0^D P_m^B \left[1 - \exp\left(- \alpha^B I_0^m \sin(\pi t/D) e^{-Kz} / P_m^B \right) \right] \mathrm{d}t. \tag{2.15}$$

The solution of this integral gives the amount of carbon assimilated at depth during one day per unit biomass. To solve it we begin by defining the **dimensionless noon irradiance** as:

$$I_*^m = \frac{\alpha^B I_0^m}{P_m^B} = \frac{I_0^m}{I_k}, \tag{2.16}$$

which represents the ratio of the photoadaptation parameter to noon irradiance. It simply tells us how higher noon irradiance is relative to the photoadaptation parameter. Using (2.16) translates the previous integral into:

$$P_T^B(z) = \int_0^D P_m^B \left[1 - \exp\left(- I_*^m e^{-Kz} \sin(\pi t/D) \right) \right] \mathrm{d}t. \tag{2.17}$$

To solve it, the expansion of the exponential function as an infinite sum is used:

$$\exp x = \sum_{n=0}^{\infty} \frac{x^n}{n!}. \tag{2.18}$$

After inserting this identity into the previous integral we obtain:

$$P_T^B(z) = \int_0^D P_m^B \left(1 - \sum_{n=0}^{\infty} \frac{\left(-I_*^m e^{-Kz} \sin\left(\pi t/D\right) \right)^n}{n!} \right) \mathrm{d}t, \tag{2.19}$$

which after some algebra becomes:

$$P_T^B(z) = -P_m^B \sum_{n=1}^{\infty} \frac{\left(-I_*^m e^{-Kz} \right)^n}{n!} \int_0^D \sin^n\left(\pi t/D\right) \mathrm{d}t. \tag{2.20}$$

Next step is to employ the following substitution:

$$x = \frac{\pi t}{D}, \tag{2.21}$$

by which the integral in the previous expression becomes:

$$\int_0^D \sin^n(\pi t/D)\,\mathrm{d}t = \frac{D}{\pi}\int_0^\pi \sin^n x\,\mathrm{d}x. \tag{2.22}$$

Normalized daily production is now:

$$P_T^B(z) = -P_m^B D \sum_{n=1}^{\infty} \frac{\left(-I_*^m e^{-Kz}\right)^n}{\pi \cdot n!}\int_0^\pi \sin^n x\,\mathrm{d}x. \tag{2.23}$$

The obtained integral is solved by recursive application of the following identity:

$$\int_0^\pi \sin^n x\,\mathrm{d}x = \frac{n-1}{n}\int_0^\pi \sin^{n-2} x\,\mathrm{d}x. \tag{2.24}$$

To apply it we first break the previous sum into sums over odd and even integers, to get:

$$\begin{aligned} P_T^B(z) = -P_m^B D\Bigg(&\sum_{n=1}^{\infty} \frac{\left(-I_*^m e^{-Kz}\right)^{2n-1}}{\pi(2n-1)!}\int_0^\pi \sin^{2n-1} x\,\mathrm{d}x \\ &+ \sum_{n=1}^{\infty} \frac{\left(-I_*^m e^{-Kz}\right)^{2n}}{\pi(2n)!}\int_0^\pi \sin^{2n} x\,\mathrm{d}x\Bigg). \end{aligned} \tag{2.25}$$

Going step by step, for $n = 1$ we have:

$$\int_0^\pi \sin x\,\mathrm{d}x = 2. \tag{2.26}$$

For $n = 2$ we have:

$$\int_0^\pi \sin^2 x\,\mathrm{d}x = \frac{\pi}{2}. \tag{2.27}$$

Subsequently, for several more values of n we have:

$$\text{n=3} \quad \int_0^{\pi} \sin^3 x \, \mathrm{d}x = \frac{2}{3} \times 2;$$

$$\text{n=4} \quad \int_0^{\pi} \sin^4 x \, \mathrm{d}x = \frac{3}{4} \times \frac{\pi}{2};$$

$$\text{n=5} \quad \int_0^{\pi} \sin^5 x \, \mathrm{d}x = \frac{4}{5} \times \frac{2}{3} \times 2;$$

$$\text{n=6} \quad \int_0^{\pi} \sin^6 x \, \mathrm{d}x = \frac{5}{6} \times \frac{3}{4} \times \frac{\pi}{2};$$

The interested reader can expand this still further, but for the sake of brevity we stop the explicit statement of these integrals here. For odd integers $(2n-1)$ the solution of (2.24) can be expressed as:

$$\int_0^{\pi} \sin^{2n-1} x \, \mathrm{d}x = 2\frac{(2n-2)!!}{(2n-1)!!}, \tag{2.28}$$

and for even integers $(2n)$ as:

$$\int_0^{\pi} \sin^{2n} x \, \mathrm{d}x = \pi\frac{(2n-1)!!}{(2n)!!}. \tag{2.29}$$

Combining these expressions with (2.25) we get:

$$\begin{aligned} P_T^B(z) = -P_m^B D\Bigg(& \sum_{n=1}^{\infty} \frac{2\left(-I_*^m e^{-Kz}\right)^{2n-1}}{\pi(2n-1)!}\frac{(2n-2)!!}{(2n-1)!!} \\ & + \sum_{n=1}^{\infty} \frac{\left(-I_*^m e^{-Kz}\right)^{2n}}{(2n)!}\frac{(2n-1)!!}{(2n)!!}\Bigg). \end{aligned} \tag{2.30}$$

Although cumbersome this expression is the exact solution for daily normalized production. We now proceed to write it in a more compact and comprehensive manner.

Putting the minus sing inside the brackets gives:

$$P_T^B(z) = P_m^B D \left(\sum_{n=1}^{\infty} \frac{2\left(-I_*^m e^{-Kz}\right)^{2n-1}}{\pi(2n-1)!} \frac{(2n-2)!!}{(2n-1)!!} - \sum_{n=1}^{\infty} \frac{\left(-I_*^m e^{-Kz}\right)^{2n}}{(2n)!} \frac{(2n-1)!!}{(2n)!!} \right). \tag{2.31}$$

We observe that the solution consists of a product of the assimilation number P_m^B, daylength D and a relatively complicated expression inside the brackets. To simplify this expression we define the $f_z\left(I_*^m e^{-Kz}\right)$ function as:

$$f_z\left(I_*^m e^{-Kz}\right) = \sum_{n=1}^{\infty} \frac{2\left(I_*^m e^{-Kz}\right)^{2n-1}}{\pi\,(2n-1)!} \frac{(2n-2)!!}{(2n-1)!!} - \sum_{n=1}^{\infty} \frac{\left(I_*^m e^{-Kz}\right)^{2n}}{(2n)!} \frac{(2n-1)!!}{(2n)!!}, \tag{2.32}$$

displayed in Figure 7 [32, 31]. This function is dimensionless and its argument is the dimensionless noon irradiance I_*^m multiplied by the e^{-Kz} term: $I_*^m e^{-Kz}$. With the given definition daily normalized production $P_T^B(z)$ now becomes:

$$P_T^B(z) = P_m^B D\, f_z\left(I_*^m e^{-Kz}\right), \tag{2.33}$$

At a given depth z, by knowing I_0^m, K, α^B and P_m^B the value of $I_*^m e^{-Kz}$ is calculated. Then the product $P_m^B D f_z(I_*^m e^{-Kz})$ gives the value of daily normalized production at depth z. To calculate production, we simply multiply (2.33) by biomass at depth $B(z)$:

$$P_T(z) = B(z) P_m^B D\, f_z\left(I_*^m e^{-Kz}\right). \tag{2.34}$$

In summary, we have derived an analytical solution for daily production at depth and now proceed to explore some of the properties of the presented solution.

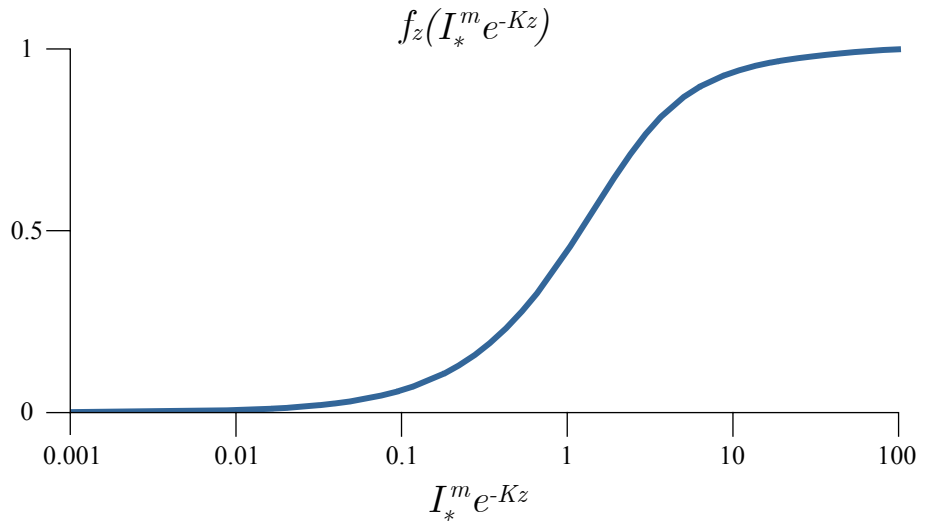

Figure 7: Dimensionless function $f_z(I_*^m e^{-Kz})$ from the analytical solution for daily production (2.33). By multiplying this function with biomass $B(z)$, the assimilation number P_m^B and daylength D daily production at depth is calculated.

2.4 PROPERTIES OF THE PRODUCTION PROFILE

In our model irradiance declines with depth, according to:

$$\frac{\mathrm{d}I}{\mathrm{d}z} = -KI. \tag{2.35}$$

Taking this into account, let us consider the change with depth of instantaneous production:

$$\frac{\mathrm{d}p^B(I(z))}{\mathrm{d}z} = \frac{\mathrm{d}p^B}{\mathrm{d}I}\frac{\mathrm{d}I}{\mathrm{d}z}. \tag{2.36}$$

The first term is positive, because the photosynthesis irradiance function is an increasing function of irradiance (1.24), whereas the second term is negative. Therefore, instantaneous production declines with depth:

$$\frac{\mathrm{d}P^B}{\mathrm{d}z} < 0. \tag{2.37}$$

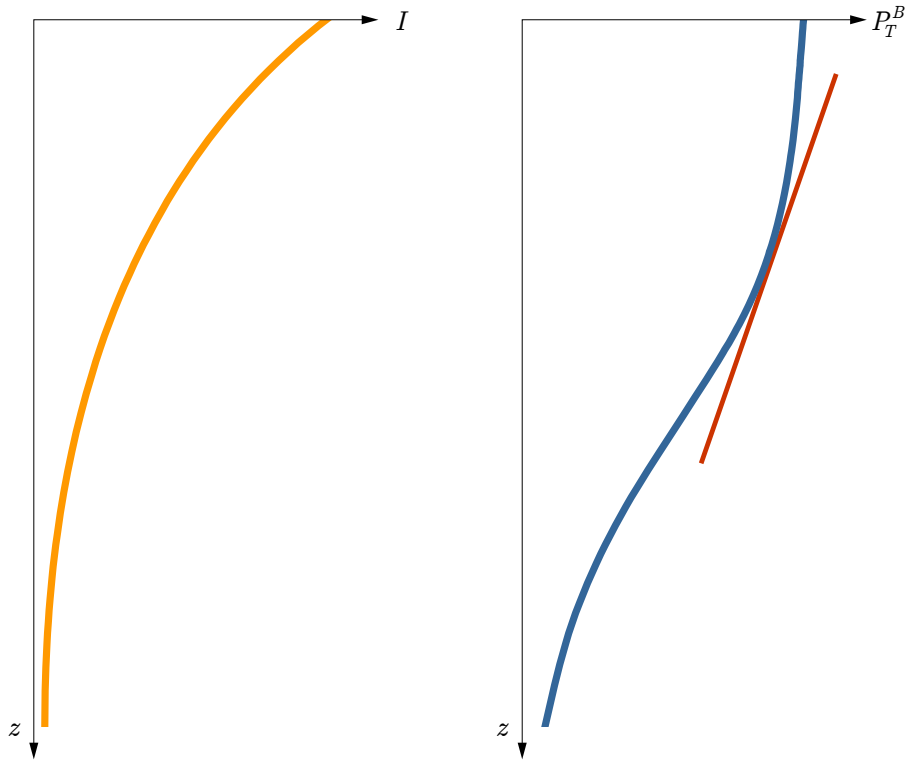

Figure 8: Decline of normalized daily production with depth (blue). Irradiance $I(z,t)$ (orange) declines exponentially with depth causing normalized production to also decline with depth, making the tangent to $P_T^B(z)$ (red line) have a negative slope with respect to depth.

Normalized daily production, being the integral over time of instantaneous production, also declines with depth (Figure 8):

$$\frac{\mathrm{d}P_T^B}{\mathrm{d}z} < 0, \tag{2.38}$$

which is easy to show by simply taking the derivative of f_z:

$$\frac{\mathrm{d}}{\mathrm{d}z} f_z(I_*^m e^{-Kz}) < 0. \tag{2.39}$$

Looking now at daily production we have:

$$P_T(z) = B(z)P_T^B(z), \tag{2.40}$$

the derivative of which with respect to depth reads:

$$\frac{\mathrm{d}P_T}{\mathrm{d}z} = \frac{\mathrm{d}B}{\mathrm{d}z}P_T^B + B\frac{\mathrm{d}P_T^B}{\mathrm{d}z}, \tag{2.41}$$

which due to (2.38) can be both positive and negative and subsequently production can acquire a subsurface maximum, in contrast to normalized production which can not.

The rate of change in daily production with respect to depth is positive if the rate of increase in biomass with depth, multiplied by normalized production, outpaces the rate of decline in normalized production multiplied by biomass:

$$\frac{\mathrm{d}B}{\mathrm{d}z}P_T^B + B\frac{\mathrm{d}P_T^B}{\mathrm{d}z} > 0. \tag{2.42}$$

By using (2.33) we derive the following condition:

$$\frac{1}{B}\frac{\mathrm{d}B}{\mathrm{d}z} > -\frac{\mathrm{d}}{\mathrm{d}z}f_z\left(I_*^m e^{-Kz}\right) \Big/ f_z\left(I_*^m e^{-Kz}\right). \tag{2.43}$$

Therefore, the relative increase in biomass with depth has to be higher than the relative decrease in production with depth. Since (2.39) is always negative the right hand side is positive.

However, it is worth noting that the given conclusions are valid for vertically uniform photosynthesis parameters, which implies a vertically uniform phytoplankton population. However, the solution (2.34) also holds in case of non-uniform photosynthesis parameters $\alpha^B = \alpha^B(z)$ and $P_m^B = P_m^B(z)$, changing the solution (2.34) to:

$$P_T(z) = B(z)P_m^B(z)D\, f_z\left(I_*^m(z)e^{-Kz}\right), \tag{2.44}$$

where now the normalized noon irradiance is also a function of depth $I_*^m(z) = \alpha^B(z)I_0^m / P_m^B(z)$. Knowing how to model the daily production profile, we now turn our attention to the biomass profile and explore how its vertical dependence is typically specified in models.

2.5 SHIFTED GAUSSIAN BIOMASS PROFILE

A prototypical function most often used to describe the biomass profile in the ocean is the Shifted Gaussian:

$$B(z) = B_0 + \frac{h}{\sigma\sqrt{2\pi}} \exp\left(-\frac{(z - z_m)^2}{2\sigma^2}\right), \tag{2.45}$$

where the biomass beneath the Gaussian curve is given by h, the depth of the maximum is at z_m and the width of the biomass peak is determined by σ. B_0 is the background biomass (Figure 9). The height of the peak biomass at z_m is $H = h/\sigma\sqrt{2\pi}$.

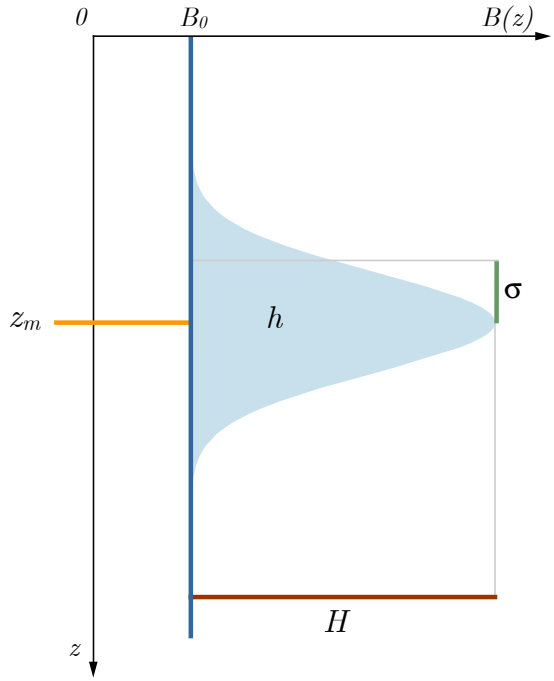

Figure 9: Sketch of the shifted Gaussian biomass profile. Integral biomass beneath the Gaussian curve is given by h (blue shaded region), depth of the maximum by z_m (orange mark) and the width of the biomass peak by σ (green line). B_0 is the background biomass (dark blue line), here equal to the surface biomass. The height above the background biomass is given by $H = h/\sigma\sqrt{2\pi}$ (red line).

The Gaussian function is suitable for describing the vertical structure of biomass and has been accepted as a standard profile for a long time [43]. It is a simple function that allows the description of the vertical structure of phytoplankton biomass for different geographical areas and seasons [40]. It has been used in many models as an initial condition for biomass, and the forms it describes are often obtained as results of numerical models [22] and measurements [45]. It is suitable for describing the structure of the deep chlorophyll maximum, which is an ubiquitous phenomenon throughout the world's oceans [9, 2].

With the shifted Gaussian biomass, daily production profile equals:

$$P_T(z) = \left[B_0 + \frac{h}{\sigma\sqrt{2\pi}} \exp\left(-\frac{(z - z_m)^2}{2\sigma^2} \right) \right] P_m^B D\, f_z\left(I_*^m e^{-Kz}\right), \tag{2.46}$$

which was obtained by direct application of (2.33) and (2.45) in (2.40). It is evident that the production profile now consists of the profile associated with the vertically uniform term in the Gaussian, namely B_0 and the vertically non-uniform term, namely the exponential component, which is dictated by three parameters: σ, z_m and h. Depending on the values of these parameters the shape of the production profile will change.

The first term will create a declining production profile, due to $B_0 \neq B(z)$, whereas the second term may create an increasing production profile. This implies that production may acquire a subsurface maximum with a shifted Gaussian biomass profile. The depth of the maximum in biomass need not coincide with the depth of maximum production. Below the maximum, both terms need to give diminishing production with increasing depth. At great depth ($z \to \infty$) normalized production and the shifted Gaussian both go to zero, but the background biomass B_0 does not. However, when multiplied to calculate daily production at great depth, their product is zero:

$$\lim_{z\to\infty} P_T(z) = B_0 P_m^B D\, f_z\left(I_*^m e^{-K\infty}\right) = 0. \tag{2.47}$$

Having background biomass constant is an unrealistic assumption for great depth and is in contradiction with observations. A remedy to this issue was proposed by [6] in the form of a Sigmoid function, which we now explore.

2.6 SHIFTED SIGMOID BIOMASS PROFILE

The Shifted Sigmoid function proposed by [6] is of the following form:

$$B(z) = B_0 \left[1 - \frac{1}{1 + \exp\big(-\sigma(z - z_m) \big)} \right], \tag{2.48}$$

where now B_0 is not the background biomass, but the surface biomass. The parameter σ dictates the slope of the biomass profile and z_m gives the mid point depth of the slope (Figure 10).

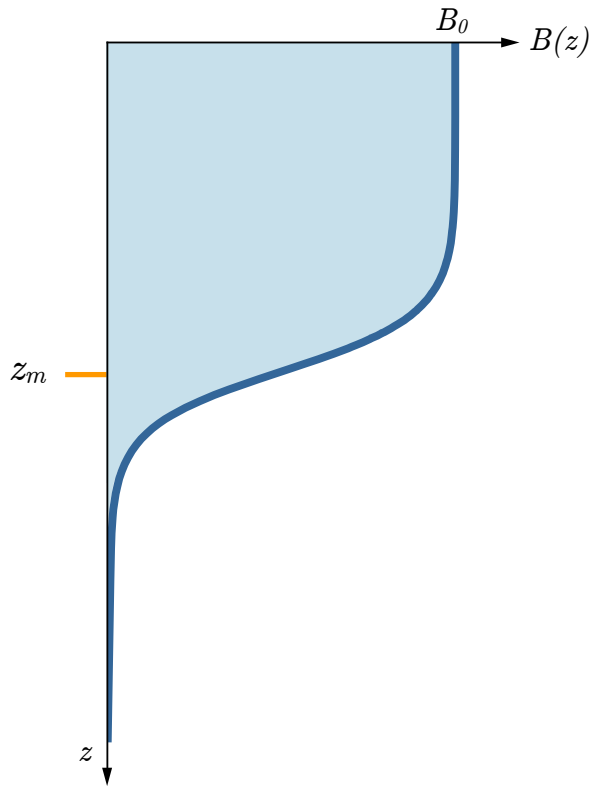

Figure 10: Sketch of the shifted Sigmoid biomass profile. Surface biomass is given by B_0, depth of the mid point by z_m (orange mark) and the slope of the biomass profile is dictated by σ. Total biomass is given by the blue shaded area.

The total biomass is now given as:

$$\int_0^\infty B(z)\,\mathrm{d}z = \frac{1}{\sigma}\ln\left(1+\exp(\sigma z_m)\right), \tag{2.49}$$

which in the limit of high σ becomes simply:

$$\lim_{\sigma\to\infty}\int_0^\infty B(z)\,\mathrm{d}z = B_0 z_m. \tag{2.50}$$

With the shifted Sigmoid daily production profile now reads:

$$P_T(z) = B_0 P_m^B D\, f_z\left(I_*^m e^{-Kz}\right)\left[1-\frac{1}{1+\exp\left(-\sigma(z-z_m)\right)}\right]. \tag{2.51}$$

Once again, in the limit of high σ we have

$$\lim_{\sigma\to\infty} P_T(z) = B_0 P_m^B D\, f_z\left(I_*^m e^{-Kz}\right), \tag{2.52}$$

which is valid from the surface up to the mid point depth z_m.

2.7 RELATION TO GROWTH MODELS

Phytoplankton growth models are dynamic models that describe the spatial-temporal distribution of biomass [61]. A typical model of this type consists of a differential equation that describes the biomass dynamics [19]. Such equations form an integral part of ecological models in which hydrodynamic equations and equations describing the rest of the ecosystem are combined [14]. In the phytoplankton growth equation, the basic term is the light saturation function, which describes the biomass growth caused by photosynthesis. The solution of the equation gives the time development of biomass which is related to primary production [26].

In order to demonstrate the connection between growth models and primary production, a simple growth model of the following form will be considered:

$$\frac{\partial}{\partial t}B(z,t) = \frac{1}{\chi}P^B(z,t)B(z,t), \tag{2.53}$$

where the normalized production is equal to $P^B(z,t) = p^B\left(I\left(z,t\right)\right)$, and χ is the carbon to chlorophyll ratio [54]. For the purposes of this demonstration, χ is constant. The equation simply states that carbon assimilated in photosynthesis increases biomass. The solution of this equation at time D (daylength) reads:

$$B(z,D) = B(z,0)\exp\left(\frac{1}{\chi}P_T^B(z)\right). \tag{2.54}$$

By writing the exponential function as a sum (2.18), previous expression becomes:

$$B(z,D) = B(z,0) + B(z,0)\left[\frac{1}{\chi}P_T^B(z) + \sum_{n=2}^{\infty}\frac{1}{n!}\left(\frac{1}{\chi}P_T^B(z)\right)^n\right]. \tag{2.55}$$

The terms in this sum have a fairly simple interpretation. Each term of the sum represents the total synthesized biomass in case the initial biomass were equal to the previous term:

$$B(z,0)\left(\frac{1}{\chi}P_T^B(z)\right)^n = \left[B(z,0)\left(\frac{1}{\chi}P_T^B(z)\right)^{n-1}\right]P_T^B(z). \tag{2.56}$$

Since primary production is the only process by which biomass accumulates in this simple growth model, all terms inside the parentheses in expression (2.55) correspond to primary production at depth z. Primary production is a process with a finite energy source that takes place in the finite dimensions of the water column, and therefore the terms in the series expansion (2.55) should converge. The exponential function is convergent over the entire set of real numbers, implying this series expansion is indeed convergent, which means that terms of higher order can be ignored in first approximation. Keeping only the first term inside

the parentheses yields a first-order approximation of the biomass at time D:

$$B(z,D) \approx B(z,0) + \frac{1}{\chi} B(z,0) P_T^B(z). \tag{2.57}$$

This implicitly assumes that the accumulation of biomass is dominantly caused by initial biomass, and the contribution from the newly synthesized biomass itself is negligible. The second term on the right is the daily production defined by (2.5), divided by χ. Therefore, the production profile provides a first approximation of the change in the biomass profile caused by primary production if biomass growth is allowed in the model.

Apart from the effect on biomass, there is also an effect growth has on the production profile. According to (2.54), for time-dependent biomass, the daily production profile is equal to:

$$P_T(z) = \chi B(z,0) \left[\exp\left(\frac{1}{\chi} P_T^B(z) \right) - 1 \right], \tag{2.58}$$

which is basically the difference between the final and initial biomass, multiplied by χ. We notice that there is an additional parameter χ in this expression. How big an influence χ has on the production profile in the growth model can be easily analysed by expressing the exponential function in the previous expression as a sum and rearranging:

$$P_T(z) = \left[1 + \sum_{n=2}^{\infty} \frac{1}{n! \chi^{n-1}} \left(P_T^B(z) \right)^{n-1} \right] B(z,0) P_T^B(z). \tag{2.59}$$

The influence of χ on the production profile is manifested only as a second-order factor. The conclusion is that the two models give an equivalent production profile in first approximation.

2.8 PROBLEMS

1. Assume the attenuation of irradiance with depth is described by the following equation:

$$\frac{\mathrm{d}I}{\mathrm{d}z} = -KI, \tag{2.60}$$

where K is the diffuse attenuation coefficient for downwelling irradiance and the z axes is positive downwards. Taking the surface irradiance just below the sea surface ($z = 0$) as known I_0 derive the solution for the irradiance profile (2.13). Subsequently use the irradiance profile to calculate $P^B(z)$ first by means of (1.6) and second by means of (1.18). Plot the two results and their difference.

2. Assume the attenuation of irradiance with depth is again described by (2.60). Restate this expression as

$$\mathrm{d}I = -KI\,\mathrm{d}z, \tag{2.61}$$

and use it in (1.14) to derive $P^B(z)$. The result should match the one obtained in the first problem, where the irradiance profile is directly used in the exponential photosynthesis irradiance function.

3. Use the photosynthesis irradiance functions given in Problem 2 of Chapter 2 in a numerical model and solve for the daily production profile for each. The irradiance profile is given by (2.14) in each case. Compare the results by plotting the numerical solutions as a function of I_*^m in the same manner that the analytical solution (2.33) is presented in Figure 7.

4. Build a numerical model in which the effect of biomass on the attenuation of irradiance with depth is taken into account with (2.11) such that the irradiance profile is given by (2.12). Calculate the daily production profile in this case and compare it to the analytical solution in which $K = K_w$. Use multiple values for k_B to explore its effect on the shape of the daily production profile.

5. Employ the shifted Gaussian in calculation of the daily production profile by using (2.46). Based on (2.41) state the condition for the maximum production at depth and derive the condition that is satisfied at that depth. Express the first derivative with respect to depth of the daily production profile in case of the shifted Gaussian and following (2.41) consider under which scenario does the production profile decrease/increase with depth. Explore the effect depth z_m and width of the maximum σ have on the shape of the production profile and the depth of the maximum in daily production.

6. Build a model of the daily production profile using the shifted Sigmoid (2.48) as the model for the biomass profile. For the normalized daily production profile use expression (2.33). Explore the effect σ and z_m have on the shape of the biomass profile as well as the production profile.

7. Build a numerical model that solves equation (2.53). Explore how the biomass profiles evolves under variable surface irradiance given by (2.14) and contrast it with the evolution over time under constant surface irradiance equal to the average daily irradiance $I_0^m \pi/2$.

3

WATERCOLUMN PRODUCTION

Having described the vertical structure in biomass and production we are now in a position to calculate the total amount of carbon assimilated in photosynthesis in the entire water column. This quantity is called watercolumn production and is of paramount importance in oceanography. In standard oceanographic practice watecolumn production is quantified by the amount of carbon assimilated during the day in the photic zone. Measurements of watercolumn production have been carried out at sea after the introduction of the radioactive carbon method in 1952 by Steeman Nielsen [56]. Since then, the development of mathematical models of watercolumn production has been of high interest to oceanographers.

In modern times remotely sensed data are merged with state of the art models to calculate global estimates of marine primary production. The backbone of all such models is the functional relation between the rate of carbon assimilation and irradiance: the photosynthesis irradiance function. While the various models differ in precise detail they all share the same structure and in this chapter we explore this structure.

We build upon the previous chapter where we have shown how to calculate daily production at depth. We proceed to extend the model and demonstrate how to calculate watercolumn production. The canonical solution for unifrom biomass [47] is presented along with the solution for mixed layer production. The assumption of uniform biomass is relaxed and exact solutions for watercolumn production with a shifted Gaussian biomass and a general solution for arbitrary biomass are derived.

3.1 PROBLEM FORMULATION

We start by defining **watercolumn production** $P_{Z,T}$ ($\mathrm{mg\,C\,m^{-2}}$) as the amount of carbon assimilated in photosynthesis in the water column during one day per square meter [47, 30]. In the notation of the model developed thus far we have:

$$P_{Z,T} = \int_0^\infty \int_0^D P(z,t)\,\mathrm{d}t\,\mathrm{d}z. \tag{3.1}$$

The notation $P_{Z,T}$ is also used when the upper limit over depth is not infinity. By expressing instantaneous production using (2.3) we have:

$$P_{Z,T} = \int_0^\infty \int_0^D B\,(z,t)\,p^B\big(\,I\,(z,t)\,\big)\,\mathrm{d}t\,\mathrm{d}z. \tag{3.2}$$

Further assuming time independent biomass and grouping the terms based on the definition of the normalized production profile (2.5) we have:

$$P_{Z,T} = \int_0^\infty B\,(z)\left(\int_0^D p^B\big(\,I\,(z,t)\,\big)\,\mathrm{d}t\right)\mathrm{d}z. \tag{3.3}$$

where the term inside the brackets is recognized as $P_T^B(z)$. Thus formulated, watercolumn production equals the vertical integral of the daily production profile $P_T(z)$ (Figure 11), that is, the vertical integral of the product between biomass $B(z)$ and normalized production $P_T^B(z)$ profiles:

$$P_{Z,T} = \int_0^\infty B(z)P_T^B(z)\,\mathrm{d}z = \int_0^\infty P_T(z)\,\mathrm{d}z. \tag{3.4}$$

Here we observe the importance of the production profile as it the central element in the calculation of watercolumn production.

Integration of $P(z,t)$ can also be done vertically first and then over time, a procedure that will shortly be used to find an analytical solution

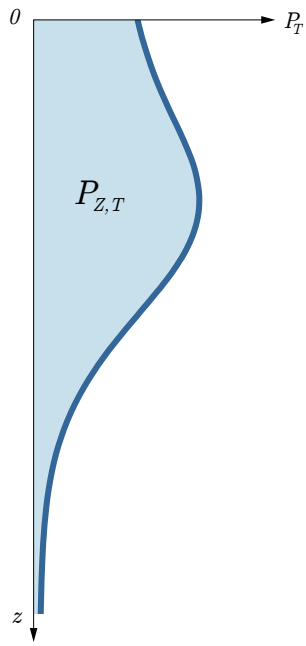

Figure 11: Sketch of watercolumn production $P_{Z,T}$ (light blue area) as the vertical integral of the daily production profile $P_T(z)$ (thick blue curve).

for watercolumn production. In this case, the vertical integral of $P(z,t)$ is the **instantaneous watercolumn production** $P_{Z,T}$ ($\mathrm{mg\,C\,m^{-2}\,h^{-1}}$):

$$P_Z(t) = \int_0^\infty B\,(z,t)\; p^B\big(\, I\,(z,t)\,\big)\,\mathrm{d}z. \tag{3.5}$$

With this definition, watercolumn production becomes an integral over daylength of instantaneous watercolumn production:

$$P_{Z,T} = \int_0^D P_Z(t)\,\mathrm{d}t. \tag{3.6}$$

The obtained expression is equal to (3.3). Having laid out the basic definitions, we now proceed to solve for $P_{Z,T}$ analytically, following [47].

3.2 ANALYTICAL SOLUTION FOR WATERCOLUMN PRODUCTION

Thus far, using the exponential photosynthesis irradiance function (1.18) and exponentially declining sinusoidal irradiance (2.13), yielded the daily normalized production profile (2.15), which we now multiply by biomass $B(z)$ to obtain:

$$P_{Z,T} = \int_0^\infty \int_0^D B(z) P_m^B \left[1 - \exp\left(-\alpha^B I_0^m \sin(\pi t/D) e^{-Kz} / P_m^B \right) \right] \mathrm{d}t \, \mathrm{d}z, \quad (3.7)$$

as the integral that needs to be solved to get watercolumn production. We begin with the simplest case, by first assuming uniform biomass:

$$B(z) = B, \quad (3.8)$$

and subsequently change the order of integration, in line with the interpretation provided in (3.6). Now we have:

$$P_{Z,T} = B P_m^B \int_0^D \int_0^\infty \left(1 - \exp\left(-\alpha^B I_0^m \sin(\pi t/D) e^{-Kz} / P_m^B \right) \right) \mathrm{d}z \, \mathrm{d}t, \quad (3.9)$$

where we have extracted B and P_m^B outside the integrals, both being independent of depth and time. With a change of variables:

$$x = I_*^m \sin(\pi t/D) e^{-Kz}, \quad (3.10)$$

the vertical integral in the expression (3.9) becomes a table integral and its solution reads:

$$\int_0^\infty \left[1 - \exp\left(-I_*^m \sin(\pi t/D) e^{-Kz} \right) \right] \mathrm{d}z = \frac{1}{K} \sum_{n=1}^\infty \frac{(-1)^{n+1}}{n \cdot n!} \left(I_*^m \sin\left(\pi t/D\right) \right)^n. \quad (3.11)$$

The obtained expression multiplied by BP_m^B gives the instantaneous watercolumn production $P_Z(t)$:

$$P_Z(t) = \frac{B P_m^B}{K} \sum_{n=1}^\infty \frac{(-1)^{n+1}}{n \cdot n!} \left(I_*^m \sin\left(\pi t/D\right) \right)^n. \quad (3.12)$$

By inserting (3.11) into (3.9) we get:

$$P_{Z,T} = \int_0^D \frac{BP_m^B}{K} \sum_{n=1}^{\infty} \frac{(-1)^{n+1}}{n \cdot n!} \left(I_*^m \sin\left(\pi t / D\right) \right)^n \mathrm{d}t. \tag{3.13}$$

Here we recognize the same integral as in (2.23) which is again solved by the application of the recursive relation (2.24), yielding:

$$\begin{aligned} P_{Z,T} = \frac{BP_m^B D}{K} \Bigg[& \sum_{n=1}^{\infty} \frac{2\left(I_*^m\right)^{2n-1}}{\pi\left(2n-1\right)\left(2n-1\right)!} \frac{(2n-2)!!}{(2n-1)!!} \\ & - \sum_{n=1}^{\infty} \frac{\left(I_*^m\right)^{2n}}{2n\left(2n\right)!} \frac{(2n-1)!!}{(2n)!!} \Bigg]. \end{aligned} \tag{3.14}$$

The presented solution is the analytical solution for daily watercolumn production. For unit biomass it is also a solution for normalized production. The expression in parentheses in (3.14) depends only on I_*^m and can be denoted as a function $f(I_*^m)$, similar to (2.31), in order to make the solution less cumbersome. With this notation, previous expression becomes simply:

$$P_{Z,T} = \frac{BP_m^B D}{K} f(I_*^m). \tag{3.15}$$

Graph of $f(I_*^m)$ is given in Figure 12. It is clear from the given solution that daily watercolumn production has a linear dependence on biomass B and daylength D. Nonlinear dependencies arise with respect to photosynthesis parameters α^B and P_m^B, and irradiance I_0^m. It is necessary to emphasize the inverse proportionality of watercolumn production and the attenuation coefficient K.

Since it was published, solution [47] has seen many applications: in the study of the interaction of mixing depth and primary production [48], in the context of Sverdrup's critical depth theory [38], in the assessment of primary production via satellites [44], as elements of climate models [44] and for explaining the dynamics of high nutrient - low chrollophyll zones [39, 46].

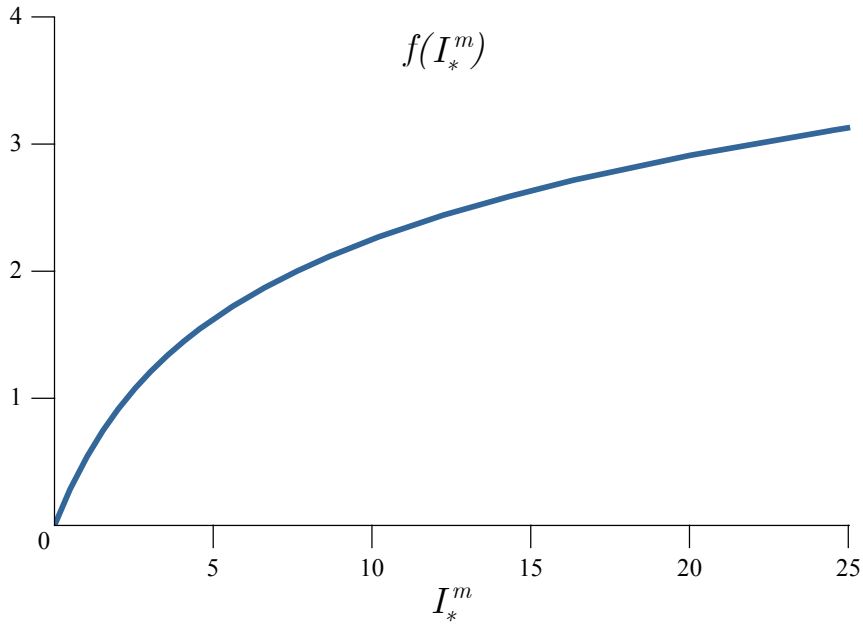

Figure 12: Dimensionless function $f(I_*^m)$ from the analytical solution for daily watercolumn production (3.15) with uniform biomass.

The assumption of an infinitely deep water column is obviously not met in the ocean. However, due to a decline in irradiance with depth, and subsequently production, the contribution of production at any given depth to watercolumn production declines with depth. Due to this, keeping infinity as the limit in the vertical integration for the open ocean is a reasonable assumption and does not lead to grave error, provided the ocean is well mixed.

Typically, the upper ocean layer is well mixed and uniform in properties, therefore the assumption of uniform biomass holds. This layer is historically referred to as the mixed layer [15]. Below the mixed layer biomass tends to be stratified, therefore the assumption of uniform biomass breaks down. We now proceed to demonstrate how to calculate mixed layer production and subsequently watercolumn production with a shifted Gaussian biomass profile.

3.3 MIXED LAYER PRODUCTION

Consider a layer in which active mixing takes place extending from the surface up to depth Z_m (Figure 13), referred to as the **mixed layer depth**. Production taking place in this layer is referred to as the **mixed layer production** ($\mathrm{mg\,C\,m^{-2}}$), stated mathematically as:

$$P_{Z_m,T} = \int_0^{Z_m} \int_0^D P(z,t)\,\mathrm{d}t\,\mathrm{d}z. \tag{3.16}$$

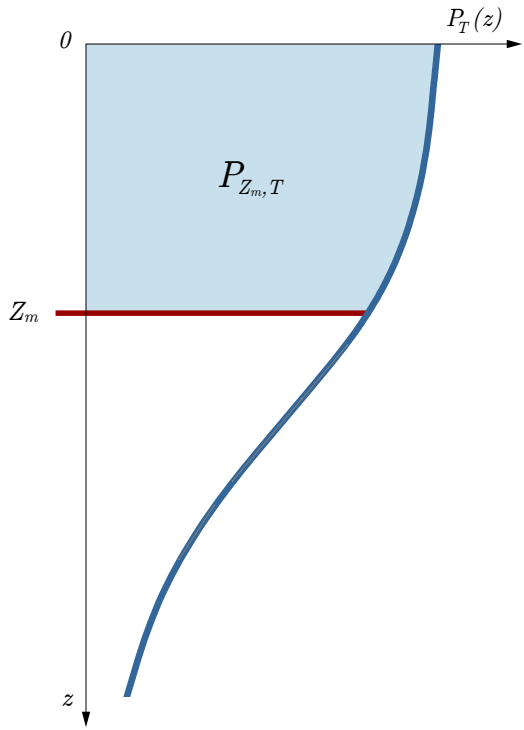

Figure 13: Sketch of mixed layer production $P_{Z_m,T}$ (light blue area) as the vertical integral of the daily production profile $P_T(z)$ (thick blue curve) from the surface $z = 0$ to the mixed layer depth Z_m (red line).

Following (3.7) the previous integral translates to:

$$P_{Z_m,T} = BP_m^B \int_0^{Z_m} \int_0^D \left[1 - \exp\left(-\alpha^B I_0^m \sin(\pi t/D) e^{-Kz}/P_m^B\right)\right] \mathrm{d}t\, \mathrm{d}z, \quad (3.17)$$

where we acknowledge biomass as being uniform in the mixed layer. To solve this integral we first observe the following:

$$P_{Z_m,T} = \int_0^{Z_m} P_T \,\mathrm{d}z = \int_0^{\infty} P_T \,\mathrm{d}z - \int_{Z_m}^{\infty} P_T \,\mathrm{d}z. \quad (3.18)$$

The first integral on the right hand side calculates watercolumn production, whereas the second one calculates production of the layer below Z_m. Given that biomass is uniform, we observe that the second integral can be interpreted as the production of an infinitely deep water column forced with surface irradiance equal to:

$$I(Z_m, t) = I_0^m e^{-KZ_m} \sin(\pi t/D), \quad (3.19)$$

as shown in Figure 14. Noon irradiance at mixed layer depth equals $I_0^m e^{-KZ_m}$. If in place of I_0^m in the expression for surface irradiance (2.9) we use $I_0^m e^{-KZ_m}$, solution (3.15) yields daily production of the layer below Z_m:

$$\int_{Z_m}^{\infty} P_T(z)\, dz = \frac{BP_m^B D}{K} f(I_*^m e^{-KZ_m}), \quad (3.20)$$

again shown in Figure 14, where in place of I_*^m we now have $I_*^m e^{-KZ_m}$. By inserting (3.15) and (3.20) into (3.18) we obtain:

$$P_{Z_m,T} = \frac{BP_m^B D}{K}\left[f\left(I_*^m\right) - f\left(I_*^m e^{-KZ_m}\right)\right], \quad (3.21)$$

as the solution for daily mixed layer production. This solution could have also been found by direct integration of (3.17) following the procedure used to solve for $P_{Z,T}$.

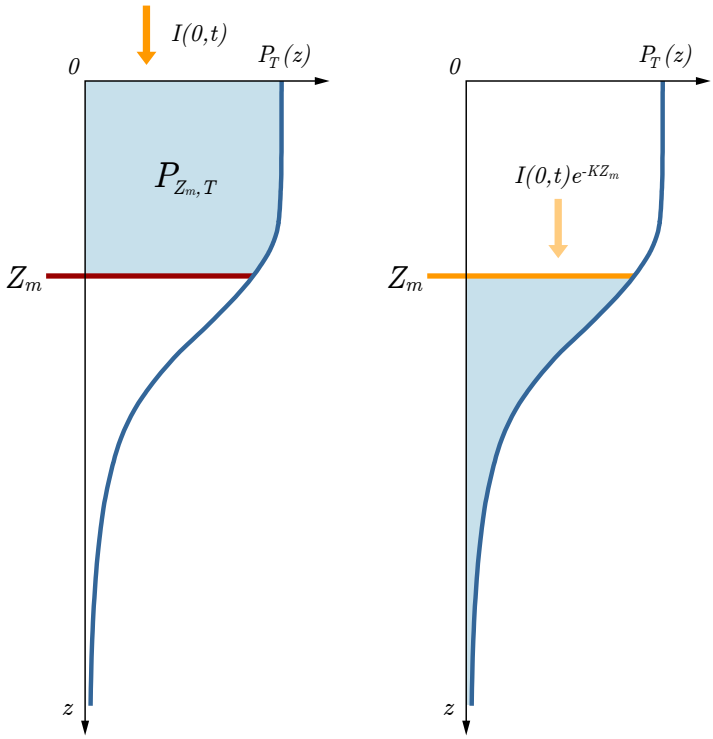

Figure 14: Mixed layer production $P_{Z_m,T}$ depicted as the difference between watercolumn production $P_{Z,T}$, forced by $I(0,t)$ and the production of the portion of the water column below the mixed layer, forced by $I(0,t)e^{-KZ_m}$.

3.4 WATERCOLUMN PRODUCTION WITH A SHIFTED GAUSSIAN BIOMASS PROFILE

The previously presented solution for the normalized production profile (2.33) can be used to solve integral (3.1) in a more general case when the biomass profile is described by the shifted Gaussian function (2.45). The contribution to watercolumn production from the constant term in the Gaussian B_0 is given by (3.15). Therefore, only the contribution from the vertically dependent term has to be found.

Following (3.4) watercolumn production equals the product of the biomass profile and the normalized production profile. Acknowledging the shifted Gasussian (2.45) in place of $B(z)$, we are interested in the solution of the following integral:

$$P_{Z,T} = \int_0^\infty \left[B_0 + \frac{h}{\sigma\sqrt{2\pi}} \exp\left(-\frac{(z-z_m)^2}{2\sigma^2} \right) \right] P_m^B D\, f_z\left(I_*^m e^{-Kz}\right) \mathrm{d}z. \quad (3.22)$$

The contribution to watercolumn production from the uniform biomass term B_0 is already known, namely (3.15), therefore:

$$P_{Z,T} = \frac{B_0 P_m^B D}{K} f(I_*^m) + \int_0^\infty \frac{h}{\sigma\sqrt{2\pi}} \exp\left(-\frac{(z-z_m)^2}{2\sigma^2} \right) P_m^B D f_z\left(I_*^m e^{-Kz}\right) \mathrm{d}z. \quad (3.23)$$

We label the integral on the right hand side as:

$$\Delta P_{Z,T} = \frac{P_m^B D h}{\sigma\sqrt{2\pi}} \int_0^\infty \exp\left(-\frac{(z-z_m)^2}{2\sigma^2} \right) f_z\left(I_*^m e^{-Kz}\right) \mathrm{d}z, \quad (3.24)$$

and it gives the contribution to watercolumn production due to the non-uniformity of the Gaussian profile. For notational simplicity, the f_z function (2.32) will be written as:

$$f_z\left(I_*^m e^{-Kz}\right) = \sum_{n=1}^\infty M(n)\, e^{-(2n-1)Kz} - \sum_{n=1}^\infty N(n)\, e^{-2nKz}, \quad (3.25)$$

where $M(n)$ and $N(n)$ contain the terms that do not depend on z. With this notation, the previous integral becomes:

$$\Delta P_{Z,T} = \frac{P_m^B D h}{\sigma\sqrt{2\pi}} \int_0^\infty \exp\left(-\frac{(z-z_m)^2}{2\sigma^2} \right) \times \left[\sum_{n=1}^\infty M(n)\, e^{-(2n-1)Kz} - \sum_{n=1}^\infty N(n)\, e^{-2nKz} \right] \mathrm{d}z. \quad (3.26)$$

In the obtained expression the sum and the integral can change places:

$$\Delta P_{Z,T} = P_m^B D \frac{h}{\sigma\sqrt{2\pi}} \left[\sum_{n=1}^{\infty} M(n) \int_0^{\infty} \exp\left(-\frac{(z-z_m)^2}{2\sigma^2} - (2n-1)Kz \right) \mathrm{d}z \right.$$
$$\left. - \sum_{n=1}^{\infty} N(n) \int_0^{\infty} \exp\left(-\frac{(z-z_m)^2}{2\sigma^2} - 2nKz \right) \mathrm{d}z \right]. \tag{3.27}$$

The same form of the integral appears in both terms, with a minor difference only in the $2n$ term in the place of $2n-1$ term in the second integral. We will first demonstrate how to solve this integral in case of odd integers, namely:

$$\int_0^{\infty} \exp\left(-\frac{(z-z_m)^2}{2\sigma^2} - (2n-1)Kz \right) \mathrm{d}z. \tag{3.28}$$

As a starting point we rewrite the argument of the exponential function into the following form:

$$-\frac{(z-z_m)^2}{2\sigma^2} - (2n-1)Kz = -\frac{1}{2\sigma^2}(z^2 - 2(z_m - (2n-1)\sigma^2 K)z + z_m^2). \tag{3.29}$$

We then introduce the following label:

$$z_m - (2n-1)\sigma^2 K = z_{2n-1}, \tag{3.30}$$

and after some algebra obtain:

$$\begin{aligned} -\frac{(z-z_m)^2}{2\sigma^2} - (2n-1)Kz &= -\frac{1}{2\sigma^2}(z^2 - 2z_{2n-1}z + z_m^2) \\ &= -\frac{1}{2\sigma^2}(z^2 - 2z_{2n-1}z + z_{2n-1}^2 - z_{2n-1}^2 + z_m^2) \\ &= -\frac{1}{2\sigma^2}(z^2 - 2z_{2n-1}z + z_{2n-1}^2) + \frac{1}{2\sigma^2}(z_{2n-1}^2 - z_m^2) \\ &= -\frac{1}{2\sigma^2}(z - z_{2n-1})^2 + \frac{1}{2\sigma^2}(z_{2n-1}^2 - z_m^2). \end{aligned} \tag{3.31}$$

Inserting this expression back into (3.28) yields:

$$\int_0^\infty \exp\left(-\frac{(z-z_m)^2}{2\sigma^2} - (2n-1)Kz\right) \mathrm{d}z = \exp\left(\frac{z_{2n-1}^2 - z_m^2}{2\sigma^2}\right) \int_0^\infty \exp\left(-\frac{(z-z_{2n-1})^2}{2\sigma^2}\right) \mathrm{d}z. \tag{3.32}$$

Employing the following change of variables:

$$x = \frac{z - z_{2n-1}}{\sqrt{2}\sigma}, \tag{3.33}$$

the integral on the right hand side becomes:

$$\int_0^\infty \exp\left(-\frac{(z-z_{2n-1})^2}{2\sigma^2}\right) \mathrm{d}z = \sqrt{2}\sigma \int_{z_{2n-1}}^\infty \exp(-x^2)\,\mathrm{d}x. \tag{3.34}$$

Now again, the integral on the right hand side of this expression can be split into two integrals:

$$\int_{z_{2n-1}}^\infty \exp(-x^2)\,\mathrm{d}x = \int_{z_{2n-1}}^0 \exp(-x^2)\,\mathrm{d}x + \int_0^\infty \exp(-x^2)\,\mathrm{d}x, \tag{3.35}$$

The solutions to these integrals are given by the error function $\Phi(x)$. Finally the solution to (3.34) is:

$$\int_0^\infty \exp\left(-\frac{(z-z_{2n-1})^2}{2\sigma^2}\right) \mathrm{d}z = \sigma\sqrt{\frac{\pi}{2}}\left(1 + \Phi\left(\frac{z_{2n-1}}{\sqrt{2}\sigma}\right)\right). \tag{3.36}$$

The solution for even integers is identical with the only difference that $2n$ appears in the place of $2n-1$.

At last the overall solution to (3.27) is:

$$\begin{aligned}\Delta P_{Z,T} =& P_m^B D \frac{h}{2} \times \\ & \left[\sum_{n=1}^{\infty} \exp\left(\frac{z_{2n-1}^2 - z_m^2}{2\sigma^2}\right) \frac{2\left(I_*^m\right)^{2n-1}}{\pi\,(2n-1)!} \frac{(2n-2)!!}{(2n-1)!!} \left(1 + \Phi\left(\frac{z_{2n-1}}{\sqrt{2}\sigma}\right)\right) \right. \\ & \left. - \sum_{n=1}^{\infty} \exp\left(\frac{z_{2n}^2 - z_m^2}{2\sigma^2}\right) \frac{\left(I_*^m\right)^{2n}}{(2n)!} \frac{(2n-1)!!}{(2n)!!} \left(1 + \Phi\left(\frac{z_{2n}}{\sqrt{2}\sigma}\right)\right) \right],\end{aligned} \tag{3.37}$$

where the $\Delta P_{Z,T}$ depends explicitly on the values of h, z_m, σ, α^B, P_m^B, I_0^m and D. The derived mathematical expression gives the quantity of carbon assimilated during one day per meter squared of the ocean surface, by phytoplankton distributed vertically according to the shifted Gaussian function (2.45), shown in Figure 9.

The shifted Gaussian is flexible enough to describe various features in the measured chlorophyll profiles and therefore this solution covers a wide range of situations encountered in the field. That flexibility is achieved by altering the parameters of the function, namely: B_0, z_m, σ and h. The disadvantage is that in addition to the six basic quantities: α^B, P_m^B, B_0, I_0^m, D and K, which appear in the canonical solution, the solution for the shifted Gaussian has three more: z_m, σ and h. To apply the solution, the values of these quantities need to be specified.

The solution was derived with the help of the solution for the nominalized production profile (2.33), which reduced (3.1), an integral over time and depth, to an integral over depth alone. This enabled the vertical integration of (3.22) to be carried out. However, there is a deeper connection between the analytical solution for watercolumn production with uniform biomass (3.15) and the production profile (2.33), which makes this possible. We now explore this connection and provide another way to derive the solution for the production profile, which will subsequently be used to derive a general solution for watercolumn production.

3.5 ALTERNATIVE DERIVATION OF THE PRODUCTION PROFILE

We begin by considering daily production in the layer extending from Z_1 to Z_2, such that $Z_1 < Z_2$, assuming uniform biomass (Figure 15). According to the notation used thus far, the production of an arbitrary layer that extends between depths Z_1 and Z_2 is equal to:

$$P_{Z_1,Z_2,T} = \int_{Z_1}^{Z_2} P_T(z)\,\mathrm{d}z = \int_{Z_1}^{\infty} P_T(z)\,\mathrm{d}z - \int_{Z_2}^{\infty} P_T(z)\,\mathrm{d}z. \tag{3.38}$$

Following a similar reasoning to the one presented in the derivation of the solution for mixed layer production, we first observe that light at depth Z_i equals $I(Z_i,t) = I_0^m e^{-KZ_i}\sin(\pi t/D)$. Therefore, if in place of Z_m in expression (3.20) we use Z_i, the solution still holds and we have:

$$\int_{Z_i}^{\infty} P_T(z)\,dz = \frac{BP_m^B D}{K} f(I_*^m e^{-KZ_i}), \tag{3.39}$$

where the $f(I_*^m e^{-Kz})$ reads:

$$\begin{aligned} f(I_*^m e^{-Kz}) = &\sum_{n=1}^{\infty} \frac{2\left(I_*^m e^{-Kz}\right)^{2n-1}}{\pi\,(2n-1)\,(2n-1)!}\frac{(2n-2)!!}{(2n-1)!!} \\ &- \sum_{n=1}^{\infty} \frac{\left(I_*^m e^{-Kz}\right)^{2n}}{2n\,(2n)!}\frac{(2n-1)!!}{(2n)!!}, \end{aligned} \tag{3.40}$$

and should not be confused with the f_z function from the solution for daily normalized production (2.32). By inserting (3.39) into (3.38) we get:

$$P_{Z_1,Z_2,T} = \frac{BP_m^B D}{K}\left[\, f\left(I_*^m e^{-KZ_1}\right) - f\left(I_*^m e^{-KZ_2}\right)\,\right], \tag{3.41}$$

According to expression (3.41), the solution for production of an arbitrary layer is equal to the production below depth Z_1 minus the production below depth Z_2. It is easy to check that in the case of $Z_1 = 0$ and $Z_2 = \infty$,

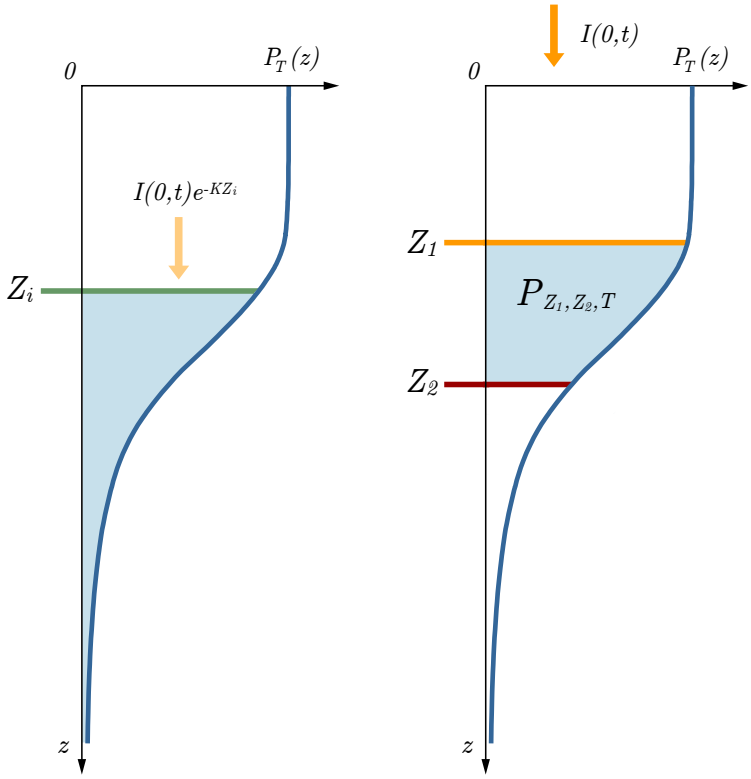

Figure 15: Production of a finite layer, from Z_1 to Z_2, depicted as the difference between watercolumn production below Z_1, forced by $I(0,t)e^{-KZ_1}$ and the production of the portion of the water column below Z_2, forced by $I(0,t)e^{-KZ_2}$

from (3.41) we get (3.15). Subsequently, by relabelling the depths Z_1 and Z_2 as:

$$\Delta Z = Z_2 - Z_1, \qquad z = Z_1, \tag{3.42}$$

we get:

$$P_{z,z+\Delta Z,T} = \frac{BP_m^B D}{K}\left[f\left(I_*^m e^{-Kz}\right) - f\left(I_*^m e^{-K(z+\Delta Z)}\right)\right]. \tag{3.43}$$

This expression gives the production in the layer extending from z to $z + \Delta Z$ (Figure 16).

Dividing by the layer thickness gives the average layer production per unit volume: where B is the uniform biomass in the layer. Since the biomass is uniform, the entire expression divided by B gives the average normalized production per unit volume:

$$\langle P_T^B \rangle = \frac{P_m^B D}{K} \left[\frac{f\left(I_*^m e^{-Kz}\right) - f\left(I_*^m e^{-K(z+\Delta Z)}\right)}{\Delta Z} \right]. \tag{3.44}$$

Production of each layer can be calculated separately and the biomass can vary between layers. For the accuracy of this solution, it is not necessary for the biomass to be equal in each layer. In the limit of $\Delta Z \to 0$, average normalized production $\langle P_T^B \rangle$ becomes $P_T^B(z)$ (Figure 16) and the previous expression becomes:

$$P_T^B(z) = -\frac{P_m^B D}{K} \lim_{\Delta Z \to 0} \frac{f\left(I_*^m e^{-K(z+\Delta Z)}\right) - f\left(I_*^m e^{-Kz}\right)}{\Delta Z}, \tag{3.45}$$

where the negative sign is simply extracted from the expression under the limit. The limit in the previous expression corresponds to the z derivative of the $f\left(I_*^m e^{-Kz}\right)$ function (3.40):

$$P_T^B(z) = -\frac{P_m^B D}{K} \frac{\mathrm{d}}{\mathrm{d}z} f\left(I_*^m e^{-Kz}\right). \tag{3.46}$$

Multiplying $1/K$ and $\mathrm{d}f/\mathrm{d}z$ we define $f_z\left(I_*^m e^{-Kz}\right)$ as:

$$f_z\left(I_*^m e^{-Kz}\right) = -\frac{1}{K} \frac{\mathrm{d}}{\mathrm{d}z} f\left(I_*^m e^{-Kz}\right). \tag{3.47}$$

With this definition, expression (3.46) becomes:

$$P_T^B(z) = P_m^B D\, f_z\left(I_*^m e^{-Kz}\right), \tag{3.48}$$

where $f_z\left(I_*^m e^{-Kz}\right)$ is obtained by differentiating (3.40) by z and dividing by K. By comparison with (2.33) we observe the two expressions are identical. Therefore, a mathematical relation existis between the f function (3.40) and the f_z function (2.32). Historically, this was the original derivation of the f_z function [32], hence the $_z$ in the subscript.

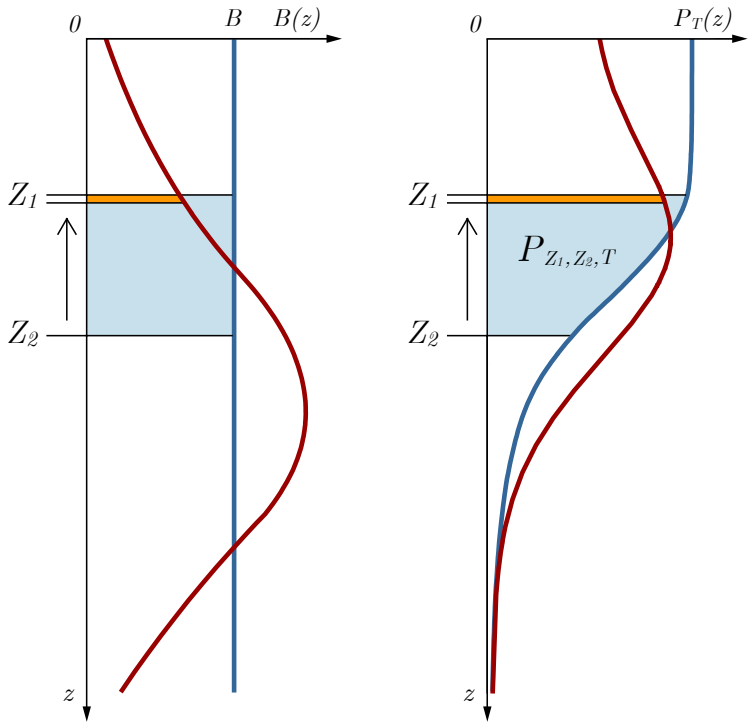

Figure 16: Illustration of the main idea in the alternative derivation of the production profile. The left image shows the biomass profiles: uniform (blue line) and non-uniform (red curve). The right figure shows the production profiles: the production profile for the uniform biomass profile (blue curve) and the production profile for the non-uniform biomass profile (red curve).

3.6 GENERAL SOLUTION

The derived relation between the f and the f_z functions enables us to find a general solution for watercolumn production in case of an arbitrary biomass profile, under the assumption that $B(z)$ is a continuous function. We start with (3.4) which we restate here for clarity:

$$P_{Z,T} = \int_0^\infty B(z) P_T^B(z)\, \mathrm{d}z. \tag{3.49}$$

By inserting (3.46) we obtain the following:

$$P_{Z,T} = -\frac{P_m^B D}{K} \int_0^\infty B(z) \frac{\mathrm{d}}{\mathrm{d}z} f\left(I_*^m e^{-Kz}\right) \mathrm{d}z. \tag{3.50}$$

Further on, proceeding with integration by parts yields:

$$P_{Z,T} = \frac{P_m^B D}{K} \left(B(0) f\left(I_*^m\right) + \int_0^\infty \frac{\mathrm{d}B(z)}{\mathrm{d}z} f\left(I_*^m e^{-Kz}\right) \mathrm{d}z \right), \tag{3.51}$$

where the following condition was used:

$$B(\infty) f(I_*^m e^{-K\infty}) = 0. \tag{3.52}$$

The derived expression (3.51) is a formal relation between the canonical solution (3.15) and any solution for watercolumn production with stratified biomass. The effect of surface biomass $B(0)$ on the magnitude of watercolumn production $P_{Z,T}$ is clearly emphasised: surface biomass is a leading factor in $P_{Z,T}$. The significance of this result is emphasized given that surface biomass is readily accessible to satellite measurement. Therefore, if the remotely-sensed surface biomass is precise, and assuming the remaining parameters of the model are characteristic of the ocean region in question, the error in the estimated watercolumn production arises solely as a consequence of the error in estimating the biomass profile, which is inaccessible to remote sensing and has to be assigned based on prior information [43].

As for the second term, it gives the contribution arising from the shape of the biomass profile. For an increase in biomass with depth, $\mathrm{d}B(z)/\,\mathrm{d}z > 0$, this contribution is positive. For a decline in biomass with depth, $\mathrm{d}B(z)/\,\mathrm{d}z < 0$, this contribution is negative. The differential change in biomass with depth $\mathrm{d}B(z)/\,\mathrm{d}z$ is multiplied by the $f(I_*^m e^{-Kz})$ function. The product $\mathrm{d}B(z) f(I_*^m e^{-Kz})$ gives the production that would occur below depth z in case the biomass below z were equal to $\mathrm{d}B(z)$. Total contribution from all infinitesimal changes in $B(z)$ is taken into account by the integral on the right hand side of (3.51). With increase in depth, the contribution from biomass variation decreases, simply because production declines with increasing depth (2.38).

3.7 BIOOPTICAL FEEDBACK

Thus far in calculating watercolumn production we have treated K as a constant independent of B. We now explore the effect of acknowledging K as a function of B. In this case, biomass too causes light attenuation. We only consider the case of uniform biomass and model the attenuation coefficient as a simple linear relation (2.11), restated here:

$$K = K_w + k_b B. \tag{3.53}$$

When the biomass is vertically uniform, solution (3.15) also applies to the case of the attenuation coefficient given by the previous expression and we have:

$$P_{Z,T} = \frac{B}{K_w + k_b B} P_m^B D f(I_*^m). \tag{3.54}$$

Now the dependence of $P_{Z,T}$ on biomass is not linear, which is a consequence of light attenuation caused by biomass. To analyse the dependence of $P_{Z,T}$ on biomass, we simply take the derivative of the resulting expression with respect to biomass:

$$\frac{\partial P_{Z,T}}{\partial B} = \frac{K_w}{(K_w + k_b B)^2} P_m^B D f(I_*^m). \tag{3.55}$$

If there is an upper limit on watercolumn production, with respect to biomass, the derivative of $P_{Z,T}$ should vanish for high values of biomass. That this is indeed the case can be verified easily by calculating the limit of the previous expression in the case when biomass tends to infinity:

$$\lim_{B \to \infty} \frac{\partial P_{Z,T}}{\partial B} = 0. \tag{3.56}$$

The obtained expression shows that the increase in production does not always follow linearly the increase in biomass, but production becomes limited. With the growth of biomass, light attenuation increases and the biomass itself prevents higher levels of production. At high biomass values, the attenuation coefficient can be written as [47]:

$$K \approx k_b B. \tag{3.57}$$

The upper limit of water column production in this case reads:

$$P_{Z,T} = P_m^B D f(I_*^m) \lim_{B\to\infty} \left(\frac{B}{K_w + k_b B} \right) = \frac{P_m^B D}{k_b} f(I_*^m). \tag{3.58}$$

Now the phytoplankton itself significantly limits the penetration of light through the water column and consequently limits the production of the water column. This effect is expressed only for high values of biomass, more precisely high concentrations of phytoplankton. At low phytoplankton concentrations, watercolumn production $P_{Z,T}$ is well approximated using only K_w for the attenuation coefficient. With increasing biomass, production increases, but so does the attenuation coefficient $K_w + k_b B$. Finally, the influence of light attenuation caused by a high concentration of phytoplankton dominates and the upper limit of production equals (3.58).

3.8 RELATION TO GROWTH MODELS

In the case of a mixed layer, an exact expression relating biomass accumulation and water column production can be derived. Let us consider a mixed layer of depth Z_m. To simplify notation we introduce the following label for the **total biomass in the mixed layer** ($\mathrm{mg\,Chl\,m^{-2}}$):

$$B_{Z_m}(t) = \int_0^{Z_m} B(z,t)\,\mathrm{d}z. \tag{3.59}$$

At initial time we assume biomass in the mixed layer as uniform:

$$B_{Z_m}(0) = B_0 Z_m. \tag{3.60}$$

Let us assume that mixed layer production $P_{Z_m}(t)$, given as:

$$P_{Z_m}(t) = \int_0^{Z_m} P(z,t)\,\mathrm{d}z, \tag{3.61}$$

leads to newly synthesized biomass. Let us also assume that the newly synthesized mixed layer biomass at time t is redistributed through the

mixed layer during a time interval Δt, so that no stratification in biomass occurs at $t + \Delta t$. Mixed layer biomass at time $t + \Delta t$ is now:

$$B_{Z_m}(t + \Delta t) = B_{Z_m}(t) + \frac{1}{\chi} P_{Z_m}(t) \Delta t. \tag{3.62}$$

Due to vertical uniformity in biomass, instantaneous mixed layer production equals:

$$P_{Z_m}(t) = \frac{1}{Z_m} B_{Z_m}(t) P^B_{Z_m}(t), \tag{3.63}$$

so that for biomass at time $t + \Delta t$ we have:

$$B_{Z_m}(t + \Delta t) = B_{Z_m}(t) + \frac{1}{\chi Z_m} P^B_{Z_m}(t) B_{Z_m}(t) \Delta t. \tag{3.64}$$

In the limit of $\Delta t \to 0$, implying instantaneous mixing of newly synthesized biomass, the previous equation becomes:

$$\frac{\partial}{\partial t} B_{Z_m}(t) = \frac{1}{\chi Z_m} P^B_{Z_m}(t) B_{Z_m}(t). \tag{3.65}$$

The solution to this equation at time D is:

$$B_{Z_m}(D) = B_{Z_m}(0) \exp\left(\frac{1}{\chi Z_m} \int_0^D P^B_{Z_m}(t) \, \mathrm{d}t \right). \tag{3.66}$$

The integral in the exponential function is given in (3.21):

$$\int_0^D P^B_{Z_m}(t) \, \mathrm{d}t = \frac{P^B_m D}{K} \Big[f\big(I^m_*\big) - f\big(I^m_* e^{-KZ_m}\big) \Big]. \tag{3.67}$$

Taking into account the initial condition (3.60) along with the previous expression, the solution to (3.65) reads:

$$B_{Z_m}(D) = B_0 Z_m \exp\left[\frac{P^B_m D}{\chi Z_m K} \left[f(I^m_*) - f(I^m_* e^{-KZ_m}) \right] \right]. \tag{3.68}$$

Mixed layer production is now the difference between $B_Z(D)$ and $B_Z(0)$ multiplied by χ:

$$P_{Z_m,T} = \chi B_0 Z_m \left[\exp \left[\frac{P_m^B D}{\chi Z_m K} \left(f(I_*^m) - f(I_*^m e^{-KZ_m}) \right) \right] - 1 \right]. \quad (3.69)$$

The implicit assumption worth stating here is that all production goes to newly sensitized biomass. If this were not the case an additional loss term should be added to the equation, which will be done if later chapters.

3.9 PROBLEMS

1. Build a numerical model for calculating watercolumn production (3.1). First, split the water column into layers, each of Δz depth. Second, split daylength D into discrete time intervals, each of Δt duration. Use all the other assumptions as in the analytical model. Now watercolumn production is given as:

$$P_{Z_m,T} = \sum_{n=1}^{N} \sum_{j=1}^{J} P_n^j \Delta t \Delta z, \tag{3.70}$$

where we have labelled production at depth z_n and time t_j as P_n^t:

$$P_n^t = P(z_n, t_j) = B(n\Delta z)\left[1 - \exp\left(- \alpha^B I_0^m \sin(\pi j \Delta t / D) e^{-Kn\Delta z} \Big/ P_m^B \right)\right], \tag{3.71}$$

where $z_n = n\Delta z$, with $n = 1, 2, ..., N$ and $t_j = j\Delta t$, with $j = 1, 2, ..., J$. Test the numerical model by calculating watercolumn production for uniform biomass. Plot the numerical solution as a function of dimensionless irradiance I_*^m in the same manner as the canonical solution shown in Figure 12.

2. Use the model from the previous problem with different photosynthesis irradiance functions (1.27, 1.28, 1.29, 1.30, 1.31). Set biomass as uniform and plot the obtained numerical solutions together with the canonical solution. Calculate the difference between the canonical solution and the numerical ones.

3. Use the model from the first problem to calculate wattercolumn production with the shifted Gaussian biomass profile (2.45). Fix all the Gaussian parameters apart from the depth of the maximum z_m, which you vary. Calculate watercolumn production as a function of z_m, by varying it from $z_m = 0$ to $z_m = 200$.

4. Use the model from the first problem with the shifted Sigmoid biomass profile (2.48). Set the mid point z_m equal to the mixed layer depth Z_m and explore the behaviour of the numerical solution for watercolumn production by varying σ. Observe the model behaviour as $\sigma \to \infty$. Compare the numerical solution to the analytical solution for mixed layer production (3.21) with a fixed $z_m = Z_m$ and a sequence of values for σ.

5. Plot the solution for mixed layer production (3.21) as a function of mixed layer depth. Calculate the average mixed layer production $P_{Z_m,T}/Z_m$ and plot it, also as a function of mixed layer depth. Discuss the difference between the two plots.

6. Calculate watercolumn production by acknowledging the dependence of the attenuation coefficient on biomass in the light penetration model (2.11). Employ uniform biomass, the shifted Gaussian biomass profile and the shifted Sigmoid biomass profile. Calculate production by varying B_0 from $B_0 = 0.01$ mg Chl m^{-3} to $B_0 = 10$ mg Chl m^{-3}.

7. Build a numerical model that solves equation (3.65). Explore how the biomass evolves over time with two models for the attenuation coefficient, first $K = K_w$ and second $K = K_w + k_B B(t)$. Plot biomass as a function of time for both cases.

4

MATRIX MODEL

The previously presented model of primary production and analytical solutions form a closed whole. With the knowledge of the values of the model parameters, daily production profile and daily watercolumn production can be calculated. The common limitation of the analytical solutions is the simple treatment of surface irradiance and the vertical uniformity of photosynthetic parameters, which somewhat limits the range of applicability of the model.

Also, the solutions are only valid for the exponential photosynthesis irradiance function [60, 42]. Other functions are also used in practice, but no analytical solutions for the daily production profile or daily watercolumn production are known for them. Therefore, the application of the model in more complex situations and with other photosynthesis irradiance functions is naturally realized by numerical methods. This chapter describes the discretization of the analytical model and the development of the matrix formalism for calculating the daily production profile and daily watercolumn production.

In a numerical model continuous time and continuous space become discrete. Consequently, integrals become sums and derivatives are expressed algebraically. In matrix notation these sums become matrix products, which are simpler to handle, both mathematically and numerically when implementing the model. The matrix equations are concise and the notation elegantly packs rather long algebraic expressions into short ones. This adds clarity to the model structure. It also simplifies model implementation.

4.1 DISCRETIZATION OF THE ANALYTICAL MODEL

Let the numerical model have N vertical levels at depths z_n, indexed by n, and J time intervals indexed by j. The depth z is positive downwards and n increases with depth so that:

$$z_n < z_{n+1}, \tag{4.1}$$

holds, as shown in Figure 17, with $n = 1, 2, ..., N$. The water column is of depth Z, such that the depth interval between two consecutive model levels is equal to:

$$\Delta z = \frac{Z}{N}. \tag{4.2}$$

The first model level is set to:

$$z_1 = \frac{\Delta z}{2}. \tag{4.3}$$

Each time interval is equal to:

$$\Delta t = \frac{D}{J}, \tag{4.4}$$

such that discrete time t_j is defined as:

$$t_j = j\Delta t, \tag{4.5}$$

with $j = 1, 2, ..., J$. The described spatial and temporal discretization enables us to rewrite the analytical expressions for the model in numerical form. We begin with the discretization of the expression for daily production (2.5) at depth z_n:

$$P_T(z_n) \approx B(z_n) \sum_{j=1}^{J} p^B\big(I(z_n, t_j)\big)\Delta t. \tag{4.6}$$

The right hand side of this expression uses biomass at depth z_n (Figure 17) and approximates daily production as a sum, rather than as an integral, like in (2.5). This sum can be denoted by $P_{n,T}$. In the limit of Δt going to zero, we have:

$$\lim_{\Delta t \to 0} P_{n,T} = P_T(z_n). \tag{4.7}$$

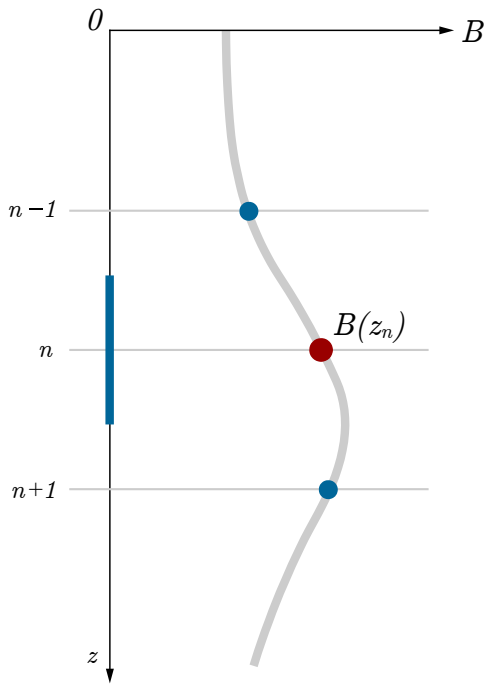

Figure 17: Vertical discretization of the biomass profile in the vicinity of depth z_n. The distance between two arbitrary vertical levels Δz need not be equal. Biomass $B(z_n)$ (red dot) represents the biomass for the entire Δz layer centred around z_n (blue line). The same holds for the vertical discretization of the production profile (not shown).

The sum on the right side of expression (4.6) approximates daily normalized production $P_T^B(z_n)$ and is denoted here by $P_{n,T}^B$:

$$P_{n,T}^B = \sum_{j=1}^{J} p^B\big(I(z_n, t_j)\big)\Delta t. \tag{4.8}$$

In this case also, in the limit when Δt tends to zero, it holds:

$$\lim_{\Delta t \to 0} P_{n,T}^B = P_T^B(z_n). \tag{4.9}$$

Therefore, both numerical expressions converge to the analytical ones in the limit of small Δt, as expected. Hence, the accuracy of the numerical calculations for a given depth z_n is dictated, and can be improved by, decreasing Δt.

Next, to numerically calculate watercolumn production $P_{Z,T}$, expression (3.1) needs to be discretized. Its discretization reads:

$$P_{Z,T} \approx \sum_{n=1}^{N} B(z_n) \left[\sum_{j=1}^{J} p^B\big(I(z_n, t_j)\big) \Delta t \right] \Delta z. \tag{4.10}$$

The double sum on the right hand side of the expression (4.10) approximates daily watercolumn production $P_{Z,T}$. In the limit when both Δt and Δz tend to zero, (4.10) goes to (3.1).

The model can also be amended such that the vertical intervals are not equal. The reason for doing this is the fact that in field work primary production measurements are often not distributed at equal depths from each other. Therefore, a given measurement is representative of a layer extending from halfway between the level, above the given level, to halfway between the given level, to the level below. Also, when the model is used to compare measurements with model predictions, setting model depths equal to the measurement depths is preferable. In this case each level z_n is assigned a depth interval Δz_n:

$$\Delta z_n = \frac{z_{n+1} - z_{n-1}}{2}, \tag{4.11}$$

for $n = 2, 3, ..., N-1$. The first vertical increment is set to:

$$\Delta z_1 = \frac{z_1 + z_2}{2}, \tag{4.12}$$

and the last one to:

$$\Delta z_N = z_N - z_{N-1}. \tag{4.13}$$

Having described the discretization of the analytical model, we now proceed to present the matrix formalism for calculating the daily production profile and watercolumn production. The formalism holds for both arbitrary and uniform vertical increments, but for pedagogical reasons will be presented with with uniform vertical increments.

4.2 MATRIX FORMALISM

With a few additional definitions, the previous sums can be concisely written using matrix formalism. We begin by first observing that irradiance at the depth z_n at the time t_j can be denoted simply as:

$$I_{nj} = I\left(z_n, t_j\right). \tag{4.14}$$

The **irradiance matrix I** (dimension $N \times J$) is defined as a matrix whose elements are I_{nj} (Figure 18). Therefore, irradiance conditions of the entire model are contained in the irradiance matrix:

$$\mathbf{I} = \begin{bmatrix} I_{11} & I_{12} & \dots & I_{1j} & \dots & I_{1J} \\ I_{21} & I_{22} & \dots & I_{2j} & \dots & I_{2J} \\ \vdots & \vdots & \ddots & \vdots & \ddots & \vdots \\ I_{n1} & I_{n2} & \dots & I_{nj} & \dots & I_{nJ} \\ \vdots & \vdots & \ddots & \vdots & \ddots & \vdots \\ I_{N1} & I_{N2} & \dots & I_{Nj} & \dots & I_{NJ} \end{bmatrix}. \tag{4.15}$$

Each row of the irradiance matrix is equal to the time series of irradiance at depth z_n, while each column is equal to the vertical profile of irradiance at time t_j. Elements of the irradiance matrix can be calculated with any optical model. For example, by using (2.13) we have:

$$I_{nj} = I_{0j} \exp\left(-K z_n\right), \tag{4.16}$$

where the surface irradiance now is given as:

$$I_{0j} = I_0\left(t_j\right). \tag{4.17}$$

Unlike the idealized surface irradiance model (2.9), surface irradiance here I_{0j} can now be any function, even discontinuous.

Next, we observe that when an individual element of the irradiance matrix I_{nj} is taken as an argument of the photosynthesis irradiance function we obtain normalized production at depth z_n and time t_j, which we label p^B_{nj}:

$$p^B_{nj} = p^B\left(I_{nj}\right). \tag{4.18}$$

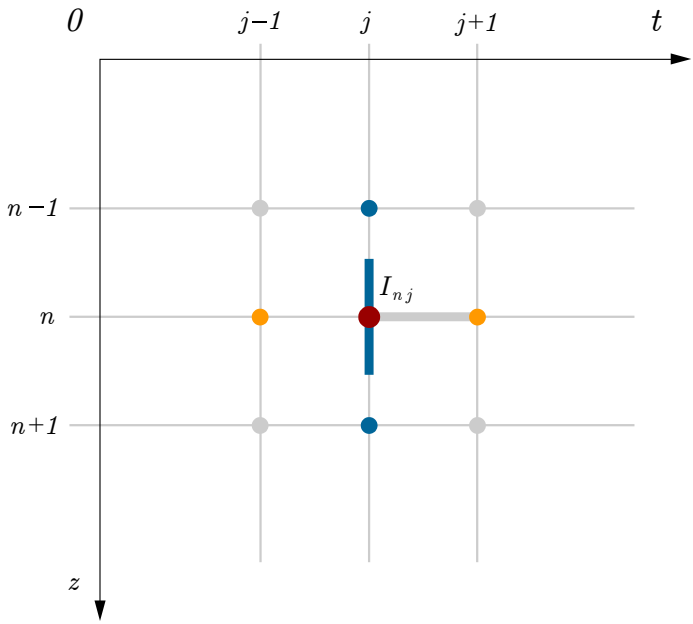

Figure 18: Sketch of the irradiance matrix $\mathbf{I}$ which collects irradiance values at depths z_n and times t_j, such that its elements are $I_{nj} = I\left(z_n, t_j\right)$ (red point). In the (z,t) plane the blue line equals Δz and the grey line equals Δt.

Subsequently, **normalized production matrix** $\mathbf{P}^B$ (dimension $N \times J$) is defined as a matrix whose elements are p^B_{nj} (Figure 19):

$$\mathbf{P}^B = \begin{bmatrix} p^B_{11} & p^B_{12} & \cdots & p^B_{1j} & \cdots & p^B_{1J} \\ p^B_{21} & p^B_{22} & \cdots & p^B_{2j} & \cdots & p^B_{2J} \\ \vdots & \vdots & \ddots & \vdots & \ddots & \vdots \\ p^B_{n1} & p^B_{n2} & \cdots & p^B_{nj} & \cdots & p^B_{nJ} \\ \vdots & \vdots & \ddots & \vdots & \ddots & \vdots \\ p^B_{N1} & p^B_{N2} & \cdots & p^B_{Nj} & \cdots & p^B_{NJ} \end{bmatrix}. \tag{4.19}$$

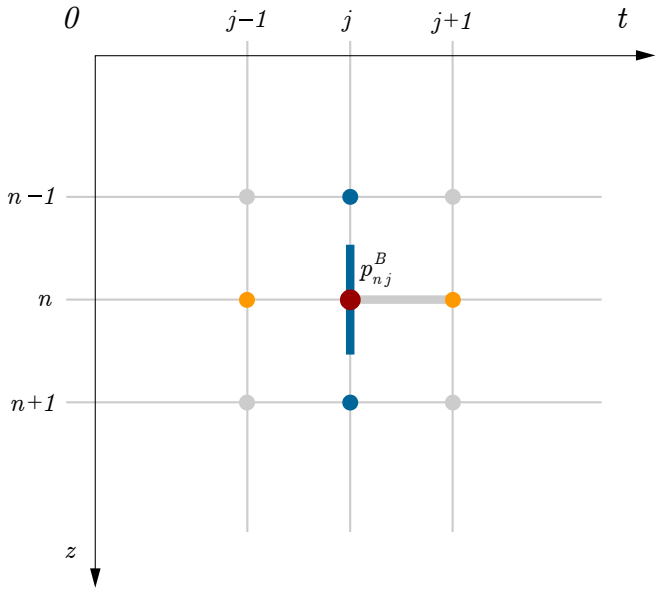

Figure 19: Sketch of the normalized production matrix $\mathbf{P}^B$ which collects normalized production values at depth z_n and time t_j, such that its elements are $p^B_{nj} = p^B(I_{nj})$. In the (z,t) plane the blue line equals Δz and the orange line equals Δt.

Each row of this matrix is equal to the time series of normalized production at depth z_n, while each column is equal to the vertical profile of normalized production at time t_j. To calculate production at depth z_n and time t_j we simply multiply each row of this matrix by the corresponding biomass at that depth:

$$P(z_n, t_j) = B\,(z_n)\; p^B\,(I_{nj})\,, \tag{4.20}$$

This expression is a discrete version of expression (2.3), now with biomass independent of time. To write the previous expression in matrix form we define the **biomass matrix B** (dimension $N \times N$) as a diagonal matrix whose elements are equal to:

$$b_{nm} = \delta_{nm} B(z_n), \tag{4.21}$$

where δ_{nm} is the Kronecker delta symbol. Written out in matrix notation the biomass matrix **B** reads:

$$\mathbf{B} = \begin{bmatrix} B(z_1) & 0 & \dots & 0 \\ 0 & B(z_2) & \dots & 0 \\ \vdots & \vdots & \ddots & \vdots \\ 0 & 0 & \dots & B(z_N) \end{bmatrix}. \tag{4.22}$$

Now, in analogy to how production at depth is calculated by multiplying biomass with normalized production, we extend the concept to matrix form in the following manner. We recognize that the matrix product of the biomass matrix with the normalized production matrix gives the **production matrix P** (dimension $N \times J$) :

$$\mathbf{P} = \mathbf{B}\mathbf{P}^B, \tag{4.23}$$

whose elements are:

$$p_{nj} = B(z_n)p^B(I_{nj}). \tag{4.24}$$

Each row of the production matrix is equal to the time series of production at depth z_n, while each column is equal to the vertical profile of production at time t_j. Therefore, the production matrix contains all the information needed to calculate watercolumn production and the daily production profile numerically. To carry out these calculations in matrix form we proceed to define another two matrices.

By defining the **time matrix** $\boldsymbol{\tau}$ (dimension $J \times 1$), which has all its elements equal and given as:

$$\tau_j = \Delta t, \tag{4.25}$$

time integration it is simply carried out as:

$$\mathbf{p}_T = \mathbf{P}\boldsymbol{\tau}, \tag{4.26}$$

and thus a **discrete daily production profile** $\mathbf{p}_T$ is obtained (dimension $N \times 1$), whose elements are equal to (4.6). The **discrete normalized daily production profile** $\mathbf{p}_T^B$ (dimension $N \times 1$) is obtained simply as:

$$\mathbf{p}_T^B = \mathbf{P}^B\boldsymbol{\tau}, \tag{4.27}$$

whose elements are equal to (4.8). Having a model for the discrete production profile, we can now move forward and calculate watercolumn production $P_{Z,T}$ in line with the double sum (4.10). To achieve this, vertical integration of $\mathbf{p}_T$ is required. The **vertical increments matrix** $\boldsymbol{\zeta}$ (dimension $1 \times N$) is defined as a matrix whose elements are equal to the vertical increment Δz around the vertical level z_n, as defined in (4.2):

$$\zeta_n = \Delta z. \tag{4.28}$$

For $\boldsymbol{\zeta}$ the following holds:

$$\sum_{n=1}^{N} \zeta_n = Z, \tag{4.29}$$

where Z is the depth of the water column. Finally, daily watercolumn production is now given as:

$$P_{Z,T} = \boldsymbol{\zeta} \mathbf{P} \boldsymbol{\tau}. \tag{4.30}$$

The given expression is analogous to expression (3.1) and is equal to its numerical counterpart (4.10). Expressions (4.26) and (4.30) are two fundamental relations of the matrix model for daily primary production. The two can be combined into the following expression for daily watercolumn production:

$$P_{Z,T} = \boldsymbol{\zeta} \mathbf{p}_T. \tag{4.31}$$

Written in this form it is obvious that the vertical increments matrix $\boldsymbol{\zeta}$ is in fact a row vector. It enables vertical summation of the daily production profile $\mathbf{p}_T$ to be carried out simply as a matrix product of $\boldsymbol{\zeta}$ with it. In the same manner the time matrix $\boldsymbol{\tau}$ is a column vector, which enables the summation over time to be carried out simply as a matrix product in (4.26).

All of the above matrix expression are mathematically equivalent to the numerical form of the basic integrals, such as (2.5) and (3.1), in the limits of small Δt and Δz_n. To demonstrate in more detail that these matrix expressions translate to the their numerical counterparts, (4.6) and (4.10), we now present a detailed derivation of the matrix model.

4.3 DERIVATION OF THE MATRIX MODEL

The expression for $P^B_{n,T}$ (4.8) can be written as a scalar product of two vectors:

$$P^B_{n,T} = \begin{bmatrix} p^B_{n1} & p^B_{n2} & \dots & p^B_{nT} \end{bmatrix} \begin{bmatrix} \Delta t & \Delta t & \dots & \Delta t \end{bmatrix}^T, \tag{4.32}$$

where:

$$p^B_{nj} = p^B\big(I(z_n, t_j)\big). \tag{4.33}$$

The given expression is valid for each vertical level z_n. Collecting p^B_{nj} elements into a matrix yields:

$$\begin{bmatrix} P^B_{1,T} \\ P^B_{2,T} \\ \vdots \\ P^B_{n,T} \\ \vdots \\ P^B_{N,T} \end{bmatrix} = \begin{bmatrix} p^B_{11} & p^B_{12} & \dots & p^B_{1j} & \dots & p^B_{1T} \\ p^B_{21} & p^B_{22} & \dots & p^B_{2j} & \dots & p^B_{2T} \\ \vdots & \vdots & \ddots & \vdots & \ddots & \vdots \\ p^B_{n1} & p^B_{n2} & \dots & p^B_{nj} & \dots & p^B_{nT} \\ \vdots & \vdots & \ddots & \vdots & \ddots & \vdots \\ p^B_{N1} & p^B_{N2} & \dots & p^B_{Nj} & \dots & p^B_{NT} \end{bmatrix} \begin{bmatrix} \Delta t \\ \Delta t \\ \vdots \\ \Delta t \\ \vdots \\ \Delta t \end{bmatrix}. \tag{4.34}$$

The given expression can be abbreviated as:

$$\mathbf{p}^B_T = \mathbf{P}^B \boldsymbol{\tau}, \tag{4.35}$$

where $\mathbf{p}^B_T$ is the normalized discrete production profile, $\boldsymbol{\tau}$ is the time matrix, and $\mathbf{P}^B$ is the normalized production matrix. Further, using (4.8), the expression (4.10) can be written as:

$$P_{Z,T} \approx \sum_{n=1}^{N} B(z_n) P^B_{n,T} \Delta z, \tag{4.36}$$

which is equal to the following dot product:

$$P_{Z,T} = \begin{bmatrix} \Delta z & \Delta z & \dots & \Delta z \end{bmatrix} \begin{bmatrix} B(z_1)P^B_{n,T} & B(z_2)P^B_{n,T} & \dots & B(z_N)P^B_{N,T} \end{bmatrix}^T. \tag{4.37}$$

The elements of the rightmost vector in the given expression correspond to the daily production at the vertical level z_n:

$$P_{n,T} = B(z_n) P^B_{n,T}. \tag{4.38}$$

Using the biomass matrix $\mathbf{B}$, defined in the previous subsection as a diagonal matrix with biomass values on the diagonal, the previous expression can be written for each vertical level and summarized as:

$$\mathbf{p}_T = \mathbf{B}\mathbf{p}^B_T, \tag{4.39}$$

where $\mathbf{p}_T$ is the discrete production profile. Inserting (4.35) for $\mathbf{p}^B_T$ yields:

$$\mathbf{p}_T = \mathbf{B}\mathbf{P}^B\boldsymbol{\tau}. \tag{4.40}$$

The given expression corresponds to the right vector in expression (4.37), while the left vector in expression (4.37) corresponds to the row matrix of vertical increments $\boldsymbol{\zeta}$. Now, daily watercolumn production as expressed by (4.37) can be written in matrix form as:

$$P_{Z,T} = \boldsymbol{\zeta}\mathbf{B}\mathbf{P}^B\boldsymbol{\tau}. \tag{4.41}$$

Expanded, the matrix product $\mathbf{B}\mathbf{P}^B$ reads:

$$\mathbf{B}\mathbf{P}^B = \begin{bmatrix} B(z_1) & 0 & \dots & 0 \\ 0 & B(z_2) & \dots & 0 \\ \vdots & \vdots & \ddots & \vdots \\ 0 & 0 & \dots & B(z_N) \end{bmatrix} \begin{bmatrix} p^B_{11} & p^B_{12} & \dots & p^B_{1T} \\ p^B_{21} & p^B_{22} & \dots & p^B_{2T} \\ \vdots & \vdots & \ddots & \vdots \\ p^B_{N1} & p^B_{N2} & \dots & p^B_{NT} \end{bmatrix} \tag{4.42}$$

Next, $\mathbf{B}\mathbf{P}^B$ is denoted by $\mathbf{P}$, which is recognized as the production matrix:

$$\mathbf{B}\mathbf{P}^B = \mathbf{P}. \tag{4.43}$$

Expanded the production matrix reads:

$$\mathbf{P} = \begin{bmatrix} p_{11} & p_{12} & \dots & p_{1T} \\ p_{21} & p_{22} & \dots & p_{2T} \\ \vdots & \vdots & \ddots & \vdots \\ p_{N1} & p_{N2} & \dots & p_{NT} \end{bmatrix}. \tag{4.44}$$

Taking all of this into account we get the expression for daily watercolumn production as:

$$P_{Z,T} = \boldsymbol{\zeta} \mathbf{P} \boldsymbol{\tau}. \tag{4.45}$$

Since according to (4.33) each element of the normalized production matrix is obtained using $p^B(I)$, it is necessary to know the irradiance at the vertical level z_n at the time instant t_j, that is $I(z_n, j\Delta t)$. Denoting $I(z_n, j\Delta t)$ with I_{nj} and collecting all elements into a matrix of the same size as $\mathbf{P}^B$, the irradiance matrix $\mathbf{I}$ emerges. Subsequently, treating $p^B[\cdot]$ as an elementwise operator acting on each element of the irradiance matrix, in accordance with (4.18), we can write the following:

$$\mathbf{P}^B = p^B[\mathbf{I}], \tag{4.46}$$

such that (4.45) becomes:

$$P_{Z,T} = \boldsymbol{\zeta} \mathbf{B} p^B[\mathbf{I}] \boldsymbol{\tau}. \tag{4.47}$$

Using the same notation the expression for the discrete production profile (4.40) can be written as:

$$\mathbf{p}_T = \mathbf{B} p^B[\mathbf{I}] \boldsymbol{\tau}. \tag{4.48}$$

Stated in this form the expression highlights the central role of the irradiance matrix in the model. We now look in more detail how to calculate its elements.

4.4 CALCULATING THE IRRADIANCE MATRIX

We have observed in the prior section that the irradiance matrix plays a central role in the matrix model. We now emphasise in more detail how to calculate its elements. In general, any optical model can be used to do this, but for simplicity we will limit ourselves here to the already used model (2.13), according to which the elements of the irradiance matrix are given as:

$$I_{nj} = I_{0j} \exp\left(-K z_n\right). \tag{4.49}$$

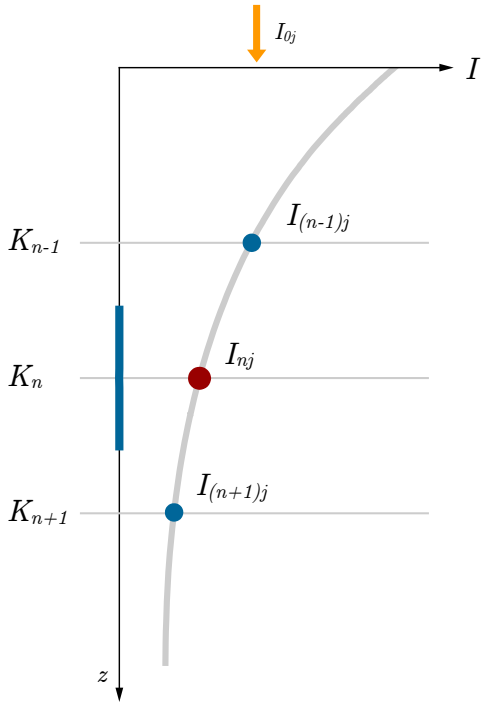

Figure 20: Calculation of irradiance at level z_n by knowing irradiance at the level above z_{n-1} for vertically dependent attenuation coefficient. Irradiance at z_n is calculated by first attenuating the irradiance at the level above $I(z_{n-1})$ over depth $\Delta z/2$ with K_{n-1} and then subsequently attenuating the obtained irradiance still further over $\Delta z/2$ with K_n.

To implement it, the model requires information on surface irradiance:

$$I_{0j} = I_0\left(t_j\right). \tag{4.50}$$

It treats the attenuation coefficient as a constant, whereas in general the attenuation coefficient is not constant, but changes with depth. To take this into account, a simple remedy is to assign different values of the attenuation coefficient for each model layer, such that K becomes K_n:

$$K_n = K(z_n). \tag{4.51}$$

Next, we recognize that irradiance at a given model level can be calculated from knowing the irradiance at the level above and the attenuation coefficient in between. If to each level a K_n value is assigned (Figure 20) it is then valid in the depth range of that level, which is Δz_n as defined in (4.2). Therefore, to get at irradiance at the level z_n we need irradiance value at the top of that layer, which is at $z_n - \Delta z/2$ and is given as:

$$I\left(z_n - \frac{\Delta z}{2}\right) = I_{(n-1)j} \exp\left(-K_{n-1}\frac{\Delta z}{2}\right). \tag{4.52}$$

Next, having irradiance at the top of the layer, it is straightforward to calculate it at the depth z_n, by simply attenuating it with K_n for half a layer depth:

$$I_{nj} = I_{(n-1)j} \exp\left(-K_{n-1}\frac{\Delta z}{2}\right) \exp\left(-K_n\frac{\Delta z}{2}\right). \tag{4.53}$$

In this manner irradiance at each level can be calculated and the irradiance matrix values populated.

4.5 ANALOGY AMONGST THE MODELS

To gain deeper insight into the mathematical structure of both the continuous and the matrix models we now employ the notion of the scalar product of functions to highlight the mathematical symmetry amongst the models. One form in which the watercolumn production integral can be written is as the vertical integral of the production profile, which itself is given as a product of the biomass profile and the normalized production profile as $P_T(z) = B(z)P_T^B(z)$, therefore we have:

$$P_{Z,T} = \int_0^\infty B(z)P_T^B(z)\,\mathrm{d}z. \tag{4.54}$$

Mathematically, the above integral is the inner product of the two functions: $B(z)$ and $P_T^B(z)$. In discrete form the approximation to this integral reads:

$$P_{Z,T} \approx \sum_{n=1}^{N} B(z_n)P_T^B(z_n)\Delta z. \tag{4.55}$$

If we now treat $B(z_n)$ and $P_T^B(z_n)$ as vectors in an N dimensional space, we can consider the above sum as a scalar product of the two vectors, analogously to the just mentioned interpretation of (4.54). To unveil where in the matrix model this analogy lies we consider equation (4.41), which by using (4.35) we unpack here as:

$$P_{Z,T} = \boldsymbol{\zeta}\mathbf{B}\mathbf{p}_T. \tag{4.56}$$

The matrix product of $\boldsymbol{\zeta}$ and $\mathbf{B}$ reads:

$$\boldsymbol{\zeta}\mathbf{B} = \begin{bmatrix} B(z_1)\Delta z & B(z_2)\Delta z & \dots & B(z_N)\Delta z \end{bmatrix}. \tag{4.57}$$

This is a row vector of the same size as $\mathbf{p}_T$ and we label it as $\mathbf{b}$, such that elementwise we have:

$$b_n = B(z_n)\Delta z. \tag{4.58}$$

Using $\mathbf{b}$ enables expression (4.56) to be rewritten as a scalar product of $\mathbf{b}$ and $\mathbf{p}_T$:

$$P_{Z,T} = \mathbf{b}\mathbf{p}_T. \tag{4.59}$$

By way of analogy this expression has the same mathematical structure as (4.54). Namely, both expressions, (4.54) and (4.56), can be thought of as inner products, with the difference that the first is an inner product over a continuous variable z and the second one is an inner product over a discrete space in which each dimension corresponds to a model depth located at z_n. In the limit of ever smaller depth intervals Δz the two expression should be equal to each other:

$$\lim_{\Delta z \to 0} \mathbf{b}\mathbf{p}_T = \int_0^\infty B(z) P_T^B(z)\, \mathrm{d}z. \tag{4.60}$$

Therefore, both models for watercolumn production can be thought of in a similar fashion, as inner products, be it over a continuous space (4.54), or over discrete space (4.56). The advantage of the matrix model comes to the fore when using measured biomass profiles, or measured surface irradiance. It is however, slightly more difficult to implement than the analytical model in case the photosynthesis parameters are depth dependent, which we now discuss.

4.6 VERTICALLY DEPENDENT PHOTOSYNTHESIS PARAMETERS

For calculating daily production at depth with vertically dependent photosynthesis parameters we have to first state the photosynthesis parameters as functions of depth. For a depth dependent initial slope we have:

$$\alpha^B = \alpha^B(z), \tag{4.61}$$

and for a depth dependent assimilation number we have:

$$P_m^B = P_m^B(z). \tag{4.62}$$

As such it is simple to include it in the analytical model for the daily production profile (2.34), by simply stating the parameters as functions of depth:

$$P_T(z) = B(z)P_m^B(z)D\, f_z\big(I_*^m(z)e^{-Kz}\big), \tag{4.63}$$

where now the dimensionless irradiance also becomes a function of depth:

$$I_*^m(z) = \frac{\alpha^B(z)I_0^m}{P_m^B(z)}. \tag{4.64}$$

However, it is now more difficult to calculate daily watercolumn production analytically. However, in the matrix model the procedure for calculating watercolumn production is straightforward, but including vertically dependent photosynthesis parameters is a bit more tricky and can done in a number of ways.

The easiest way to proceed is to amend (4.48), the matrix model analogue to (4.63), by taking into account the vertical dependence of photosynthesis parameters. Subsequently, we have $p^B[\cdot]$ act on each row of the normalized production matrix with different values of photosynthesis parameters:

$$\mathbf{P}^B = \sum_{n=1}^{N} p^B\Big[\mathbf{EI}\big|\ \alpha^B(z_n), P_m^B(z_n)\Big], \tag{4.65}$$

where $\mathbf{E}$ is a matrix with a single unit element on the diagonal in the row corresponding to the model level n. In such a way $\mathbf{E}$ is used to select each row of the irradiance matrix. This expression corresponds to:

$$p_{nj}^B = p^B\Big(I_{nj}\big|\ \alpha^B(z_n), P_m^B(z_n)\Big), \tag{4.66}$$

where we have used the notation from (1.20) to highlight the vertical dependence of the photosynthesis parameters. In this manner each row of the production matrix can have different values of photosynthesis parameters. Whilst the construction of the normalized production matrix $\mathbf{P}^B$, as stated in (4.65), takes a bit more effort, the remainder of the model stays the same.

4.7 PROBLEMS

1. Build the irradiance matrix as defined in (4.16). Write a code which plots the irradiance profile at a desired time step, corresponding to a matrix column. Write a code which plots the irradiance time series at a desired depth, corresponding to a matrix row. Finally plot the the entire irradiance matrix. Observe how changing surface irradiance and the attenuation coefficient changes the light field and the irradiance matrix.

2. Build a normalized production matrix by using the photosynthesis irradiance function directly on the irradiance matrix (4.18). Write a code which accepts various photosynthesis irradiance functions (1.27, 1.28, 1.29, 1.30, 1.31). Plot the the normalized production matrices and the differences amongst each. Change the values of the photosynthesis parameters to observe how the production matrix changes.

3. Write a code which builds the biomass matrix (4.2) with biomass given by either the shifted Gaussian (2.45) of the shifted Sigmoid function (2.48). Use the biomass matrix to calculate the production matrix as defined in (4.23). Plot the the production matrix for different photosynthesis irradiance functions (1.27, 1.28, 1.29, 1.30, 1.31).

4. Build the irradiance matrix by acknowledging the effect of biomass on the underwater light field. Use this irradiance matrix to calculate the production matrix. Alter the parameters of the biomass profile to observe how the production matrix changes with the shape of the biomass profile.

5. Using the matrix model calculate the production profile (4.26) and watercolumn production (4.30). Also implement the code using loops, as in (4.6) and (3.1). Contrast the code with the code for the matrix model.

6. Amend the irradiance model (4.53) to take into account non uniform model level separations as stated in (4.11). Subsequently, write out the matrix model equations given in section 5.3 now using non uniform model level separations. Start with equation (4.37) and work your way through to equation (4.45).

7. Build the normalized production matrix with depth dependent photosynthesis parameters, as stated in (4.65), and use it to calculate the daily production profile and daily watercolumn production. Study the effect of using depth dependent photosynthesis parameters on both the shape of the production profile and the magnitude of daily watercolumn production.

Part II

DYNAMICS

5

CRITICAL DEPTH THEORY

Thus far we laid out the basics of bio optical models of primary production and hinted at dynamical relations between production and growth. We now take the next step and place the theory in a broader dynamical context. We begin by presenting, what is in oceanographic terms considered a rather famous hypotheses: the Critical Depth Hypothesis.

Due to the interaction of the ocean with the atmosphere the topmost layer of the ocean is well mixed. This layer is referred to as the mixed layer. The critical depth theory deals with the interplay between production, losses and mixing in the mixed layer. It asserts a depth horizon, termed the critical depth, and predicts that mixing beyond the critical depth reduces mixed layer light conditions beyond the levels that can sustain positive growth. Vice versa, mixed layers shallower than the critical depth are favourable for phytoplankton growth, since mixed layer light levels give rise to production which surpasses losses. It is this predictive power that makes the theory testable and its application to the real ocean has sparked much interest and debate over the years [52].

We proceed by outlining the basic mathematical formulation of the Critical Depth Hypothesis, first given by Sverdrup in 1953 [58]. We then give a modern synthesis [33], provide the exact analytical solution for the critical depth, place the theory in a dynamical context, calculate the steady state biomass and finally present a conservation principle which arises due to the biooptical feedback in the model.

5.1 PROBLEM FORMULATION SENSU SVEDRUP

Consider a mixed layer of depth Z_m (Figure 21) in which production is given as a linear function of light (1.7). Due to mixing the layer is optically homogenous such that (2.13) holds for irradiance. Combining the two assumptions gives production at depth as:

$$P(z,t) = B\alpha^B I_0(t) \exp(-Kz), \tag{5.1}$$

where B is the mixed layer biomass, such that the total mixed layer biomass is given as $B_{Z_m} = BZ_m$.

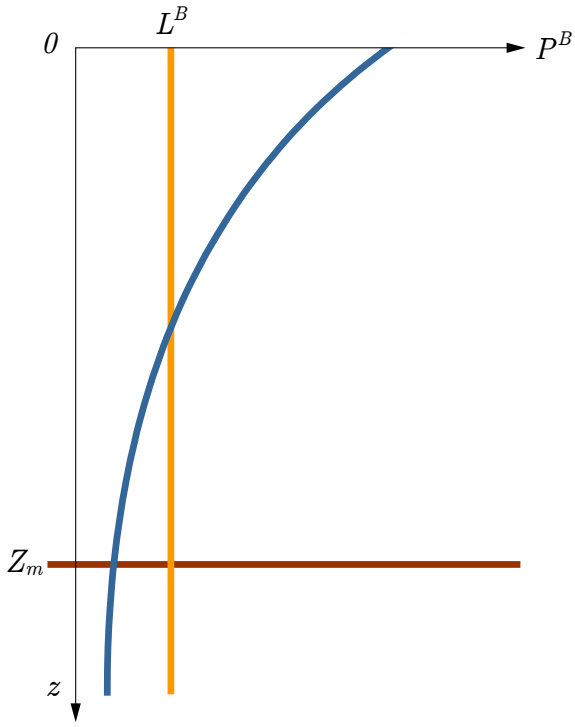

Figure 21: Depiction of the vertical dependence of normalized production P^B (blue curve) and losses L^B (orange line) in a water column with a mixed layer of depth Z_m (red line). Photosynthesis declines with depth due to the reduction in light intensity, whereas losses are assumed constant due to active mixing.

Following (3.16) and integrating the previous expression (over time and depth) yields the mixed layer production:

$$P_{Z_m,T} = \int_0^{Z_m} \int_0^{D} P(z,t)\,\mathrm{d}t\,\mathrm{d}z = \frac{B\alpha^B I_T}{K}(1 - e^{-KZ_m}), \tag{5.2}$$

where I_T stands for the total available light energy at the surface received during one day:

$$I_T = \int_0^{D} I_0(t)\,\mathrm{d}t. \tag{5.3}$$

Now assume, in line with Figure 21, a depth-independent, biomass-specific, **loss rate** L^B, such that the total loss $L(z,t)$ at each depth and time is given by:

$$L(z,t) = BL^B, \tag{5.4}$$

where L^B is the loss rate per unit biomass in the broadest sense (respiration, grazing), which can be parametrized in numerous ways [62]. Integrating this expression (over time and depth) yields mixed layer losses as:

$$L_{Z_m,T} = \int_0^{Z_m} \int_0^{D} L(z,t)\,\mathrm{d}t\,\mathrm{d}z = BL_T^B Z_m, \tag{5.5}$$

with $L_T^B = 24\ L^B$, where the 24 comes due to integration over the entire day. We stress that temporal integration is carried out over daylight hours for primary production and over 24 hours for the loss term.

Following Sverdrup [58] the **critical depth** Z_c (m) is defined as the depth for which the following holds:

$$P_{Z_c,T} = L_{Z_c,T}, \tag{5.6}$$

or stated explicitly for Sverdup's model:

$$\frac{\alpha^B I_T}{K}\left(1 - e^{-KZ_c}\right) = 24\ L^B Z_c. \tag{5.7}$$

The obtained equation is a transcendental one. Luckily, it is solvable using the Lambert W function, but prior to presenting the exact solution we will first interpret this expression.

For active mixing proceeding exactly to the critical depth $Z_m = Z_c$, mixed layer production equals losses and therefore no biomass accumulation takes place. In order for biomass accumulation to take place, production needs to exceed losses:

$$\frac{\alpha^B I_T}{K}\left(1 - e^{-KZ_m}\right) > 24\, L^B Z_m, \tag{5.8}$$

which occurs when mixing does not proceed to the critical depth $Z_m < Z_c$. If mixing proceeds beyond the critical depth $Z_m > Z_c$ losses dominate:

$$\frac{\alpha^B I_T}{K}\left(1 - e^{-KZ_m}\right) < 24\, L^B Z_m, \tag{5.9}$$

and biomass accumulation will not take place. To know which condition is satisfied we proceed to solve (5.7) to obtain Z_c.

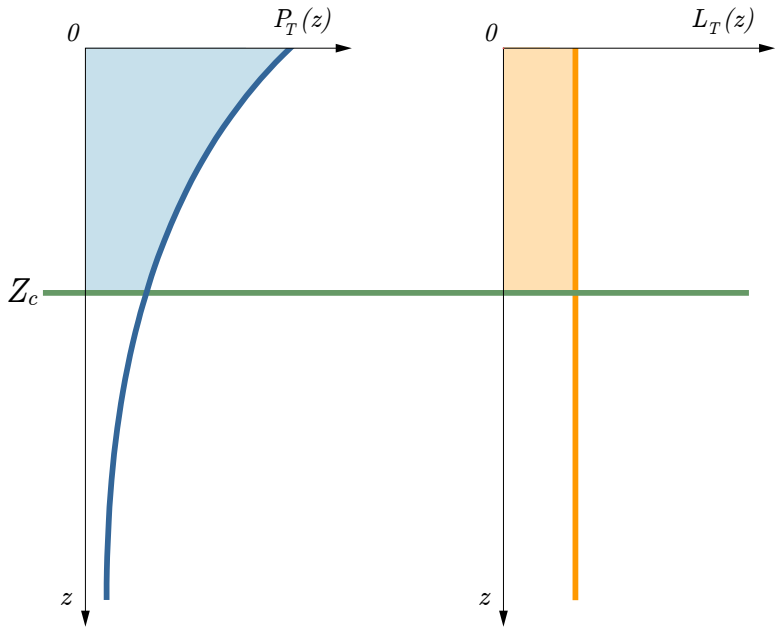

Figure 22: Graphical representation of the critical depth Z_c (green line) as the depth at which vertically integrated production (blue surface) equals vertically integrated losses (orange surface).

5.2 EXACT SOLUTION FOR SVEDRUP'S CRITICAL DEPTH

A straightforward approach to solving (5.7) is to use the Lambert W function, which is the inverse of xe^x [8, 21]. Take the following equation:

$$xe^x = a, \tag{5.10}$$

where both x and a are real numbers. The Lambert W function, denoted simply as W, solves the above equation as:

$$x = W(a). \tag{5.11}$$

For our purposes that is as much as we need to know about the Lambert W function. The interested reader is referred to [8, 18, 20, 57, 23] for more details on the function.

In order to solve (5.7) and find an exact expression for Sverdrup's critical depth, by using the Lambert W function, we start by rewriting (5.7) as:

$$1 - e^{-KZ_c} = \frac{L_T^B}{\alpha^B I_T} KZ_c. \tag{5.12}$$

By multiplying the attenuation coefficient with the critical depth we define ζ_c as the optical depth corresponding to the critical depth:

$$\zeta_c = KZ_c. \tag{5.13}$$

By dividing surface production with losses we define A as:

$$A = \frac{\alpha^B I_T}{L_T^B}. \tag{5.14}$$

Now our starting expression turns into:

$$1 - e^{-\zeta_c} = \frac{\zeta_c}{A}, \tag{5.15}$$

and after a little algebra we get:

$$(\zeta_c - A)e^{(\zeta_c - A)} = -Ae^{-A}. \tag{5.16}$$

The obtained expression is now in the form of (5.10) and we simply solve it by using the Lambert W function to obtain:

$$\zeta_c = W\Big(-Ae^{-A}\Big) + A. \tag{5.17}$$

More technical details on the derivation of the solution are found in [33]. Fully expanded, by using (5.13) and (5.14), the solution reads:

$$Z_c = \frac{1}{K}\left[W\left(-\frac{\alpha^B I_T}{L_T^B}\exp\left(\frac{-\alpha^B I_T}{L_T^B}\right)\right) + \frac{\alpha^B I_T}{L_T^B}\right]. \tag{5.18}$$

Having obtained an exact expression for Z_c we can easily compare it to Z_m to ascertain if production exceeds losses in the mixed layer. It is at this stage that the Critical Depth Hypothesis comes into play.

5.3 CRITICAL DEPTH HYPOTHESIS

Critical Depth Hypothesis states that the spring bloom can be initiated once the mixed layer depth becomes shallower than the critical depth [58, 52]. This typically occurs in spring due to the onset of stratification. To explore it from a dynamical standpoint, we follow up on the relation of mixed layer production to growth (3.65) augmented with a loss term:

$$B_{Z_m}(t+\Delta t) = B_{Z_m}(t) + \frac{1}{\chi}\Big(P_{Z_m}(t) - L_{Z_m}\Big)\Delta t. \tag{5.19}$$

Once again, in the limit of $\Delta t \to 0$ we have:

$$\frac{\mathrm{d}}{\mathrm{d}t}B_{Z_m}(t) = \frac{1}{\chi}\Big(P_{Z_m}(t) - L_{Z_m}\Big). \tag{5.20}$$

For Sverdrup's model, due to active mixing $B_{Z_m} = BZ_m$, and taking into account (5.2) and (5.5), whilst averaging over 24 hours, we obtain:

$$\frac{\mathrm{d}B}{\mathrm{d}t} = \frac{1}{24\chi Z_m}\left[\frac{\alpha^B I_T}{K}\big(1 - e^{-KZ_m}\big) - L_T^B Z_m\right]B, \tag{5.21}$$

The expression in the brackets is plotted in Figure 23.

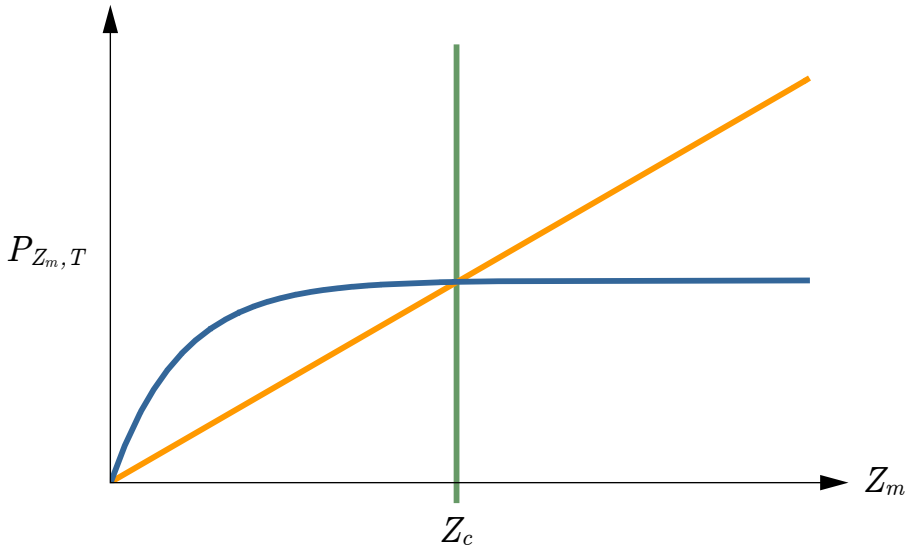

Figure 23: Graphical representation of equation (5.21). Mixed layer production (blue curve) is higher/lower than mixed layer losses (orange line) when the mixed layer depth Z_m is shallower/deeper than the critical depth Z_c (green line).

Following Figure 23 production is higher than losses when the mixed layer depth is shallower than the critical depth: graphically the blue curve (production) is above the orange curve (losses). Production is lower than losses when the mixed layer depth is deeper than the critical depth: graphically the blue curve (production) is below the orange curve (losses). In the brackets on the right hand side of (5.21) we observe the difference between mixed layer production and losses. Therefore, we conclude the following:

$$\begin{aligned} \frac{\mathrm{d}B}{\mathrm{d}t} &> 0 \qquad Z_m < Z_c; \\ \frac{\mathrm{d}B}{\mathrm{d}t} &= 0 \qquad Z_m = Z_c; \\ \frac{\mathrm{d}B}{\mathrm{d}t} &< 0 \qquad Z_m > Z_c. \end{aligned} \tag{5.22}$$

In this simple model biomass grows when $Z_m < Z_c$ and declines when $Z_m > Z_c$. If $Z_m = Z_c$ biomass does not change over time.

5.4 STEADY STATE

As biomass changes over time so does the attenuation coefficient (2.11), altering the light field and changing normalized production, which finally has dynamical consequences. Although slight, this alteration in the model makes equation (5.21) nonlinear with respect to B:

$$\frac{\mathrm{d}B}{\mathrm{d}t} = \frac{1}{24\chi Z_m}\left[\frac{\alpha^B I_T}{K_w + k_B B}\Big(1 - \exp\big(-(K_w + k_B B)Z_m\big)\Big) - L_T^B Z_m\right] B. \tag{5.23}$$

Also, the inclusion of the bio-optical feedback now makes the production term a decreasing function of biomass. Therefore, a steady state solution $B^* > 0$ is plausible (Figure 24). Naturally, a trivial steady state $B^* = 0$ is also a solution.

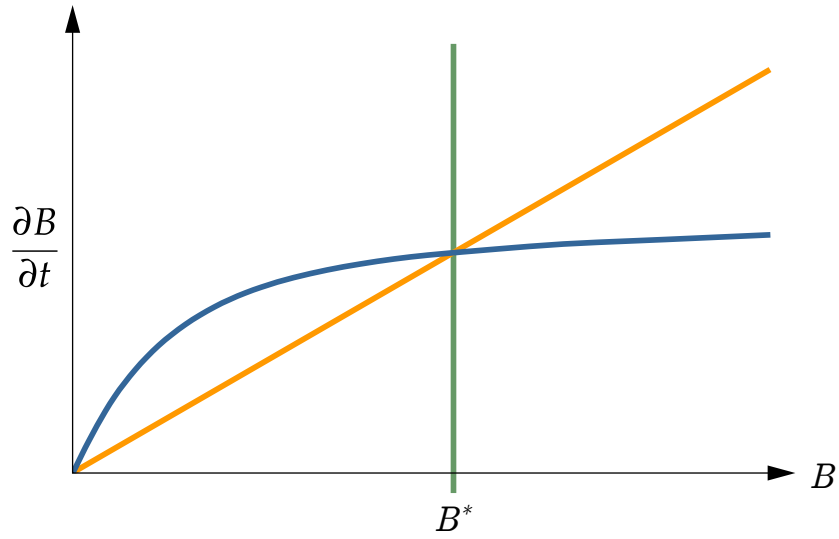

Figure 24: Graphical representation of equation (5.23). Mixed layer production (blue curve) is higher/lower than mixed layer losses (orange line) when the biomass B is lower/higher than the steady state biomass B^* (green line). Note the difference from Figure 23: the abscissa here marks biomass B (state variable), whereas in Figure 23 abscissa marks the mixed layer depth (model parameter).

Once at steady state, production equals losses, implying the right hand side of (5.23) equals zero, which holds when:

$$\frac{\alpha^B I_T}{K_w + k_B B}\Big(1 - \exp\big(-(K_w + k_B B)Z_m\big)\Big) = L_T^B Z_m. \tag{5.24}$$

With a little algebra, and using the definition of A (5.14), we have:

$$1 - \exp\big(-(K_w + k_B B)Z_m\big) = \frac{(K_w + k_B B)Z_m}{A}. \tag{5.25}$$

Solving this equation would give us B^*. By observing that it is of the same form as (5.15), we can solve it in the same way, which yields the following solution for steady state biomass:

$$B^* = \frac{1}{k_B Z_m}\Big(W_0\Big(-Ae^{-A}\Big) + A\Big) - \frac{K_w}{k_B}. \tag{5.26}$$

By observing that the expression in the brackets is given by (5.17) we get:

$$B^* = \frac{K_w}{k_B}\left(\frac{Z_c}{Z_m} - 1\right), \tag{5.27}$$

where Z_c now stands for the critical depth in the case of clear water $K = K_w$. Plot of this solution, with Z_c and Z_m expressed as optical depths, is given in Figure 25. For the biomass in the mixed layer of depth Z_m to be sustained we require $B^* > 0$, translating (5.27) into:

$$Z_c > Z_m, \tag{5.28}$$

which is recognized as the critical depth criterion. The trivial state state $B^* = 0$ is reached when the previous condition is not met.

However, it must be highlighted that interpretation of the prior result is not trivial. By observing that at steady state production equals losses, so must the critical depth equal the mixed layer depth (5.22), otherwise production will not equal losses and biomass will change with time. Therefore, at steady state Z_c should equal Z_m and (5.27) would yield zero. This however is not correct, since Z_c in (5.27) takes into account only attenuation due to water ($K = K_w$) whereas attenuation occurs due to water and phytoplankton ($K = K_w + k_B B$), whenever $B > 0$. We now explore these relations in more detail.

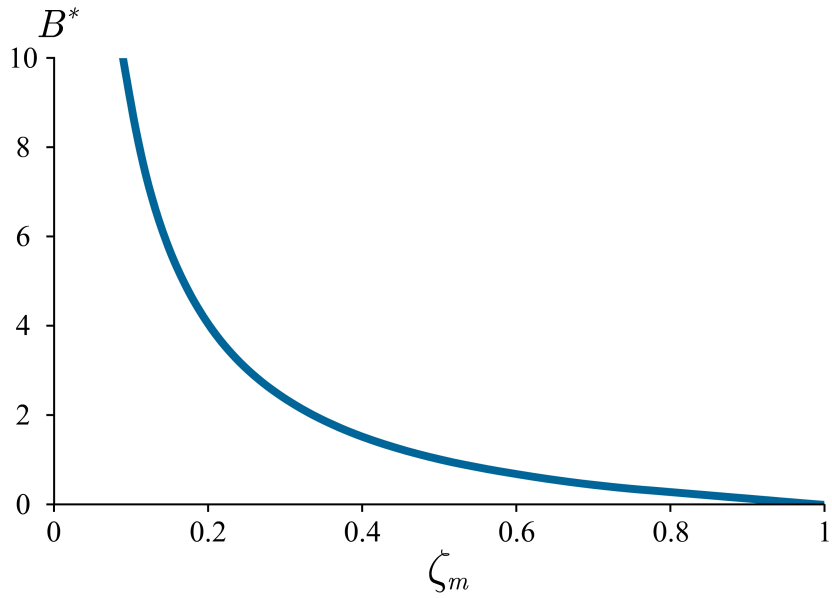

Figure 25: Steady state biomass (5.27) as a function of Z_m for $K_w/k_B = 1$ and $\zeta_c = 1$. After ζ_m becomes larger than 1 the critical depth criterion is violated and biomass can no longer be sustained.

5.5 CRITICAL DEPTH CONSERVATION PRINCIPLE

Considering that Z_c in equation (5.27) is not optically coupled to phytoplankton biomass, such that Z_c in equation (5.18) is determined by K_w and not by K as given in (2.11), theoretically we are led to distinguish two critical depths. The first one we relabel as the optically-uncoupled critical depth C and the second one as the optically coupled critical depth S. We give the following definitions:

Optically uncoupled critical depth C is the critical depth associated with $k_B = 0$ and is defined as:

$$C = \frac{1}{K_w}\left(W_0\left(-Ae^{-A}\right) + A\right). \tag{5.29}$$

Optically uncoupled critical depth is independent of time $C \neq C(t)$.

Optically coupled critical depth S is the critical depth associated with $k_B \neq 0$ and is defined as:

$$S = \frac{1}{K_w + k_B B}\left(W_0\left(-Ae^{-A}\right) + A\right). \tag{5.30}$$

Optically coupled critical depth is time dependent $S = S(t)$.

With these definitions steady state biomass (5.27) is now:

$$B^* = \frac{K_w}{k_B}\left(\frac{C}{Z_m} - 1\right). \tag{5.31}$$

For $C < Z_m$ this equation yields negative biomass, which is physically unrealistic. However, $C < Z_m$ corresponds to clear-water at steady state, implying absence of phytoplankton. Hence, the solution is only valid for C/Z_m larger than one, which is in accordance with the Critical Depth Hypothesis.

With the above, we are now in a position to calculate the light intensity at the base of the mixed layer at steady state and compare it to the light intensities at C and S. By inserting (2.11) and (5.31) into (2.13), irradiance at the base of the mixed layer is shown to equal irradiance at the optically uncoupled critical depth:

$$I(Z_m) = I_0 \exp\left(-K_w C\right) = I(C), \tag{5.32}$$

although the two depths Z_m and C need not be equal (Figure 26). Therefore, at steady state light intensity at the base of the mixed layer equals the light intensity at the optically-uncoupled critical depth. Although the mixed layer depth does not equal the optically uncoupled critical depth $Z_c \neq C$, their light levels are equal, due to shading by phytoplankton. It is important to stress that $I(C)$ is biomass independent. We can also calculate S at steady state by inserting (5.31) into (5.30), which after some algebra gives:

$$S^* = Z_m, \tag{5.33}$$

where we have labelled the optically coupled critical depth at steady state as S^*. Therefore, at steady state the optically coupled critical depth equals the mixed layer depth, but the clear-water critical depth does not (Figure 26).

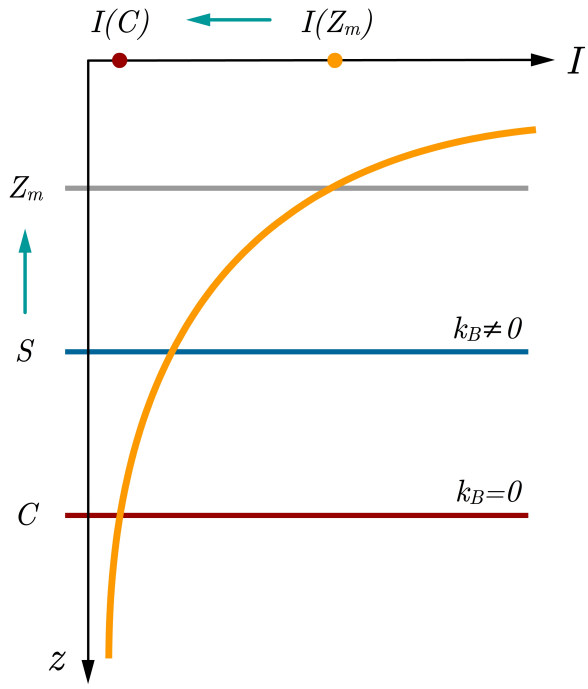

Figure 26: Sketch of the relation between mixed layer depth Z_m, optically-uncoupled critical depth C and optically coupled critical depth S. With time, S converges to Z_m, while C remains constant. Simultaneously, irradiance at the mixed layer base $I(Z_m)$ converges to irradiance at the clear-water critical depth $I(C)$. Finally, at steady state we have $S^* = Z_m$ and $I(Z_m) = I(C)$.

Having demonstrated the relations that hold at steady state we now explore the dynamical approach to the steady state. Assume the initial condition of the system is given by $B_0 \neq B^*$ and $S_0 \neq Z_m$. We already have an equation for the time evolution of biomass, namely (5.23) and are now interested into deriving an equation describing the time evolution of S. We can simply take the time derivative of (5.30) to obtain:

$$\frac{\mathrm{d}S}{\mathrm{d}t} = -\left(\frac{k_B}{K_w + k_B B}\frac{\mathrm{d}B}{\mathrm{d}t}\right)S. \tag{5.34}$$

According to this result the optically coupled critical depth declines as biomass grows and vice versa.

The previous expression is reducible to:

$$\frac{\mathrm{d}S}{\mathrm{d}B} = -\frac{k_B S}{K_w + k_B B}, \tag{5.35}$$

which can be integrated by separation of variables. Integration from $S(0) = S_0$ to $S(t) = S$ gives:

$$S = S_0 \left(\frac{K_w + k_B B_0}{K_w + k_B B} \right), \tag{5.36}$$

whereas the integration from $S(t) = S$ to $S(\infty) = S^*$, while acknowledging (5.33), gives:

$$S = Z_m \left(\frac{K_w + k_B B^*}{K_w + k_B B} \right). \tag{5.37}$$

This result was first derived by [39] (their equation 4.5) for a non-linear photosynthesis irradiance model with discrete time. As demonstrated here, it also holds for Svedrup's linear photosynthesis irradiance model.

The derived equation can be generalized by rearranging (5.34), recognizing (2.11) and applying the chain rule, to obtain:

$$\frac{\mathrm{d}(KS)}{\mathrm{d}t} = 0, \tag{5.38}$$

demonstrating that the product of the attenuation coefficient and the optically coupled critical depth remains constant over time. Given initial conditions (K_0, S_0), when the critical depth criterion is met the system ends in a steady state characterized by $S = Z_m$ and $B = B^*$. When the critical depth criterion is not met the system ends in the trivial steady state characterized by $S = C$ and $B = 0$. It is important to highlight that on the approach to these states the system moves along a trajectory which keeps the KS product constant.

Following the definition (5.30) and acknowledging (5.17) we observe that the quantity which is conserved is in fact the critical depth expresses as an optical depth ζ_c (5.17) and therefore we can restate the previous expression simply as:

$$\frac{\mathrm{d}\zeta_c}{\mathrm{d}t} = 0. \tag{5.39}$$

We term this the Critical Depth Conservation Principle. Working backwards from it stems equation (5.37).

5.6 NONLINEAR FORMULATION

Prior analysis was given for Sverdrup's model which has a linear photosynthesis irradiance function (5.1). We now lift this limitation and present a more general model formulation which can accommodate any photosynthesis irradiance function. First we introduce the formulation for the exponential photosynthesis irradiance function (1.18). The modification to Svedrup's model comes only to equation (5.2) which now transforms into:

$$P_{Z_m,T} = \int_0^{Z_m}\int_0^{D} P(z,t)\,\mathrm{d}t\,\mathrm{d}z = \frac{BP_m^B D}{K_w + k_B B}\Big[\, f\big(I_*^m\big) - f\big(I_*^m e^{-(K_w+k_B B)Z_m}\big)\,\Big]. \tag{5.40}$$

The remaining model assumptions hold. The equation describing biomass evolution over times now becomes:

$$\frac{\partial B}{\partial t} = \frac{1}{24\chi Z_m}\left[\frac{P_m^B D}{K_w + k_B B}\Big[\, f\big(I_*^m\big) - f\big(I_*^m e^{-(K_w+k_B B)Z_m}\big)\,\Big] - L_T^B Z_m\right] B. \tag{5.41}$$

To simplify notation we introduce the **average normalized instantaneous mixed layer production** $\langle P\rangle_{Z_m}^B$ as:

$$\langle P\rangle_{Z_m}^B = \frac{P_m^B D}{24(K_w + k_B B)Z_m}\Big[\, f\big(I_*^m\big) - f\big(I_*^m e^{-(K_w+k_B B)Z_m}\big)\,\Big], \tag{5.42}$$

turning (5.41) into:

$$\frac{\mathrm{d}B}{\mathrm{d}t} = \frac{1}{\chi}\Big(\langle P\rangle_{Z_m}^B - L^B\Big)B. \tag{5.43}$$

This equation describes the time evolution of mixed layer biomass as the difference between average mixed layer production and losses. The production term is expressed as an average one day and over depth, due to the equation expressing change in biomass per cubed meter. In general, the above equation is valid for any photosynthesis irradiance

function, one just has to pay attention to how $\langle P \rangle^B_{Z_m}$ is specified. The exact formulation would be:

$$\langle P \rangle^B_{Z_m} = \frac{P^B_{Z_m}}{Z_m}, \tag{5.44}$$

whereas a reasonable first approximation would be to use the daily average, as was just done:

$$\langle P \rangle^B_{Z_m} = \frac{P^B_{Z_m,T}}{24 Z_m}. \tag{5.45}$$

The formulation depends on what the modelling goals are. If resolving the seasonal cycle the latter works just fine, whereas when resolving diurnal dynamics the former should be used.

In both cases, when calculating average mixed layer production it is important to use instantaneous light conditions, calculate instantaneous production and then take the average. Calculating average light conditions and then production will not yield the same result, due to the nonlinearity in the production light relation, as given by the photosynthesis irradiance function.

5.7 PROBLEMS

1. Use different photosynthesis irradiance functions (1.27, 1.28, 1.29, 1.30, 1.31) in the calculation of the instantaneous production profile. Plot all the profiles on the same graph along with a uniform loss term in the same manner as Figure 21. Observe at which depth each function crosses the loss rate.

2. Numerically calculate instantaneous mixed layer production as:

$$P_{Z_m} = \sum_{n=1}^{N} P_n \Delta z, \tag{5.46}$$

where $P_n = P(z_n)$ with $z_n = n\Delta z$, for $n = 1, 2, ..., N$ and $N = Z_m/\Delta z$. Use all the photosynthesis irradiance functions (1.27, 1.28, 1.29, 1.30, 1.31). Plot the integrated production and losses as a function of Z_m in the same manner as shown in Figure 23 for each photosynthesis irradiance function. Numerically calculate the critical depth in each case.

3. Numerically solve equation (5.19) using calculated mixed layer production from the previous problem. Include the biooptical feedback by modelling the attenuation coefficient as:

$$K(t) = K_w + k_B B(t). \tag{5.47}$$

Run the model with various photosynthesis irradiance functions (1.27, 1.28, 1.29, 1.30, 1.31) until steady state is reached. Plot the calculated biomass $B(t)$ as a function of time in each case. Numerically solve for the critical depth at each time step $S(t)$ and plot it as a function of time. Finally, plot the product of $K(t)$ and $S(t)$ as a function of time.

4. Recreate Figure 23 using equation (5.23) where saturation of photosynthesis is not modelled and subsequently equation (5.41) where saturation of photosynthesis is modelled. Observe the difference between the two by studying mixed layers of varying depth.

5. Recreate figure Figure 25 numerically by running the numerical model to steady state, first by using equation (5.23) and subsequently by using equation (5.41). Numerically calculate the optically uncoupled critical depth C and test whether solution (5.31) correctly predicts the steady state for both cases.

6. Run the model by using (5.41) and calculate the irradiance at the base of the mixed layer $I(Z_m)$ and at the optically coupled critical depth $I(S)$ at each time step. Compare it to the irradiance at the optically uncoupled depth, calculated using (5.32).

7. Observe how the mixed layer biomass evolves under variable surface irradiance given by (2.14) and contrast it with the evolution over time under constant surface irradiance equal to the average daily irradiance $I_0^m \pi/2$. Use both averaging approaches, (5.44) and (5.45), to explore the difference between simulations.

6

MIXED LAYER DYNAMICS

In the previous chapter the foundations of the critical depth theory were laid out with a linear photosynthesis irradiance function used to derive the presented results. We now expand on the developed concepts and explore mixed layer dynamics in more detail, first by relaxing the assumption of linearity in the photosynthesis irradiance function and subsequently deriving more general results applicable to any photosynthesis irradiance function.

The chapter opens with the derivation of equations for the time evolution of average and total mixed layer biomass. The difference between average and total mixed layer production is discussed and the dependence of both on mixed layer depth derived analytically. Steady state solutions for average and total mixed layer biomass are derived and their stability analysed. The link between stability of steady states and the critical depth criterion is established. The critical depth criterion is shown to be a necessary condition for the stability of the non-trivial steady state. When it is met the non-trivial steady state is stable and when it is not met the trivial steady state is stable.

Mixed layer depth is then treated as a function of time. The asymmetry in the response of average and total mixed layer biomass to mixed layer shallowing/deepening is discussed at length. The response of primary production to mixed layer shallowing is relevant during the onset of spring stratification, whereas the response to deepening is relevant during autumn and winter when convective mixing dominates.

6.1 AVERAGE AND TOTAL MIXED LAYER BIOMASS

Up to now we have worked with biomass B, which was given as a concentration of chlorophyll per meter cubed. In the case of a mixed layer (Figure 28) we are also interested in the **total mixed layer biomass** B_Z ($\mathrm{mg\,Chl\,m^{-2}}$), defined here as:

$$B_Z = \int_0^{Z_m} B(z)\,\mathrm{d}z. \tag{6.1}$$

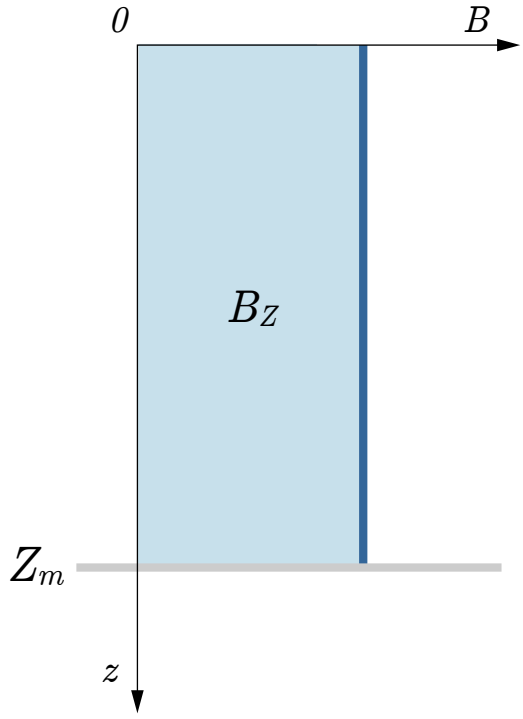

Figure 27: Total mixed layer biomass B_Z (light blue area) is given as a vertical integral of average biomass B (dark blue line) from the surface up to the mixed layer depth Z_m (grey line). Due to mixing average mixed layer biomass is by definition constant with depth.

Given the assumption of instantaneous mixing the following holds:

$$B_Z = BZ_m. \tag{6.2}$$

In this chapter we will refer to B as average biomass and B_Z as total biomass. As we have demonstrated in the prior chapter time evolution of average biomass is given by (5.43). In a similar fashion we can also begin with the equation for the time evolution of biomass at a given depth:

$$\frac{\mathrm{d}B}{\mathrm{d}t} = \frac{1}{\chi}\Big(p^B(I) - L^B\Big)B. \tag{6.3}$$

By vertically integrating this equation we arrive at:

$$\frac{\mathrm{d}}{\mathrm{d}t}\int_0^{Z_m} B\,\mathrm{d}z = \frac{1}{\chi}\left(\int_0^{Z_m} Bp^B(I)\,\mathrm{d}z - \int_0^{Z_m} L^B B\,\mathrm{d}z\right), \tag{6.4}$$

which using (6.1) becomes:

$$\frac{\mathrm{d}B_Z}{\mathrm{d}t} = \frac{1}{\chi}\left(\int_0^{Z_m} Bp^B(I)\,\mathrm{d}z - L^B B_Z\right). \tag{6.5}$$

Note the difference in the production term between the equations for total and average biomass. In the equation for average biomass the production term is divided by Z_m, whereas in the equation for total biomass it is not. However, for a time independent mixed layer depth $Z_m \neq Z_m(t)$ and time independent surface irradiance $I_0 \neq I_0(t)$, both (6.3) and (6.5) are interchangeable simply due to the fact that mixing keeps the biomass uniform in the mixed layer, expressed mathematically as (6.2). Using that expression we can write the production term in the equation for total biomass as:

$$\int_0^{Z_m} Bp^B(I)\,\mathrm{d}z = \frac{B_Z}{Z_m}\int_0^{Z_m} p^B(I)\,\mathrm{d}z. \tag{6.6}$$

Now we can expand $B_Z = BZ_m$ in each term in equation (6.5) and recover equation (6.3). Therefore the equations are fundamentally the same equation when the mixed layer is depth is constant with time.

Both equations have stable steady states, B^* and B_Z^*, which are also linked by (6.2). To derive expressions for these steady states, we now proceed to generalize the steady state solution (5.31) from the prior chapter, which was derived for a linear photosynthesis irradiance function. By using (2.11) and (2.13) as the light model, irradiance in the mixed layer becomes:

$$I(z) = I_0 \exp\big(-(K_w + k_B B)z\big). \tag{6.7}$$

Further on, irradiance at the mixed layer depth reads (Figure 28):

$$I(Z_m) = I_0 \exp\big(-(K_w + k_B B)Z_m\big), \tag{6.8}$$

which written using total biomass becomes:

$$I(Z_m) = I_0 \exp\big(-K_w Z_m - k_B B_Z\big). \tag{6.9}$$

By taking the time derivative of the prior expression we get:

$$\frac{\mathrm{d}I(Z_m)}{\mathrm{d}t} = -\left(k_B Z_m \frac{\mathrm{d}B}{\mathrm{d}t}\right) I(Z_m). \tag{6.10}$$

and further eliminating time gives us:

$$\frac{\mathrm{d}I(Z_m)}{\mathrm{d}B} = -k_B Z_m I(Z_m). \tag{6.11}$$

A general form of this result was first derived by [25] (their equation 22). By separation of variables and integration from the initial state $B(0) = B_0$ to the steady state $B(\infty) = B^*$, we get:

$$B^* = \frac{K_w}{k_B}\left(\frac{1}{K_w Z_m} \ln \frac{I_0}{I^*(Z_m)} - 1\right), \tag{6.12}$$

as the expression for steady state biomass, where $I^*(Z_m)$ is the irradiance at mixed layer depth at steady state. To be dimensionally consistent the first term in the brackets has to be dimensionless, which implies that the term $\ln(I_0/I^*(Z_m))/K_w$ has the dimension of depth and this is in fact the optically uncoupled critical depth, as defined in (6.15) for a linear production model [33]. Therefore we have:

$$C = \frac{1}{K_w} \ln \frac{I_0}{I^*(Z_m)}. \tag{6.13}$$

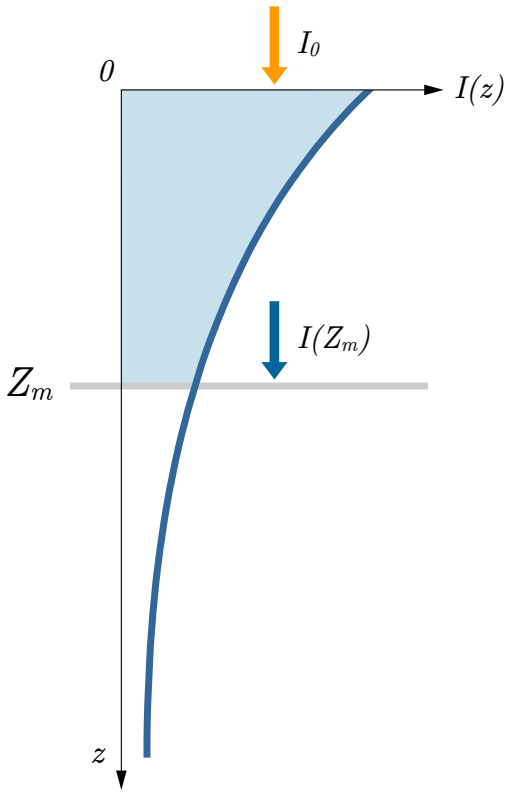

Figure 28: Irradiance at the mixed layer depth $I(Z_m)$ (blue arrow) calculated using expression (6.8), based on surface irradiance (orange arrow) attenuated due to water and mixed layer biomass.

Combining the previous two expressions we derive the following expression for average biomass at steady state:

$$B^* = \frac{K_w}{k_B}\left(\frac{C}{Z_m} - 1\right). \tag{6.14}$$

It is important to note that this result is general and does not depend on the specific formulation of the photosynthesis irradiance function. The production light relation, as dictated by the photosynthesis irradiance

function determines C and therefore B^*. We stress that C is the optically uncoupled critical depth and is the solution to:

$$\int_0^C P^B(I)\,\mathrm{d}z = L^B C, \tag{6.15}$$

under irradiance attenuated only due to water:

$$\frac{\mathrm{d}I}{\mathrm{d}z} = -K_w I, \tag{6.16}$$

implying that biooptical coupling is not present in the model. With no biooptical coupling irradiance at C is simply:

$$I(C) = I_0 \exp\left(-K_w C\right). \tag{6.17}$$

By expressing $I^*(Z_m)$ from (6.13) at steady state, we arrive at:

$$I^*(Z_m) = I_0 \exp\left(-K_w C\right). \tag{6.18}$$

We observe that irradiance at the mixed layer depth at steady state equals the irradiance at the optically uncoupled critical depth:

$$I^*(Z_m) = I(C). \tag{6.19}$$

This result was already demonstrated for the linear photosynthesis irradiance model (5.32). Here we see it is generalized to any photosynthesis irradiance function.

Finally, having derived the solution for average steady state biomass, it is straightforward to find the total steady state biomass, by simply multiplying (6.14) with the mixed layer depth (Figure 29):

$$B_Z^* = \frac{K_w}{k_B}\Big(C - Z_m\Big). \tag{6.20}$$

According to this expression total steady state biomass is proportional to the depth difference between the optically uncoupled critical depth and the mixed layer depth. In case of a mixed layer approaching zero the solution gives:

$$\lim_{Z_m \to 0} B_Z^* = \frac{K_w}{k_B} C. \tag{6.21}$$

This is a finite quantity, in comparison to the solution for average steady state biomass (6.14), which diverges when Z_m goes to zero.

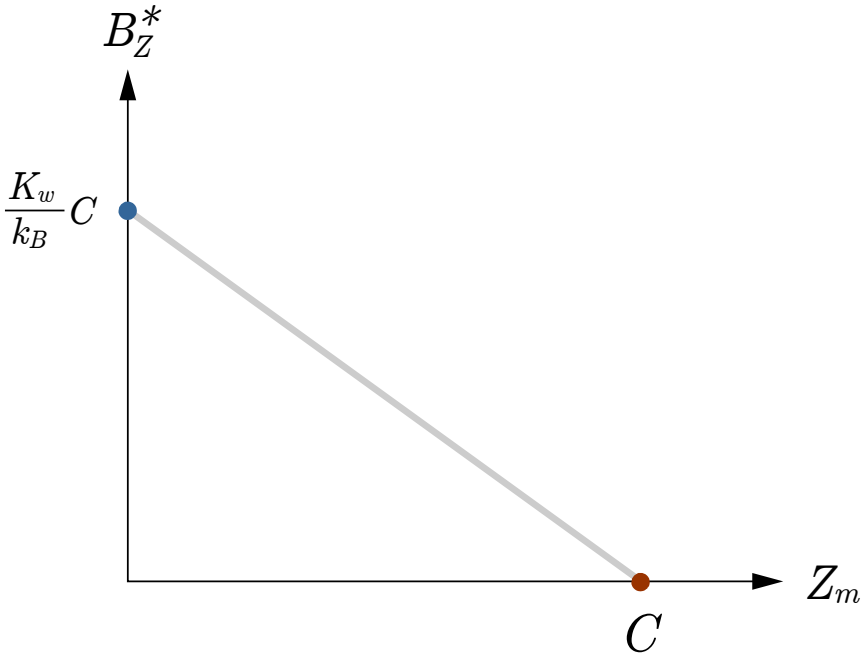

Figure 29: The solution for total mixed layer biomass at steady state B_Z^* (6.20) as a function of mixed layer depth Z_m (grey line). When the mixed layer depth crosses the optically uncoupled critical depth C, total biomass goes to zero (red point). When the mixed layer goes to zero total biomass goes to $K_w C/k_B$. The slope of the steady state solution (blue line) is given by $-K_w/k_B$.

6.2 AVERAGE AND TOTAL MIXED LAYER PRODUCTION

Central term to both equations for the time evolution of biomass, be it average biomass (6.3), or total biomass (6.5), is the production term. As biomass changes so too does the production term. The physical mechanism responsible for a change in the production term is light attenuation caused by biomass. Increasing biomass reduces the underwater irradiance, which then reduces production and vice versa. This interplay is central to understanding the effect of the biooptical feedback on system stability. Here we explore the time dependence of the production term and the relation between average and total mixed layer production.

For constant mixed layer depth and constant surface irradiance, time derivative of total instantaneous mixed layer production is:

$$\frac{\mathrm{d}}{\mathrm{d}t}\int_0^{Z_m} Bp^B(I)\,\mathrm{d}z = \frac{\mathrm{d}B}{\mathrm{d}t}\int_0^{Z_m} p^B(I)\,\mathrm{d}z + B\int_0^{Z_m}\frac{\mathrm{d}p^B(I)}{\mathrm{d}t}\,\mathrm{d}z, \tag{6.22}$$

where biomass terms come out of the integral due to biomass being constant with depth. The first term on the right hand side arises simply due to the change in biomass with time. Looking more closely at the integrand in the second term on the right hand side we have:

$$\frac{\mathrm{d}p^B(I)}{\mathrm{d}t} = \frac{\mathrm{d}p^B(I)}{\mathrm{d}I}\frac{\mathrm{d}I}{\mathrm{d}t}, \tag{6.23}$$

where the chain rule was applied. Invoking (1.24) the first derivative is always positive. The second one can easily be calculated by taking the time derivative of (6.7) to obtain:

$$\frac{\mathrm{d}I(z)}{\mathrm{d}t} = -\left(k_B z\frac{\mathrm{d}B}{\mathrm{d}t}\right) I(z), \tag{6.24}$$

which can be both positive or negative, depending on the sign of $\mathrm{d}B/\,\mathrm{d}t$. Using the derived expressions and taking the $\mathrm{d}B/\,\mathrm{d}t$ term out of the integral, enables us to rewrite (6.22) as:

$$\frac{\mathrm{d}}{\mathrm{d}t}\int_0^{Z_m} Bp^B(I)\,\mathrm{d}z = \frac{\mathrm{d}B}{\mathrm{d}t}\int_0^{Z_m}\left(p^B(I) - \left(k_B z B\right)\frac{\mathrm{d}p^B(I)}{\mathrm{d}I}I(z)\right)\mathrm{d}z. \tag{6.25}$$

We observe that the second term arises due the change in the light field caused by a change in biomass. All the quantities in it are positive, but given the minus sign, the contribution to the change of the production term depends on the sign of $\mathrm{d}B/\,\mathrm{d}t$, as expected. Without the biooptical feedback, which corresponds to $k_B = 0$, this term is zero and there is no effect of biomass on the light field and subsequently on the production term. In that case normalized mixed layer production is time independent and determined only by surface irradiance, attenuation due to water and the photosynthesis parameters. To gain more insight it is useful to look at these relations with $k_B = 0$.

At this stage we highlight the difference between average normalized instantaneous mixed layer production $\langle P \rangle^B_{Z_m}$ and total normalized instantaneous mixed layer production $P^B_{Z_m}$. The two are related simply via:

$$\langle P \rangle^B_{Z_m} = \frac{P^B_{Z_m}}{Z_m}, \tag{6.26}$$

where $P^B_{Z_m}$ is restated here for clarity:

$$P^B_{Z_m} = \int_0^{Z_m} p^B(I)\,\mathrm{d}z. \tag{6.27}$$

Total instantaneous mixed layer production can be viewed as a function of mixed layer depth $P^B_{Z_m} = P^B_{Z_m}(Z_m)$. As such it is an increasing function of mixed layer depth (Figure 30), shown by taking the derivative of (6.27) with respect to Z_m and acknowledging that production is positive by definition:

$$\frac{\partial P^B_{Z_m}}{\partial Z_m} = p^B\big(I(Z_m)\big) > 0. \tag{6.28}$$

However, average normalized instantaneous mixed layer production is a decreasing function of mixed layer depth:

$$\frac{\partial \langle P \rangle^B_{Z_m}}{\partial Z_m} = \frac{1}{Z_m}\left(\frac{\partial}{\partial Z_m}\int_0^{Z_m} p^B(I)\,\mathrm{d}z - \frac{1}{Z_m}\int_0^{Z_m} p^B(I)\,\mathrm{d}z\right). \tag{6.29}$$

The first term on the right hand side is recognized as (6.28), while the second is recognized as (6.26). Acknowledging this yields:

$$\frac{\partial \langle P \rangle^B_{Z_m}}{\partial Z_m} = \frac{1}{Z_m}\left[p^B\big(I(Z_m)\big) - \langle P \rangle^B_{Z_m}\right] < 0. \tag{6.30}$$

Because production declines with depth average mixed layer production $\langle P \rangle^B_{Z_m}$ will be higher than production at the mixed layer depth $p^B\big(I(Z_m)\big)$ (Figure 30). Therefore, average normalized instantaneous mixed layer production is a decreasing function of depth. Taking these insights into account we can proceed to analyse the response of mixed layer biomass, both average and total, to changing mixed layer depth.

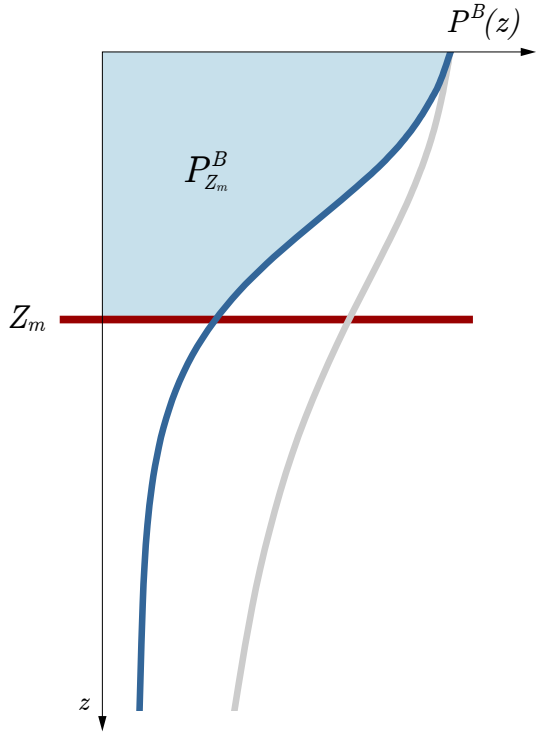

Figure 30: Total normalized mixed layer production (6.27) (light blue area) as a vertical integral of the instantaneous production profile (blue curve). Average mixed layer production (6.26) (grey curve) is a decreasing function of depth and the total mixed layer production is an increasing function of depth.

We now assume that mixed layer depth is time dependent, $Z_m = Z_m(t)$, and proceed to explore how mixed layer biomass responds. Two scenarios emerge naturally: mixed layer can become shallower, say as a result of heating, or it can become deeper, say as a result of convection. Thus far we have considered only the non-trivial steady state $B^* \neq 0$, implicitly assuming that the critical depth criterion is met. However, when the mixed layer depth is time dependent it may cross the optically uncoupled critical depth and the trivial steady state $B = 0$ has to be considered as well. Which of the two the states is stable can be answered using stability analysis, which we now proceed to do.

6.3 STABILITY ANALYSIS

Equation (6.3) describing the time evolution of average biomass can be written as:

$$\frac{\mathrm{d}B}{\mathrm{d}t} = f(B), \tag{6.31}$$

where now the function on the right hand side equals:

$$f(B) = \frac{1}{\chi}\left(\frac{1}{Z_m}\int_0^{Z_m} Bp^B(I)\,\mathrm{d}z - L^B B\right). \tag{6.32}$$

A plot of $f(B)$ is given below. At the point where $f(B) = 0$ we have a steady state. In our case there are two steady states (fixed points): the trivial steady state $B^* = 0$ and the non-trivial steady state $B^* \neq 0$ given by (6.14). Either can be stable or unstable. To classify them we will use linear stability analysis.

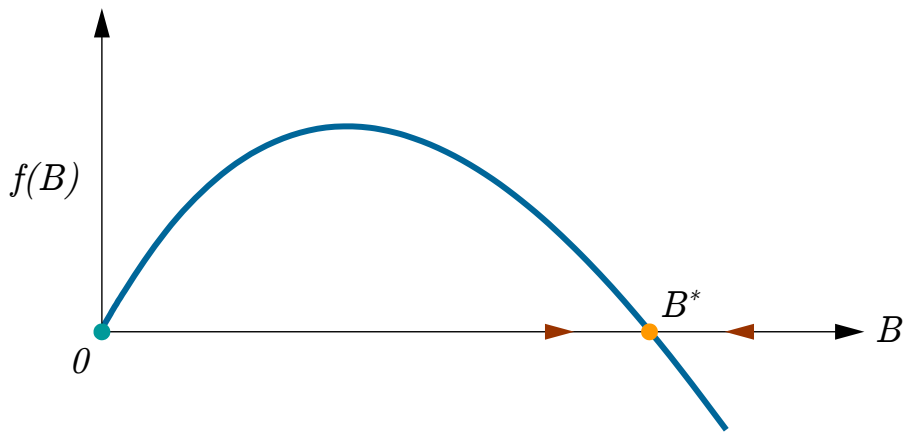

Figure 31: Plot of the $f(B)$ function from equation (6.31). Null points of $f(B)$ correspond to steady states: a trivial steady state $B^* = 0$ (green circle) and a non-trivial steady state $B^* \neq 0$ given by (6.14) (orange circle). As plotted the trivial steady state is unstable and the non-trivial is stable, as indicated by red arrows. This situation arises when $Z_m < C$.

Assume B^* is a fixed point and let δB be a small perturbation around B^*, such that we can approximate B in the vicinity of B^* as:

$$B = B^* + \delta B, \tag{6.33}$$

where $\delta B = \delta B(t)$. We are interested in how δB changes with time. If it declines to zero we will refer to the steady state as stable, whereas if it goes to infinity, we will refer to the steady state as unstable. To study how δB changes with time we take the derivative of the above to arrive at:

$$\frac{\mathrm{d}}{\mathrm{d}t}\delta B = f(B), \tag{6.34}$$

where (6.31) was used. By acknowledging (6.33) we get:

$$\frac{\mathrm{d}}{\mathrm{d}t}\delta B = f(B^* + \delta B), \tag{6.35}$$

which upon Taylor expansion around B^* yields:

$$\frac{\mathrm{d}}{\mathrm{d}t}\delta B = f(B^*) + \left.\frac{\mathrm{d}f(B)}{\mathrm{d}B}\right|_{B^*} \delta B, \tag{6.36}$$

where higher order terms were not considered. Acknowledging that $f(B^*) = 0$ leads to:

$$\frac{\mathrm{d}}{\mathrm{d}t}\delta B = \left.\frac{\mathrm{d}f(B)}{\mathrm{d}B}\right|_{B^*} \delta B, \tag{6.37}$$

The solution of which is simply:

$$\delta B(t) = \delta B(0) \exp\left(\left.\frac{\mathrm{d}f(B)}{\mathrm{d}B}\right|_{B^*} t\right), \tag{6.38}$$

where $\delta B(0)$ is the initial perturbation to B^*. Therefore, we are led to differentiate two situations: stable and unstable. The condition for stability reads:

$$\left.\frac{\mathrm{d}f(B)}{\mathrm{d}B}\right|_{B^*} < 0, \tag{6.39}$$

and the condition for instability reads:

$$\left.\frac{\mathrm{d}f(B)}{\mathrm{d}B}\right|_{B^*} > 0. \tag{6.40}$$

We observe that the first derivative of $f(B)$ determines stability.

The derivative of (6.32) with respect to B reads:

$$\frac{\mathrm{d}f(B)}{\mathrm{d}B} = \frac{1}{\chi}\left(\frac{1}{Z_m}\int_0^{Z_m} p^B(I)\,\mathrm{d}z + \frac{1}{Z_m}\int_0^{Z_m} B\frac{\mathrm{d}p^B(I)}{\mathrm{d}B}\,\mathrm{d}z - L^B\right). \tag{6.41}$$

To evaluate it at B^* we have to select a $p^B(I)$ function and carry out the differentiation, which is straightforward to do. An alternative route would be to recognize that at the non-trivial steady state $B^* > 0$ average production equals losses:

$$\frac{1}{Z_m}\int_0^{Z_m} p^B(I)\,\mathrm{d}z = L^B, \tag{6.42}$$

therefore the first and the third term on the right hand side cancel out at steady state B^*, leaving us with:

$$\left.\frac{\mathrm{d}f(B)}{\mathrm{d}B}\right|_{B^*} = \frac{1}{\chi}\frac{B}{Z_m}\int_0^{Z_m}\frac{\mathrm{d}p^B(I)}{\mathrm{d}B}\,\mathrm{d}z. \tag{6.43}$$

But, at the trivial steady state $B^* = 0$, this expression vanishes. Therefore, let us first observe what happens as biomass approaches zero. With $B^* \to 0$ prior expression also goes to zero and (6.41) becomes:

$$\lim_{B^*\to 0}\frac{\mathrm{d}f(B)}{\mathrm{d}B} = \frac{1}{\chi}\left(\frac{1}{Z_m}\int_0^{Z_m} p^B(I)\,\mathrm{d}z - L^B\right). \tag{6.44}$$

The vanishing of the (6.43) term reflects the fact that at low biomass, the contribution to light attenuation due to biomass, is negligible. Now if the mixed layer is sufficiently deep the average mixed layer production will be lower than the loss rate:

$$\frac{1}{Z_m}\int_0^{Z_m} p^B(I)\,\mathrm{d}z < L^B. \tag{6.45}$$

Therefore near zero biomass the slope of $f(B)$ shown in Figure 31 will be negative, as now shown in Figure 32. Following (6.39) the trivial steady state will be stable.

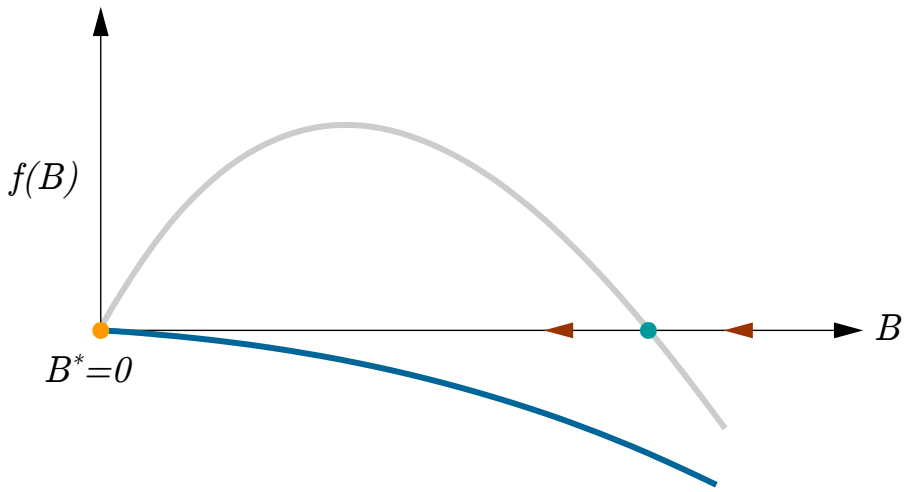

Figure 32: Plot of the $f(B)$ function from equation (6.31) when the trivial steady state is stable. When the loss term dominates over the production term the trivial steady state $B^* = 0$ (orange circle) becomes stable. The non-trivial steady state $B^* \neq 0$ given by (6.14) (green circle) is now the unstable fixed point. This situation arises when $Z_m > C$.

On the contrary, if the opposite of the prior expression holds, namely:

$$\frac{1}{Z_m} \int_0^{Z_m} p^B(I)\, \mathrm{d}z > L^B, \tag{6.46}$$

the slope of $f(B)$ at zero will be positive and the trivial steady state will be unstable. The trivial steady state being unstable opens the possibility for an existence of a non-trivial steady state. Looking at Figure 31 we observe that for there to be a non-trivial steady state the function $f(B)$ has to intersect the B axis at a point $B^* > 0$, implying the derivative of $f(B)$ at the non-trivial steady state (6.43), has to be negative. Using the chain rule in (6.43) produces:

$$\left.\frac{\mathrm{d}f(B)}{\mathrm{d}B}\right|_{B^*} = \frac{1}{\chi}\frac{B}{Z_m}\int_0^{Z_m} \frac{\mathrm{d}p^B(I)}{\mathrm{d}I}\frac{\mathrm{d}I}{\mathrm{d}B}\,\mathrm{d}z. \tag{6.47}$$

Following (6.7) we have:

$$\frac{\mathrm{d}I}{\mathrm{d}B} = -k_B z I, \tag{6.48}$$

and given (1.24) makes the previous expression negative, implying the non-trivial steady state is stable, according to (6.39).

The non-trivial steady state is stable due to the biooptical feedback. Without it the production term would be linear in B and $f(B)$ would not intersect the B axis. The steady states would either be zero, in case the loss term dominates, or infinity, in case the production term dominates. With the biooptical feedback, the biomass effects the underwater light field and for a given mixed layer depth higher biomass implies lower irradiance and vice versa. Consequently, lower irradiance implies less normalized production. Therefore the production term saturates with respect to biomass (also shown in Figure 24), while the loss term keeps growing linearly with biomass. Change of biomass per unit time is given as the difference between the two. This implies that the $f(B)$ function has to cross the B axis at some point, which is the non-trivial steady state B^*.

Thanks to this analysis we observe the deeper connection between the critical depth criterion and the stability of steady states. In this context the critical depth criterion can be reinterpreted as the criterion for change in stability properties of the trivial and the non-trivial steady state. With the critical depth criterion met (6.46), the non-trivial steady state is stable:

$$Z_m < C, \qquad B_u^* = 0, \qquad B_s^* > 0, \tag{6.49}$$

where B_s^* stands for stable and B_u^* stands for unstable. With the critical depth criterion not being met (6.45), the trivial steady state is stable:

$$Z_m > C, \qquad B_s^* = 0, \qquad B_u^* > 0. \tag{6.50}$$

In the jargon of dynamical system theory with Z_m crossing C the trivial steady state goes from a source to a sink, whereas the non-trivial steady state goes from a sink to a source. The critical depth C is the bifurcation point for the mixed layer depth Z_m.

6.4 MIXED LAYER DEEPENING

Assume the mixed layer biomass is at steady state and also assume zero biomass below the mixed layer, due to unfavourable growth conditions. Let the mixed layer depth be increasing with time (Figure 33), such that:

$$\frac{\mathrm{d}Z_m}{\mathrm{d}t} > 0. \tag{6.51}$$

Deepening does not effect total biomass directly, therefore (6.5) still holds:

$$\frac{\partial B_Z}{\partial t} = \frac{1}{\chi}\left(\int_0^{Z_m(t)} Bp^B(I)\,\mathrm{d}z - L^B B_Z \right), \tag{6.52}$$

now with the recognition that $Z_m = Z_m(t)$.

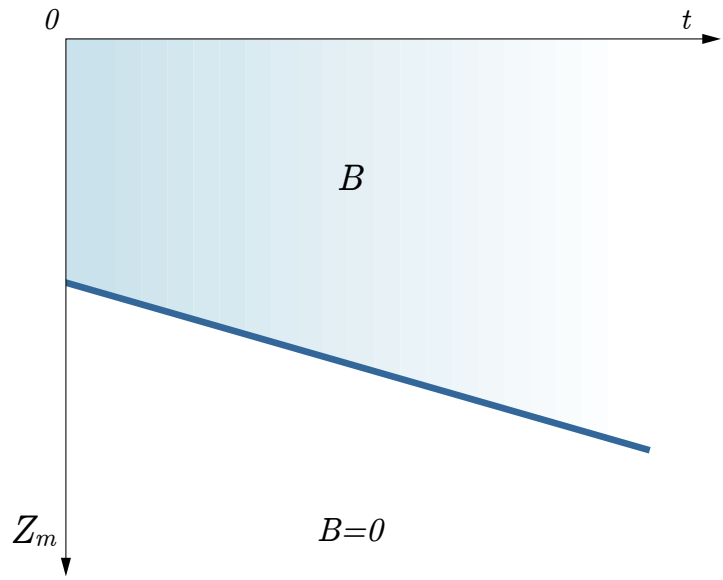

Figure 33: During mixed layer deepening (blue line) average biomass B (light blue surface) gets diluted due to entrainment of water from below the mixed layer, but the total mixed layer biomass B_Z is not affected (assuming no production, nor losses). We assume zero biomass below the mixed layer.

Due to the change in $Z_m(t)$ the production term gets affected and production now changes with time as:

$$\begin{aligned}\frac{\mathrm{d}}{\mathrm{d}t}\int_0^{Z_m} Bp^B(I)\,\mathrm{d}z = \frac{\mathrm{d}B}{\mathrm{d}t}\int_0^{Z_m}\left(p^B(I) - \left(k_B z B\right)\frac{\mathrm{d}p^B(I)}{\mathrm{d}I}I(z)\right)\mathrm{d}z \\ + Bp^B\Big[I(Z_m(t))\Big]\frac{\mathrm{d}Z_m(t)}{\mathrm{d}t}.\end{aligned} \tag{6.53}$$

where the Leibnitz integral rule was applied which produced the third term on the right hand side, which does not appear in (6.22) when the mixed layer depth did not change with time. It reflects the increase in total mixed layer production resulting from an increase in mixed layer depth. It is positive, implying it acts to increase total mixed layer production during deepening. Whether or not the resulting derivative of total mixed layer production with time will be positive or negative depends on the sum of the three terms.

The factor determining this is the sign of $\mathrm{d}B/\,\mathrm{d}t$. When it is positive the first term on the right hand side is positive and the second one is negative, reflecting the fact that less light penetrates through the mixed layer. However, when it is negative the first term is negative and the second one is positive, reflecting the fact that now more light penetrates through the mixed layer. Whether or not $\mathrm{d}B/\,\mathrm{d}t$ will be positive or negative, we can explore by looking at the equation for average mixed layer biomass, which now gets augmented to account for the effect of deepening.

During deepening average biomass gets diluted due to entrainment of water from below the mixed layer, which we assumed has zero biomass. To account for this an additional term appears in the biomass equation (6.3):

$$\frac{\partial B}{\partial t} = \frac{1}{\chi}\left(\frac{1}{Z_m}\int_0^{Z_m} Bp^B(I)\,\mathrm{d}z - L^B B\right) - \frac{1}{Z_m}\frac{\mathrm{d}Z_m}{\mathrm{d}t}B. \tag{6.54}$$

Therefore an asymmetry in the two equations arises. To analyse the consequences of this asymmetry we explore the response of average and total biomass in the following scenario.

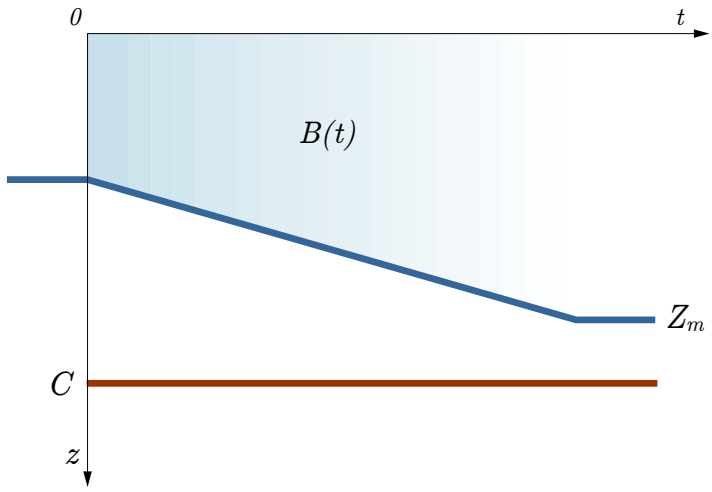

Figure 34: Response of mixed layer biomass to deepening under $Z_m(t) < C$. The system is initially at steady state with average biomass B_1^*. During deepening biomass changes with time. After deepening stops the system acquires a new steady state with average biomass B_2^*, which following (6.14) is less than B_1^*. Following (6.20) the same argument holds for total biomass.

Assume the system is at steady state B_1^* and $(B_Z^*)_1$ given by (6.14) and (6.20). Changing Z_m will then change the steady state and in both cases the new steady state will be of lower biomass, be it average B_2^* or total biomass $(B_Z^*)_2$, given that the final mixed layer depth is deeper than the initial. Because the steady state is stable the system will tend towards this new steady state and average and total biomass will both decline with time. However, if the system is not initially at steady state, biomass may both decline or increase with time depending on the initial condition in relation to the final steady state.

The response to deepening can also be interpreted using the notion of the critical depth. The optically coupled critical depth will converge towards the mixed layer depth. If initially at steady state S will be equal to the mixed layer depth. During deepening S will change and once the mixed layer settles onto the new depth S will continue changing with time until it too equals this new mixed layer depth.

6.5 MIXED LAYER SHALLOWING

Let the mixed layer depth be decreasing with time, such that:

$$\frac{\mathrm{d}Z_m}{\mathrm{d}t} < 0. \tag{6.55}$$

Below the mixed layer we assume zero biomass. With no production, nor losses, shallowing does not effect average biomass directly, therefore (6.3) still holds:

$$\frac{\partial B}{\partial t} = \frac{1}{\chi}\left(\frac{1}{Z_m(t)} \int_0^{Z_m(t)} B p^B(I)\,\mathrm{d}z - L^B B\right). \tag{6.56}$$

again with the recognition that $Z_m = Z_m(t)$ (Figure 35).

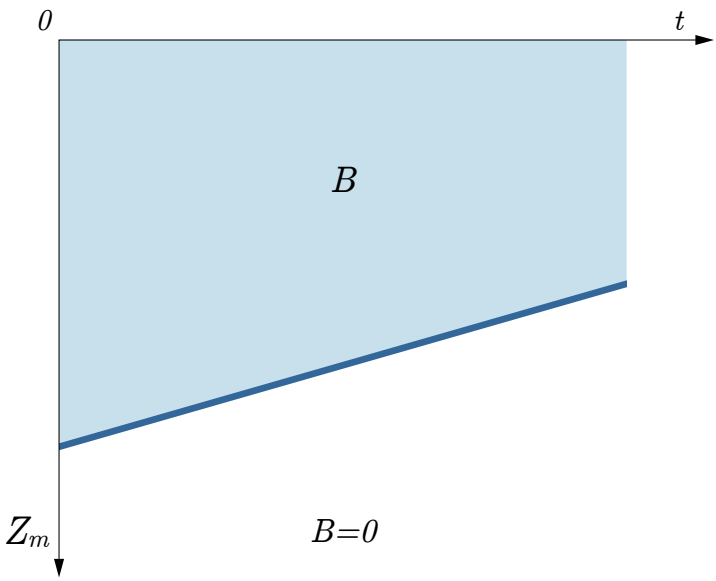

Figure 35: During mixed layer shallowing (blue line) average mixed layer biomass B (light blue surface) does not get diluted, but the total mixed layer biomass B_Z is reduced due to detrainment of biomass which now finds itself below the mixed layer (assuming no production, nor losses). We assume zero biomass below the mixed layer.

Although average biomass is not affected directly by shallowing, the production term is, and therefore subsequently biomass gets affected. To see how the production term changes now, we can explore this change in the same manner as was done in expression (6.53):

$$\begin{aligned}\frac{\mathrm{d}}{\mathrm{d}t}\int_0^{Z_m} Bp^B(I)\,\mathrm{d}z = \frac{\mathrm{d}B}{\mathrm{d}t}\int_0^{Z_m}\left(p^B(I) - \left(k_B z B\right)\frac{\mathrm{d}p^B(I)}{\mathrm{d}I}I(z)\right)\mathrm{d}z \\ - Bp^B\Big[I(Z_m(t))\Big]\left|\frac{\mathrm{d}Z_m(t)}{\mathrm{d}t}\right|,\end{aligned} \tag{6.57}$$

with the difference that now the time derivative of the mixed layer depth has a negative sign. The third term on the right hand side now reflects the decrease in total mixed layer production resulting from a decrease in mixed layer depth. It is negative implying it acts to decrease total mixed layer production during shallowing. This occurs due to detrainment of biomass from the mixed layer during shallowing. The biomass which now finds itself below the mixed layer no longer contributes to mixed layer production.

In line with this reasoning total biomass is affected by shallowing directly, since now a portion of biomass gets detrained from the mixed layer and the equation for total biomass now becomes:

$$\frac{\partial B_Z}{\partial t} = \frac{1}{\chi}\left(\int_0^{Z_m(t)} Bp^B(I)\,\mathrm{d}z - L^B B_Z\right) - \frac{1}{Z_m}\left|\frac{\mathrm{d}Z_m}{\mathrm{d}t}\right|B_Z. \tag{6.58}$$

Therefore, once again an asymmetry arises in the equations. Whereas during deepening it was the equation for average biomass in which an additional term appeared, now it is the equation for total biomass in which an additional term appears. Here too in order to analyse the consequences of the asymmetry in the equations for average and total biomass we explore the response of average and total biomass in the following scenario.

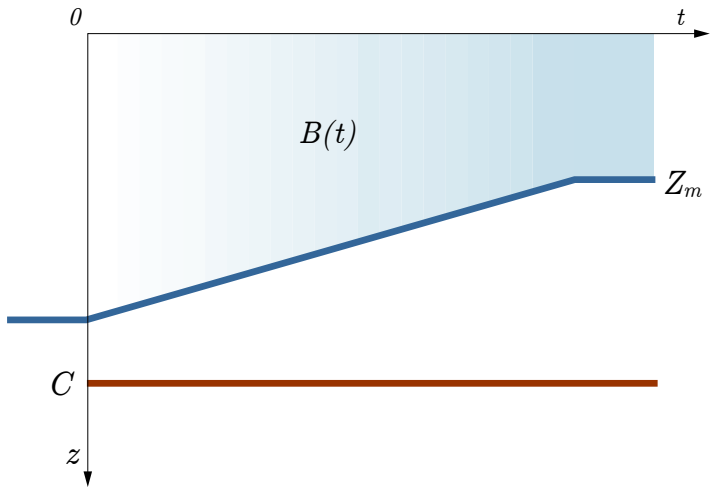

Figure 36: Response of mixed layer biomass to shallowing under $Z_m(t) < C$. The system is initially at steady state with average biomass B_1^*. During shallowing biomass changes with time. After shallowing stops the system acquires a new steady state with average biomass B_2^*, which following (6.14) is higher than B_1^*. Following (6.20) the same argument holds for total biomass.

Assume the system is at steady state B_1^* and $(B_Z^*)_1$ given by (6.14) and (6.20). Changing Z_m will then change the steady state and in both cases the new steady state will be of higher biomass, be it average B_2^* or total biomass $(B_Z^*)_2$, given that the final mixed layer depth is shallower than the initial. Because the steady state is stable the system will tend towards this new steady state and average and total biomass will both increase with time. However, if the system is not initially at steady state, biomass may both decline or increase with time depending on the initial condition in relation to the final steady state.

The response to shallowing can also be interpreted using the notion of the critical depth. The optically coupled critical depth will converge towards the mixed layer depth. If initially at steady state S will be equal to the mixed layer depth. During shallowing S will change and once the mixed layer settles onto the new depth S will continue changing with time until it too equals this new mixed layer depth.

6.6 CROSSING THE CRITICAL DEPTH

In the above analysis it was assumed that the mixed layer depth does not cross the critical depth at any time, therefore the non-trivial steady state is the stable steady state. However, as it was demonstrated in the stability analysis the trivial steady state becomes the stable steady state once the mixed layer crosses the critical depth. This behaviour can be summarised using a bifurcation diagram. If we treat the mixed layer depth Z_m as a parameter and plot the steady state solution B_Z^* as a function of Z_m we obtain Figure 37.

Starting from $Z_m = 0$ there are two steady states $B_Z^* = 0$ and $B_Z^* > 0$. The $B_Z^* = 0$ is the unstable state and $B_Z^* > 0$ is the stable state, implying all initial conditions with $Z_m < C$ lead towards $B_Z^* > 0$. However, upon the mixed layer crossing the critical depth C, the non-trivial steady state vanishes and the only stable steady state left is the trivial steady state. In the jargon of dynamical systems theory the critical depth C is the bifurcation point for the mixed layer biomass.

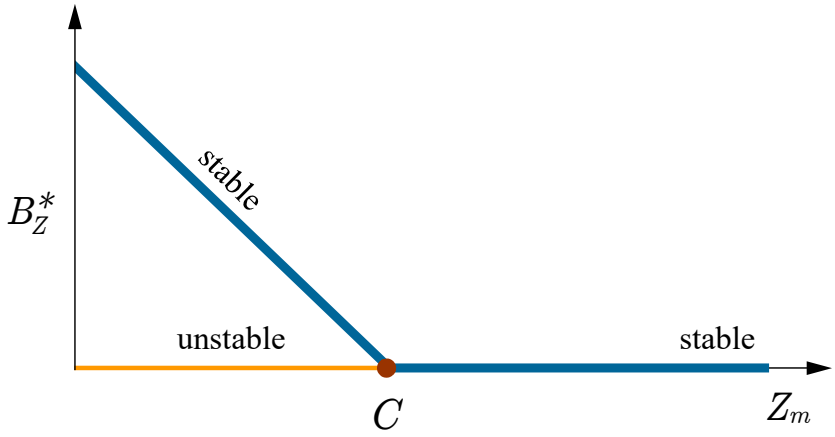

Figure 37: Bifurcation diagram for total biomass B_Z with the mixed layer depth Z_m as the bifurcation parameter. For Z_m shallower than the optically uncoupled critical depth C zero biomass is the unstable steady state (orange line) and $B^* > 0$, given by (6.20), is the stable steady state (blue line). Once Z_m becomes deeper than C, zero biomass becomes the stable steady state (blue line).

6.7 PROBLEMS

1. Make a numerical model which calculates the time evolution of average (6.3) and total (6.5) mixed layer biomass. Run the model to steady state and compare the simulation results to the analytical solutions for steady state (6.14) and (6.20). Observe how the model behaves if the initial condition is set to above or below the steady state solution.

2. For the above model simulations calculate the irradiance at the base of the mixed layer and observe it as a function of time. Compare the irradiance at steady state to the irradiance predicted by expression (6.19).

3. Plot the normalized mixed layer production (6.27) as a function of mixed layer depth. Observe how the function behaves in the limit of large mixed layer depth. Contrast this plot with the plot of average normalized mixed layer production (6.26), also as a function of mixed layer depth. Again, observe how average normalized mixed layer production behaves in the limit of large mixed layer depth. Finally, plot the instantaneous normalized production profile (2.2) on the same plot as average normalized mixed layer production, as shown qualitatively in Figure 30. Observe the difference between production and average mixed layer production at the mixed layer base.

4. Carry out the stability analysis from section 7.3 with the linear photosynthesis irradiance function. State the obtained expressions (6.41) and (6.43) explicitly.

5. Make a numerical model with a linearly increasing mixed layer depth:

$$Z_m(t) = Z_m(0) + w_m t, \tag{6.59}$$

where $Z_m(0)$ is the mixed layer depth at initial time and w_m is the rate of deepening. Numerically simulate the evolution of total mixed layer biomass $B_Z(t)$ using (6.52) and the evolution of average mixed layer

biomass $B(t)$ using (6.54). Plot the time evolution $B_Z(t)$ and $B(t)$. Also plot the time evolution of normalized mixed layer production $P^B_{Z_m}(t)$ and mixed layer production $P_{Z_m}(t)$. Finally, make the simulations with varying values of w_m.

6. Modify the previous model to a numerical model with a linearly shallowing mixed layer depth:

$$Z_m(t) = Z_m(0) - w_m t, \tag{6.60}$$

where $Z_m(0)$ is the mixed layer depth at initial time and w_m is the rate of shallowing. Numerically simulate the evolution of total mixed layer biomass $B_Z(t)$ using (6.58) and the evolution of average mixed layer biomass $B(t)$ using (6.56). Plot the time evolution $B_Z(t)$ and $B(t)$. Also plot the time evolution of normalized mixed layer production $P^B_{Z_m}(t)$ and mixed layer production $P_{Z_m}(t)$. Finally, make the simulations with varying values of w_m.

7. Start the model at initial mixed layer depth $Z_m(0) = Z_i$ and with steady state biomass corresponding to that depth, calculated using (6.14) for B^* and (6.20) for B^*_Z. Modify the prior model such that after a time period T mixed layer stops deepening/shallowing and settles onto a final mixed layer depth, such that $Z_m(t) = Z_f$, for $t > T$. For the cases of mixed layer deepening/shallowing, run this model with different initial conditions to observe the difference in the response of mixed layer biomass. Start the model with initial biomass below or above the steady state biomass and observe under which conditions the biomass grows or declines over time.

7

BIOMASS PROFILE

In a physical sense phytoplankton cells are particles suspended in a fluid under gravity. Naturally, some cells are not neutrally buoyant and sink through the water column. Sinking acts to remove phytoplankton from the sunlight uppermost part of the ocean and if not prevented the ultimate faith of all cells would simply lie in the abyss.

The process opposing sinking is mixing. Thus far we have taken mixing to be instantaneous and ignored sinking, which is a rather strong assumption. A more realistic one would be to have the strength of mixing vary, as naturally occurs in the ocean. Mixing, if not too strong and not too deep, keeps the cells close to the surface and phytoplankton populations can be sustained.

In addition the biological processes act as well, namely production and losses, which act to increase or decrease biomass irrespective of mixing and sinking. In this context mixing and sinking act to redistribute biomass vertically. The vertical distribution of biomass affects the light field, which subsequently sets the rate of production at depth.

Therefore, all the mentioned processes act simultaneously to produce a vertically dependent biomass profile. In this chapter we proceed to build models which describe this vertical structure. We focus on the role of light, mixing and sinking and explore steady state solutions for the biomass profile. We derive mathematical conditions which describe properties of steady state solutions.

7.1 PROBLEM FORMULATION

Consider now that mixing is not instantaneous so that the assumption of uniform biomass no longer holds and we have:

$$B = B(z,t). \tag{7.1}$$

Assume that the initial condition on biomass is known:

$$B_0 = B(z,0). \tag{7.2}$$

The processes which act to change the biomass profiles over time are both biological and physical. Of biological processes we will model primary production and losses, whereas of the physical we will model mixing and sinking. For the production term we use (2.2):

$$P^B(z,t) = p^B\big(I(z,t)\big), \tag{7.3}$$

with the accompanying light model:

$$\frac{\mathrm{d}I}{\mathrm{d}z} = (K_w + k_B B)I, \tag{7.4}$$

such that irradiance at depth becomes:

$$I(z,t) = I_0(t)\exp\left(-\int_0^z \big(K_w + k_B B(z',t)\big)\,\mathrm{d}z'\right), \tag{7.5}$$

with z' as a dummy variable for integration. For the losses we use a vertically uniform loss term:

$$L^B(z,t) = L^B. \tag{7.6}$$

With only these two processes taken into account the growth equation becomes:

$$\frac{\partial B}{\partial t} = \frac{1}{\chi}\Big(P^B(z,t) - L^B\Big)B. \tag{7.7}$$

This equation holds in case of no mixing and no sinking. Together with equation (7.5) it forms an integro-differential system, the backbone of which is the bio-optical feedback. We now explore the dynamics of (7.5) and (7.7) in more detail. Afterwards we model sinking and mixing, one by one, before we turn to studying their combined effects.

7.2 COMPENSATION DEPTH

Due to attenuation, irradiance declines with depth (2.13) and so does production (2.38). Assuming normalized production at the surface is larger than losses:

$$P^B(0) > L^B, \tag{7.8}$$

there will be a depth at which production will equal losses, termed the **compensation depth** z_c (m) (Figure 38):

$$P^B(z_c) = L^B. \tag{7.9}$$

In principle, using an inverse of P^B the compensation depth could be expressed explicitly as:

$$z_c = (P^B)^{-1}(L^B), \tag{7.10}$$

where $(P^B)^{-1}$ stands for the inverse. In practice, using the exponential photosynthesis irradiance function (1.18) in (7.9) yields:

$$P_m^B\Big(1 - \exp\Big(-\alpha^B I(z_c)\Big/P_m^B\Big)\Big) = L^B, \tag{7.11}$$

from which the compensation irradiance $I_c = I(z_c)$ follows as:

$$I_c = -\frac{P_m^B}{\alpha^B}\ln\left(1 - \frac{L^B}{P_m^B}\right). \tag{7.12}$$

To express z_c form I_c the irradiance model itself needs to be inverted. Using (7.5) as the irradiance model gives I_c as:

$$I_c = I_0 \exp\left(-\int_0^{z_c}\Big(K_w + k_B B(z')\Big)\,\mathrm{d}z'\right). \tag{7.13}$$

By combining the previous two expressions we get:

$$K_w z_c + k_B \int_0^{z_c} B(z')\,\mathrm{d}z' = -\ln\left(-\frac{P_m^B}{\alpha^B I_0}\ln\left(1 - \frac{L^B}{P_m^B}\right)\right). \tag{7.14}$$

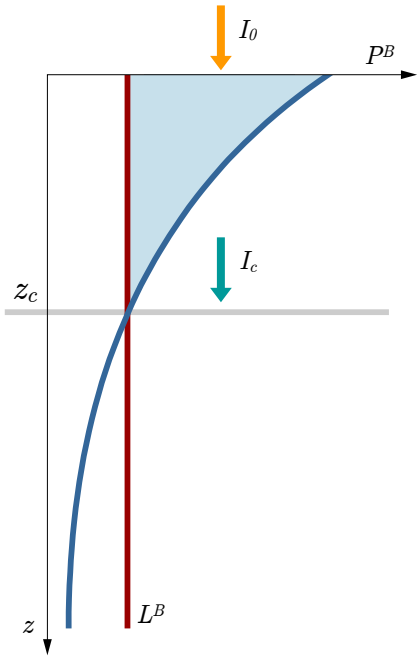

Figure 38: Due to the attenuation of light photosynthesis P^B (blue curve) declines with depth and has to at some depth equal the loss rate L^B (red line). This depth is called the compensation depth z_c (grey line).

Taking the time derivative of the obtained expression, while acknowledging $z_c = z_c(t)$, yields:

$$\frac{\partial z_c}{\partial t} = -\frac{k_B}{K_w + k_B B(z_c)} \int_0^{z_c} \frac{\partial B(z')}{\partial t} \, \mathrm{d}z', \tag{7.15}$$

where the Leibnitz integral rule was applied. We observe that as the biomass above the compensation depth grows, which it does by definition, the compensation depth becomes shallower (Figure 38). Therefore, with time all the biomass will be accumulated in a very thin surface layer:

$$\lim_{t \to \infty} B(z,t) = \int_0^{\infty} B(z)\delta(z) \, \mathrm{d}z. \tag{7.16}$$

7.3 THE EFFECT OF SINKING ON THE BIOMASS PROFILE

Let us assume the phytoplankton sink with a **sinking speed** w ($\mathrm{m\,s^{-1}}$). For now, assume that biomass is conserved, such that neither production nor losses affect B. In this case we can write:

$$B(z, t + \Delta t) = B(z - w\Delta t, t) \tag{7.17}$$

This expression states that biomass at depth z and time $t + \Delta t$ came from depth $z - w\Delta t$ and time t (Figure 39). In the limit of small Δt, Taylor series expansion of both sides around $B(z, t)$ gives:

$$B(z, t) + \frac{\partial B}{\partial t}\Delta t \approx B(z, t) - w\frac{\partial B}{\partial z}\Delta t. \tag{7.18}$$

Cancelling terms on both sides yields the **advection equation**:

$$\frac{\partial B}{\partial t} + w\frac{\partial B}{\partial z} = 0. \tag{7.19}$$

The exact solution to this equation, under no flux boundary condition at the surface, is set by the initial condition $B_0(z)$ and reads:

$$B(z, t) = B_0(z - wt). \tag{7.20}$$

It is important to stress that the shape of the initial condition does not change with time, it simply gets advected with depth. Therefore, the ultimate fate of any phytoplankton is to sink out of the photic zone (Figure 39).

Now assume that during Δt production and losses also affect B. Equation (7.17) now becomes:

$$B(z, t + \Delta t) = B(z - w\Delta t, t)\left[1 + \frac{1}{\chi}\left(P^B(z - w\Delta t, t) - L^B\right)\Delta t\right]. \tag{7.21}$$

This expression states that during sinking, production acts to increase biomass and losses act to decrease biomass. Phytoplankton that started off at depth $z - w\Delta t$ and time t will experience production given by $B(z - w\Delta t, t)P^B(z - w\Delta t, t)$ and losses given by $B(z - w\Delta t, t)L^B$. Once

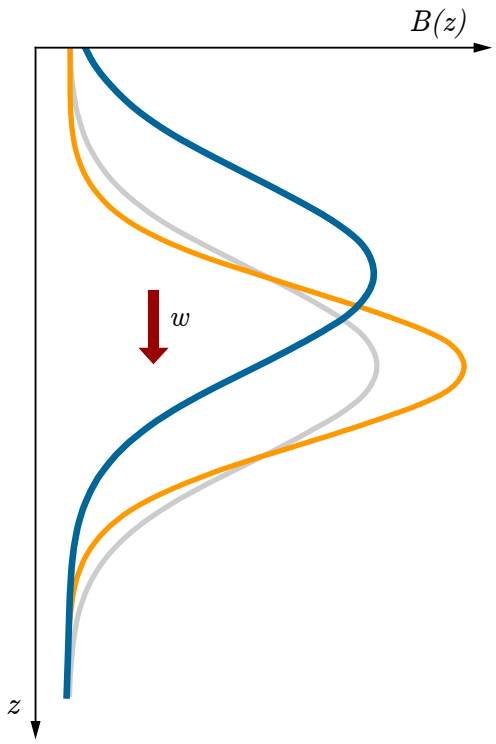

Figure 39: Subjected to sinking the phytoplankton will simply be "washed out" out of the photic zone. Each phytoplankton cell increases its depth due to sinking w (red arrow). The biomass profile (blue curve) gets advected with depth (grey curve), but it also changes shape due to production and losses during sinking (orange curve).

again, in the limit of small Δt, Taylor series expansion of both $B(z,t)$ and $P^B(z,t)$ gives:

$$\begin{aligned} B(z,t) + \frac{\partial B}{\partial t}\Delta t \approx B(z,t) - w\frac{\partial B}{\partial z}\Delta t \\ + \frac{1}{\chi}\left[B(z,t) - w\frac{\partial B}{\partial z}\Delta t\right]\left[P^B(z,t) - w\frac{\partial P^B}{\partial z}\Delta t\right]\Delta t \\ + \frac{1}{\chi}\left[B(z,t) - w\frac{\partial B}{\partial z}\Delta t\right]L^B\Delta t. \end{aligned} \tag{7.22}$$

Keeping only the leading order terms yields the following equation:

$$\frac{\partial B}{\partial t} + w\frac{\partial B}{\partial z} = \frac{1}{\chi}\left(P^B(z,t) - L^B\right)B, \tag{7.23}$$

which describes the combined effects of sinking, production and losses. The solution to this equation at steady state $\partial B/\partial t = 0$ is:

$$B^*(z) = 0. \tag{7.24}$$

To gain insight into as to why this is the solution we switch our point of view to what is called the **Lagrangian description** of fluid motion.

Consider a water parcel at depth z_0 at time $t = 0$ (Figure 40). Its biomass concentration is equal to $B(z_0, 0) = B_0(z_0)$. Without production, nor losses, biomass in the water parcel does not change over time. Cells simply sink such that the biomass concentration found at that depth, namely $B_0(z_0)$, will at later time be at depth $z_0 + wt$. Eventually, all cells sinks out of the photic zone.

Now, let us add the effects of production and losses during sinking. Due to sinking, instantaneous production experienced by the cells changes with depth. At any given time, instantaneous normalized production is calculated at the depth at which the cells are located, given as $P^B(z_0 + wt, t)$, whereas losses are constant with depth (7.6). Therefore, the equation describing the change of biomass at $z_0 + wt$ over time is:

$$\left.\frac{\partial B}{\partial t}\right|_{z_0+wt} = \frac{1}{\chi}\left(P^B(z_0 + wt, t) - L^B\right)B(z_0 + wt). \tag{7.25}$$

Formally, by changing the coordinate system from a stationary one, to the one sinking with speed w we have transformed a partial differential equation (7.23) to an ordinary differential equation (7.25). The formal solution to the obtained equation is:

$$B(z_0 + wt, t) = B_0(z_0)\exp\left[\frac{1}{\chi}\int_0^t \left(P^B(z_0 + wt, t') - L^B\right)\mathrm{d}t'\right], \tag{7.26}$$

with t' is a dummy variable for integration.

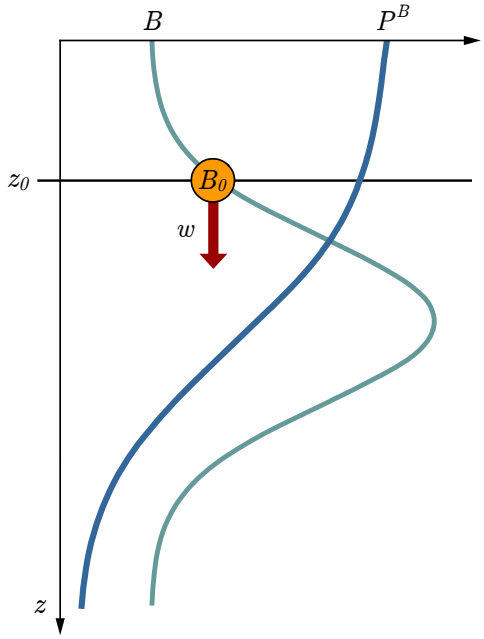

Figure 40: A patch of phytoplankton with biomass B_0 found at depth z_0 (orange circle) sinks with speed w (red arrow). As it sinks it experiences varying light conditions $I(z_0 + wt, t)$ and subsequently production $P^B(z_0 + wt, t)$.

With the bio-optical feedback (7.5) in place, $P^B(z_0 + wt, t)$ is arguably complicated to calculate. Using (1.18) for the photosynthesis irradiance functions gives:

$$P^B(z_0 + wt, t) = P_m^B \left(1 - \exp\left(-\alpha^B I(z_0 + wt, t) \Big/ P_m^B\right)\right), \tag{7.27}$$

which is coupled to the light penetration model:

$$I(z_0 + wt, t) = I_0(t) \exp\left(-\int_0^{z_0+wt} \left(K_w + k_B B(z', t)\right) \mathrm{d}z'\right), \tag{7.28}$$

such that irradiance at depth $z_0 + wt$ requires information on biomass from the surface up to that depth. Therefore, to calculate the change in biomass at depth, information on biomass above that depth is required.

However, valuable insight can be gained by ignoring the bio-optical feedback and finding an analytical solution to (7.26). This solution is valid in the regime of:

$$k_B B \ll K_w. \tag{7.29}$$

In this case light at depth $z_0 + wt$ becomes:

$$I(z_0 + wt, t) = I_0(t) \exp\big(-K_w(z_0 + wt)\big), \tag{7.30}$$

and normalized production reads:

$$P^B(z_0 + wt, t) = P_m^B \left[1 - \exp\left(-\frac{\alpha^B I_0(t)}{P_m^B} \exp\big(-K_w(z_0 + wt)\big)\right)\right]. \tag{7.31}$$

Going back to (7.26) this expression has to be integrated over time. For simplicity, we set $I_0(t) = I_0^m$ such that the integral we need to solve is:

$$\int_0^t P^B(z_0 + wt, t')\,\mathrm{d}t' = \int_0^t P_m^B \left[1 - \exp\left(-\frac{\alpha^B I_0^m}{P_m^B} \exp\big(-K_w(z_0 + wt')\big)\right)\right] \mathrm{d}t'. \tag{7.32}$$

Using (2.18) and following the same procedure we used in finding the analytical solution for the daily production profile (2.33), transforms the prior expression into:

$$\int_0^t P^B(z_0 + wt, t')\,\mathrm{d}t' = -P_m^B \sum_{n=1}^{\infty} \frac{(-I_*^m)^n}{n!} \int_0^t \exp\big(-K_w(z_0 + wt')\big)^n \mathrm{d}t. \tag{7.33}$$

The integral on the right hand side is a standard form integral and the solution to (7.26) reads:

$$B(z_0 + wt, t) = B_0(z_0) \exp\left[\frac{P_m^B}{\chi} \sum_{n=1}^{\infty} \frac{(I_*^m)^n \exp\left(-K_w n(z_0 + wt)\right)}{K_w\ w\ n\ n!} - L^B t\right]. \tag{7.34}$$

We observe that with time both exponentials go to zero, irrespective of $B_0(z_0)$, justifying (7.24) as the solution to (7.23) at infinite time and consistent with the conclusion that sinking phytoplankton cells get washed out of the photic zone.

7.4 THE EFFECT OF MIXING ON THE BIOMASS PROFILE

Let us assume the phytoplankton are actively mixed due to turbulence (Figure 41). We model the effect of turbulence by modifying the sinking speed such that it has an additional random component:

$$w = \langle w \rangle + w', \tag{7.35}$$

where $\langle w \rangle$ is the average and w' is the random component, whose average is by definition zero. The average is taken over a characteristic time scale T chosen to be short enough such that there is a change in the average, but long enough such that the fluctuations cancel out [10]. The averaging is defined by:

$$\langle x \rangle = \frac{1}{T} \int_0^T x(t)\, \mathrm{d}t. \tag{7.36}$$

We assume that w is depth independent, implying mixing is uniform throughout the water column. Due to mixing we also model biomass as having an average component $\langle B \rangle$ and a fluctuation B', such that biomass reads:

$$B = \langle B \rangle + B', \tag{7.37}$$

with the property that the average of B' is by definition zero. Prior to inserting these two expression into (7.23) we acknowledge that due to $w \neq w(z)$ we can rewrite it as:

$$\frac{\partial B}{\partial t} + \frac{\partial}{\partial z}(wB) = \frac{1}{\chi}\Big(P^B(z,t) - L^B\Big)B. \tag{7.38}$$

Now, after inserting w from (7.35) and B from (7.37) we get:

$$\frac{\partial}{\partial t}\Big(\langle B \rangle + B'\Big) + \frac{\partial}{\partial z}\Big[\Big(\langle w \rangle + w'\Big)\Big(\langle B \rangle + B'\Big)\Big] = \frac{1}{\chi}\Big(P^B(z,t) - L^B\Big)\Big(\langle B \rangle + B'\Big). \tag{7.39}$$

By averaging this equation using (7.36), it transforms into:

$$\frac{\partial \langle B \rangle}{\partial t} + \frac{\partial}{\partial z}\Big(\langle w \rangle \langle B \rangle + \langle w'B' \rangle\Big) = \frac{1}{\chi}\Big(P^B(z,t) - L^B\Big)\langle B \rangle, \tag{7.40}$$

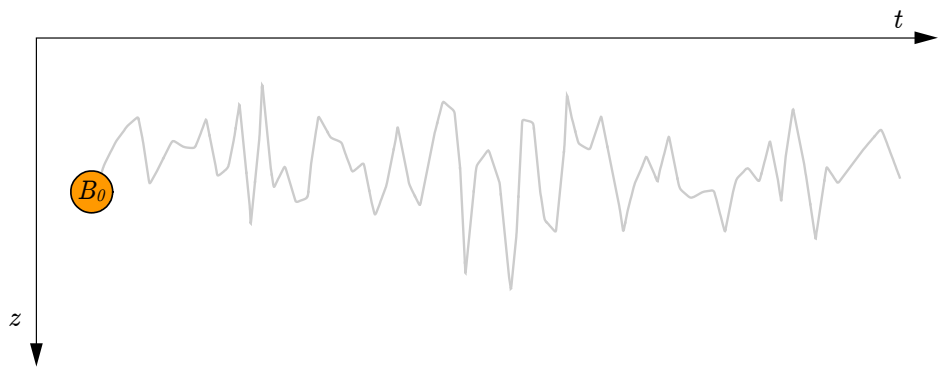

Figure 41: Lagrangian view of random motion due to turbulence. A patch of phytoplankton (orange circle) will experience fluctuations in its position (grey) due to the random component of velocity (7.35). In an Eulerian description this effect is parametrised via the turbulent mixing flux (7.41).

where we have acknowledged that the average of a product is not the same as the product of the averages. The third term on the left hand side is typically parametrized as:

$$-\frac{\partial}{\partial z}\left\langle w'B'\right\rangle = M\frac{\partial\left\langle B\right\rangle}{\partial z}, \tag{7.41}$$

where M is the **mixing coefficient** ($\mathrm{m^2\,s^{-1}}$). With this our equation becomes:

$$\frac{\partial B}{\partial t} + w\frac{\partial B}{\partial z} = \frac{1}{\chi}(P^B(z,t) - L^B)B + M\frac{\partial^2 B}{\partial z^2}, \tag{7.42}$$

where we have written $\left\langle B\right\rangle$ simply as B, with the understanding that biomass is a function of depth and time $B = B(z,t)$.

The derived equation can also be written using the notion of **flux** F ($\mathrm{mg\,Chl\,m^{-2}\,s^{-1}}$), with contributions from sinking and mixing:

$$F = wB - M\frac{\partial B}{\partial z}. \tag{7.43}$$

In this notation the above equation becomes simply:

$$\frac{\partial B}{\partial t} = \frac{1}{\chi}(P^B(z,t) - L^B)B - \frac{\partial F}{\partial z}. \tag{7.44}$$

As a first step in our analysis we set $w = 0$ and focus on the effects of mixing in shaping the biomass profile, along with production and losses. Our starting equation is:

$$\frac{\partial B}{\partial t} = \frac{1}{\chi}(P^B(z,t) - L^B)B + M\frac{\partial^2 B}{\partial z^2}, \tag{7.45}$$

coupled to equation (7.5) for irradiance. The problem as stated requires specification of boundary conditions. At the surface we specify no flux as the boundary condition:

$$M\frac{\partial B}{\partial z}\bigg|_0 = 0, \tag{7.46}$$

whereas at infinite depth we specify zero biomass:

$$B(\infty, t) = 0. \tag{7.47}$$

Our primary interest lies in exploring the properties of the non-trivial steady state $B^* > 0$. At steady state equation (7.45) reduces to:

$$M\frac{\partial^2 B^*}{\partial z^2} = -\frac{1}{\chi}(P^B(z) - L^B)B^*. \tag{7.48}$$

We note that at steady state production is time independent and we write $P^B(z,t) = P^B(z)$. The stated boundary conditions provide enough information to qualitatively describe the steady state solution to (7.48).

At the surface, boundary condition (7.46) sets the slope of B^* to zero, implying there is a maximum in biomass at the surface (Figure 42):

$$B(0) = B_m. \tag{7.49}$$

To see if this is a local, or a global maximum, we observe the second derivative of B. Since above z_c production exceeds losses, following (7.48) from the surface till z_c we have:

$$\frac{\partial^2 B^*}{\partial z^2} < 0, \qquad z < z_c, \tag{7.50}$$

implying the biomass profile declines with depth (Figure 42):

$$\frac{\partial B^*}{\partial z} < 0. \tag{7.51}$$

At the compensation depth z_c, by definition (7.9), production equals losses, therefore by again following (7.48) we have:

$$\left.\frac{\partial^2 B^*}{\partial z^2}\right|_{z_c} = 0, \tag{7.52}$$

implying there is an inflexion point z_i at the compensation depth (Figure 42). Below the inflexion point the second derivative changes sign:

$$\frac{\partial^2 B^*}{\partial z^2} > 0, \qquad z > z_c, \tag{7.53}$$

pushing the slope of B up. Because the normalized production $P^B(z)$ declines with depth it only crosses the loss term at z_c, therefore there is no other inflexion point and the biomass profile continues to decline with depth, finally ending in $B^*(\infty) = 0$.

We can gain more information on B^* by integrating (7.48) from the surface to depth z:

$$\left.\frac{\partial B^*}{\partial z}\right|_z = -\frac{1}{M\chi}\int_0^z \left(P^B(z') - L^B\right) B^*(z')\,\mathrm{d}z', \tag{7.54}$$

where we have acknowledged the surface boundary condition (7.46), with z' as a dummy variable for integration. According to the obtained expression the slope of the steady state biomass profile is dictated by the difference between integrated production and losses, divided by M (Figure 42). It is inversely proportional to mixing coefficient M, implying that mixing acts to reduce gradients in the biomass profile.

In light of equation (7.15), which describes the time evolution of the compensation depth, we can look whether the compensation depth can acquire a steady state:

$$\frac{\partial z_c}{\partial t} = 0. \tag{7.55}$$

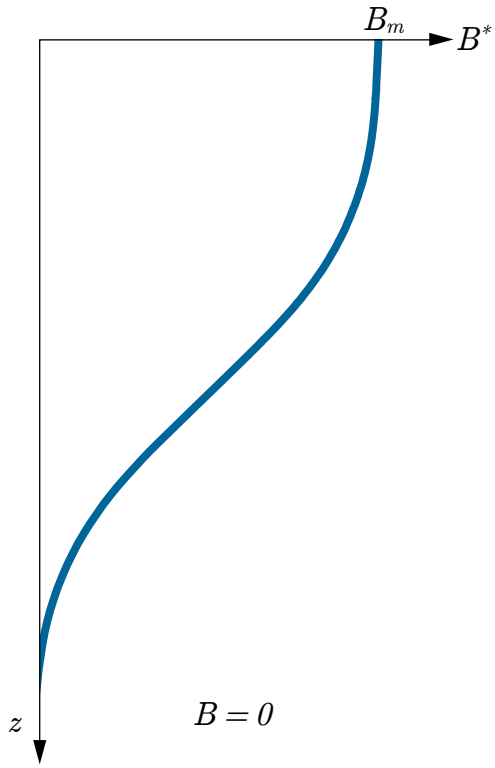

Figure 42: Subjected to mixing phytoplankton may acquire a steady state biomass profile (blue curve). Maximum biomass B_m is attained at the surface and declines with depth. The slope of the biomass profile is determined by the difference between vertically integrated production and losses up to that depth (7.54).

Inserting (7.45) into (7.15), whilst acknowledging (7.46), leads to:

$$\frac{\partial z_c}{\partial t} = -\frac{k_B}{K_w + k_B B(z_c)} \left[\frac{1}{\chi} \int_0^{z_c} \left(P^B(z', t) - L^B \right) B \, \mathrm{d}z' + M \frac{\partial B}{\partial z} \bigg|_{z_c} \right]. \quad (7.56)$$

For this expression to equal zero the following has to hold:

$$\frac{1}{\chi} \int_0^{z_c} \left(P^B(z', t) - L^B \right) B \, \mathrm{d}z' = -M \frac{\partial B}{\partial z} \bigg|_{z_c}. \quad (7.57)$$

Since by definition above z_c production exceeds losses, the term on the right hand side acts to balance the excess production on the left hand side and a steady state is possible. Physically, the term on the right hand side is the turbulent flux and it is positive, implying that excess production above z_c gets mixed downwards.

7.5 COMBINED EFFECTS OF SINKING AND MIXING

We now proceed to model sinking cells in a turbulent environment, such that the evolution of biomass is described by:

$$\frac{\partial B}{\partial t} + w\frac{\partial B}{\partial z} = \frac{1}{\chi}\left(P^B(z,t) - L^B\right)B + M\frac{\partial^2 B}{\partial z^2}. \tag{7.58}$$

Having both mixing and sinking acting simultaneously changes the surface boundary condition to:

$$wB(0) - M\frac{\partial B}{\partial z}\bigg|_0 = 0, \tag{7.59}$$

It is still a no flux boundary, just that the flux now consists of an advective and a diffusive term. The bottom boundary condition (7.47) is unaltered.

Once again, we aim to explore the steady state solution, in which case (7.58) reads:

$$w\frac{\partial B^*}{\partial z} = \frac{1}{\chi}\left(P^B(z) - L^B\right)B^* + M\frac{\partial^2 B^*}{\partial z^2}. \tag{7.60}$$

The surface boundary condition now implies that the slope of the steady state biomass profile at the surface is no longer zero, but given as:

$$\frac{\partial B^*}{\partial z}\bigg|_0 = \frac{w}{M}B^*(0) > 0. \tag{7.61}$$

This further implies the biomass profile may have a subsurface maximum. Given the bottom boundary condition (7.47) we see that as depth increases B^* has to decline to zero, which is clearly less than $B^*(0)$, meaning that B^* has to have a global maximum somewhere from the surface till great depth (Figure 43). To achieve this the first derivative has to change sing

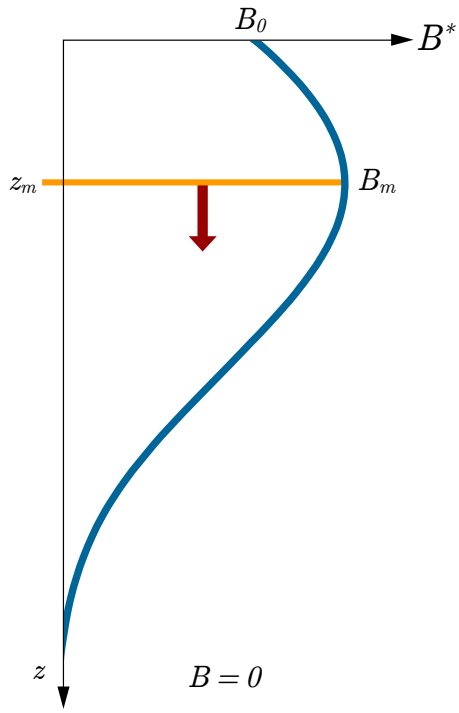

Figure 43: Steady state biomass profile (green curve) in case of production, losses, sinking (red arrow) and mixing. Maximum biomass B_m is attained below the surface at depth z_m, which is shallower than the compensation depth z_c (7.64). The slope of the biomass profile is given by (7.66). At the depth of the maximum z_m (orange line), the difference between vertically integrated production P_{z_m} and losses L_{z_m} is balanced by sinking wB_m.

at some depth and become negative. At the depth where this occurs the first derivative of B^* is zero and the second derivative is less than zero:

$$\left.\frac{\partial B^*}{\partial z}\right|_{z_m} = 0, \qquad \left.\frac{\partial^2 B^*}{\partial z^2}\right|_{z_m} < 0, \tag{7.62}$$

and we label this depth z_m (Figure 43).

Acknowledging the conditions for the maximum (7.62) directly in (7.60) leads to:

$$M\left.\frac{\partial^2 B^*}{\partial z^2}\right|_{z_m} = -\frac{1}{\chi}\left(P^B(z_m) - L^B\right)B^*(z_m) < 0. \tag{7.63}$$

For this to hold the production term has to be larger than the loss term. By definition, it is positive above the compensation depth z_c, meaning that the depth of the maximum has to be shallower than the compensation depth:

$$z_m < z_c. \tag{7.64}$$

In comparison to (7.52) at the compensation depth we now have:

$$\left.\frac{\partial^2 B^*}{\partial z^2}\right|_{z_c} = \frac{w}{M}\left.\frac{\partial B^*}{\partial z}\right|_{z_c}, \tag{7.65}$$

therefore the inflexion point is no longer located at z_c. Since the depth of the maximum is shallower than the compensation depth it must be that the inflexion point is also shallower than the compensation depth. However, due to $B(\infty) = 0$ there must be a second inflection point deeper than z_m. At this second inflexion point the first derivative of biomass has to be less than zero since biomass has already reached the global maximum. In order for this to hold the loss term has to be greater than the production term, which by definition occurs below the compensation depth and this condition is met.

Once again, we can gain more information on B^* by integrating (7.60) from the surface to depth z:

$$\left.\frac{\partial B^*}{\partial z}\right|_{z} = -\frac{1}{M}\int_0^z \frac{1}{\chi}\left(P^B(z') - L^B\right)B^*(z')\,\mathrm{d}z' + \frac{w}{M}B^*, \tag{7.66}$$

where we have acknowledged the surface boundary condition (7.59), with z' as a dummy variable for integration. By comparison with (7.54) the slope of the steady state biomass profile is now dictated by the difference between integrated production and losses, divided by M, supplemented by an additional term wB^*/M, which arises due to sinking. It is due to this additional term, which is always positive for $B^* > 0$, that the biomass slope can change sing, making a subsurface maximum plausible. At the depth of the maximum z_m, the previous expression becomes:

$$B^*(z_m) = \frac{1}{w}\int_0^{z_m} \frac{1}{\chi}\left(P^B(z) - L^B\right)B^*\,\mathrm{d}z, \tag{7.67}$$

Therefore, at steady state excess production over losses occurring above the maximum is matched by sinking at depth z_m (Figure 43). We also observe that biomass at the maximum is inversely related to the sinking speed w.

Here again, we can use equation (7.15) to check whether the compensation depth can acquire a steady state. Inserting (7.58) into (7.15), whilst acknowledging (7.59), gives:

$$\frac{\partial z_c}{\partial t} = -\frac{k_B}{K_w + k_B B(z_c)} \left[\frac{1}{\chi} \int_0^{z_c} \left(P^B(z', t) - L^B \right) B \, \mathrm{d}z' + M \frac{\partial B}{\partial z}\bigg|_{z_c} - wB(z_c) \right]. \tag{7.68}$$

For this to equal zero we require:

$$\frac{1}{\chi} \int_0^{z_c} \left(P^B(z', t) - L^B \right) B \, \mathrm{d}z' = -M \frac{\partial B}{\partial z}\bigg|_{z_c} + wB(z_c). \tag{7.69}$$

We see that the flux term on the right hand side acts to balance the excess production on the left hand side and a steady state is possible. The difference here being that the flux consists of sinking and mixing, whereas in the prior expression (7.57) it was only due to mixing. However, in both cases a steady state is reached, with the compensation depth being fixed in time.

7.6 STRONG MIXING

Of particular interest is the case of instantaneous active mixing, holding the biomass in the mixed layer uniform, enabling us to use (5.43) for the mixed layer biomass evolution, transforming (7.15) into:

$$\frac{\partial z_c}{\partial t} = -\left(\frac{k_B}{K_w + k_B B}\frac{\partial B}{\partial t}\right) z_c. \tag{7.70}$$

Above the compensation depth growth surpasses losses, whereas below it we have the opposite. At steady state, when total mixed layer production equals losses, this implies:

$$z_c^* < Z_m, \tag{7.71}$$

in order for mixed layer losses to equal mixed layer production. We have used z_c^* to mark the compensation depth at steady state. Since at steady state we have $S^* = Z_m$ prior expression becomes:

$$z_c^* < S^*, \tag{7.72}$$

as expected. In conclusion, the depth at which production equals the loss rate is the compensation depth, whereas the depth at which average mixed layer production equals the loss rate is the critical depth. Since the production profile is a decreasing function of depth (2.38), average mixed layer production will be higher than the production at the base of the mixed layer:

$$\langle P \rangle_{Z_m}^B > P_T^B(Z_m). \tag{7.73}$$

This is the mathematical explanation for why mixing acts favourably to increase production below the compensation depth. With no mixing, production below the compensation depth is lower than the loss rate and therefore growth below the compensation depth is negative. With active mixing instantaneous production below the compensation depth is still less than the loss rate, but now, due to mixing, it is the average production that matters and this is higher than the loss rate. Therefore, biomass is sustainable all the way to the mixed layer depth to which the optically coupled critical depth converges to, provided $Z_m < C$. For $Z_m > C$ loss rate surpasses the average production and growth is negative throughout mixed layer.

7.7 PROBLEMS

1. It is interesting to observe that the sinking term can be eliminated from the model (7.58) by using the following transformation [50]:

$$B = \exp\left(\frac{w}{2M}z\right)\tilde{B}. \tag{7.74}$$

Inserting the above in (7.58), carrying out the derivatives and cancelling the exponential term $\exp(wz/2M)$ yields:

$$\frac{\partial \tilde{B}}{\partial t} = \left[\frac{1}{\chi}\left(P^B(z,t) - L^B\right) - \frac{w^2}{4M}\right]\tilde{B} + M\frac{\mathrm{d}^2\tilde{B}}{\mathrm{d}z^2}. \tag{7.75}$$

Carry out the described procedure and derive (7.75). Interpret the effect the term $w^2/4M$ has on the equation.

2. Extend the model (7.58) to include the effect of nutrients on production. To achieve this a nutrient equation has to be coupled to the biomass equation:

$$\frac{\partial N}{\partial t} = -\frac{\nu}{\chi}(P^B(z,t) - L^B)B + M\frac{\partial^2 N}{\partial z^2}, \tag{7.76}$$

with ν as the nitrogen to chlorophyll ratio. This equation requires an initial condition on nutrient concentration, stated as:

$$N_0 = N(z,0). \tag{7.77}$$

It also requires two boundary conditions: at the surface and at depth. The surface boundary condition is that of no flux:

$$M\frac{\partial N}{\partial z}\bigg|_0 = 0, \tag{7.78}$$

whereas the bottom boundary condition is that of constant nutrient concentration in the deep ocean:

$$N(\infty) = N_d. \tag{7.79}$$

The production term now becomes:

$$P^B(z,t) = \frac{N(z,t)}{N(z,t)+N_k} p^B\big(I(z,t)\big). \tag{7.80}$$

Study the model first under no sinking of phytoplankton $w = 0$ in (7.58). Multiplying the biomass equation (7.58) with ν, add it to the nutrient equation (7.76) and derive the following for steady state:

$$B^* = \frac{N_d^* - N}{\nu}. \tag{7.81}$$

Observe if a subsurface maximum in biomass appears. Subsequently set $w > 0$ in (7.58) and derive analogue expressions to (7.66) for both biomass and nutrients. Under which conditions does a subsurface maximum in biomass appear?

3. Consider a finite depth water column, with a bottom at Z_b. The equation describing biomass evolution is the same as in the infinite water column case (7.58). The surface boundary condition also remains the same as (7.59), but at the bottom a no flux boundary condition is now in place:

$$wB(Z_b) - M\frac{\partial B}{\partial z}\bigg|_{Z_b} = 0. \tag{7.82}$$

To study the effect of a bottom on the steady state solution it is noteworthy first to study equation (7.58) at steady state without the production and the loss term:

$$w\frac{\partial B^*}{\partial z} = M\frac{\partial^2 B^*}{\partial z^2}. \tag{7.83}$$

This equation describes the distribution of inert sinking particles under mixing. Given the closed boundary conditions, the total number of such particles remains constant. Verify that:

$$B^*(z) = B^*(0)\exp\left(\frac{v}{M}z\right), \tag{7.84}$$

is the solution for inert particles at steady state. Now add the production and loss terms and study biomass at steady state in comparison to the solution for inert particles. How does the closed bottom boundary condition affect $B^*(z)$ in comparison to the infinite water column case?

8

NUMERICAL SIMULATIONS

The analytical approach laid out thus far, while instructive, has its limitations. It is useful to study the properties of steady state solutions, but given the problems are non linear, it is difficult to solve for the time dependent solutions exactly. Due to this we have to resolve to numerical methods to study the time evolution of the system. Here we provide basic numerical methods which can be used to study the dynamics of biomass, light and production profiles in the ocean. The methods we present are rather elementary and are by no means the state of the art. The goal is to demonstrate the basics of numerical modelling. Interested reader is encouraged to explore more detailed numerical methodology in [10, 49] and a paper devoted specifically to modelling biomass profiles in the ocean [24].

The partial differential equation describing the time evolution of the biomass profile (7.58) consists of four terms: local change, advective term, mixing term and the reaction term, which itself consists of the production and loss terms. Coupled to it is the light penetration model (7.5), which has to be solved simultaneously. To translate such a coupled system into numerical form requires proper numerical treatment of each term in order for the numerical model to exhibit stable behaviour and yield correct solutions. To achieve these goals, the numerical schemes we use have to exhibit certain mathematical properties and securing such properties is no easy feet. Nonetheless, once secured, the ensuing numerical simulations help us to pierce deeper into the dynamics of biomass, light and production in the ocean.

8.1 PROBLEM FORMULATION

The equation we wish to solve numerically is the partial differential equation (7.58), which we restate here for clarity:

$$\frac{\partial B}{\partial t} + w\frac{\partial B}{\partial z} = \frac{1}{\chi}\left(P^B(z,t) - L^B\right)B + M\frac{\partial^2 B}{\partial z^2}. \tag{8.1}$$

It is classified in the literature as the **advection diffusion reaction** equation. The advection term is due to sinking, the diffusion term is due to mixing and the reaction term is due to production and losses.

On the left hand side of the equation we have a time derivative of biomass, which makes biomass what is called a **prognostic variable**. Prognostic variables fully describe the state of the system at any time. They are calculated from equations such as (8.1) along with initial and boundary conditions. Another common term in the literature for such variables is state variables. Complementary to prognostic are **diagnostic variables**, which can be calculated from the knowledge of prognostic variables. In our model light is one such variable. It is calculated with the light penetration model (7.5), also restated here for clarity:

$$I(z,t) = I_0(t)\exp\left(-\int_0^z \left(K_w + k_B B(z',t)\right)\mathrm{d}z'\right). \tag{8.2}$$

The two equations from an **integro-differential system** and in order to solve it by numerical means, terms in the equations have to be converted to their numerical counterparts, which is referred to as **discretization**. The mathematical procedure of discretization is not unique, and the analytical model can have numerous numerical representations, referred to as **numerical schemes**.

Before proceeding to explore numerical schemes it is important to stress that each numerical scheme has its limitations. To demonstrate this let us imagine that an analytical solution to our problem is known. The task of the numerical model is then to reproduce this solution. How precise the numerical result will be depends on a few factors. First, the numerical scheme has to reproduce the analytical equation in the limit of

small time and spatial steps. This property is referred to as **consistency**. Second, it has to be stable and not blow up, in other words not give infinite solutions due to numerical instabilities. This property is referred to as **stability**. Third, the solution it produces has to converge onto the analytical solution. This property is referred to as **convergence**. Securing consistency, stability and convergence of numerical schemes is not an easy undertaking.

Hawing explained the basic underpinnings of numerics, to fully specify the problem at hand, we need to set initial and boundary conditions. The biomass equation requires an initial condition and two boundary conditions. We set the initial condition as:

$$B(z,0) = B_0(z), \tag{8.3}$$

where $B_0(z)$ is a known function. Once again, at the surface we specify a no flux boundary condition:

$$wB(0) - M\frac{\partial B}{\partial z}\bigg|_0 = 0, \tag{8.4}$$

and at infinite depth we specify zero biomass:

$$B(\infty,0) = 0. \tag{8.5}$$

The initial and boundary conditions have to be translated to their numerical counterparts. Whilst this is easily doable for the initial condition, for boundary conditions the procedure is not trivial. Also, the irradiance model requires a boundary condition in the form of surface irradiance:

$$I(0,t) = I_0(t), \tag{8.6}$$

were we assume $I_0(t)$ is known. The irradiance model also uses the initial condition on biomass to calculate $I(z,0)$. Having specified the model fully in analytical form, we now proceed to translate it to its numerical counterpart.

8.2 NUMERICAL MODEL SETUP

We begin the model setup by first defining discrete depths z_n as:

$$z_n = (n - 1/2)\Delta z, \tag{8.7}$$

where n is the depth index ($n = 1, 2, ..., N$) and Δz is the separation between the two consecutive depths. Note the first depth is at $\Delta z/2$. Discrete time t_j is defined as:

$$t_j = j\Delta t, \tag{8.8}$$

where j is the time index ($j = 1, 2, ..., J$) and Δt is the time step. This configuration is shown in Figure 44, referred to as the **numerical grid**.

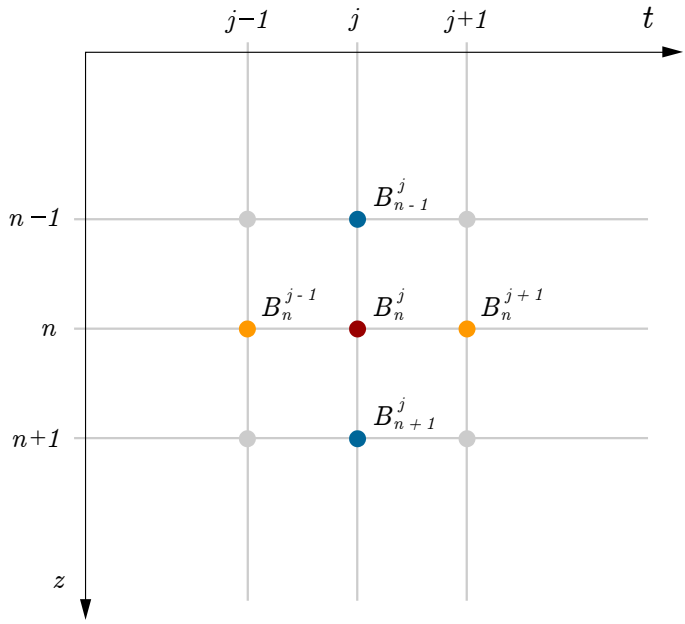

Figure 44: Numerical grid used to represent model variables, here shown for biomass B. In a numerical model a continuous variable, such as $B(z, t)$ becomes a discrete variable $B^j_n = B(z_n, t_j)$. By changing index n we change depth (blue circles), whereas by changing index j we change time (orange circles).

With the grid defined the continuous model variables, such as irradiance, production and biomass now become discrete variables:

$$I(z,t) \rightarrow I(z_n,t_j) = I_n^j, \tag{8.9}$$

$$P(z,t) \rightarrow P(z_n,t_j) = P_n^j, \tag{8.10}$$

$$B(z,t) \rightarrow B(z_n,t_j) = B_n^j. \tag{8.11}$$

With the variables discretized the next step is to discretize the model equations themselves. The equation we proceed to solve is (8.1) coupled to the light penetration model (8.2).

Having defined the numerical counterparts, B_n^j and I_n^j, to continuous variables, $B(z,t)$ and $I(z,t)$, our goal now is to calculate biomass at the next time step $B_n^{j+1} = B(z_n, t_j + \Delta t)$ from the knowledge of biomass at the current time step $B_n^j = B(z_n,t_j)$. To this end we have to discretize each term of equation (8.1). We proceed from left to right. The first term on the left hand side of equation (8.1) is the time derivative, which now has to be approximated numerically.

To demonstrate the principle of numerical approximation we simplify equation (8.1) to a growth model of the following form:

$$\frac{\partial B}{\partial t} = \frac{1}{\chi}\left(P_m^B - L^B\right)B, \tag{8.12}$$

where $B = B(z,t)$. This simple model describes the growth of phytoplankton under light saturation, subjected to constant losses, under no sinking nor mixing. The equation is a standard growth equation with the well known analytical solution:

$$B(z,t) = B(z,0)\exp\left[\frac{1}{\chi}\left(P_m^B - L^B\right)t\right]. \tag{8.13}$$

The model in this form will suffice for now in order to gradually build up a numerical scheme which can solve (8.1) with all processes taken into account. To solve (8.12) numerically we need to rewrite the time derivative in numerical form, which we now proceed to do.

8.3 TIME DERIVATIVE

Generally, we can write $B(z, t + \Delta t)$ as a Taylor series around $B(z, t)$:

$$B(z, t + \Delta t) = B(z, t) + \left.\frac{\partial B}{\partial t}\right|_{(z,t)} \Delta t + \frac{1}{2}\left.\frac{\partial^2 B}{\partial t^2}\right|_{(z,t)} (\Delta t)^2 + ..., \tag{8.14}$$

where Δt is positive. Keeping only the first order term provides a numerical approximation for the time derivative:

$$\left.\frac{\partial B}{\partial t}\right|_{(z,t)} \approx \frac{B(z, t + \Delta t) - B(z, t)}{\Delta t}, \tag{8.15}$$

which is referred to as the Euler scheme [49], to be more specific the forward in time Euler scheme [10], or simply the forward in time scheme (Figure 45). Using the newly established notation (8.11) we arrive at:

$$\left.\frac{\partial B}{\partial t}\right|_{(z_n,t_j)} \to \frac{1}{\Delta t}\left(B_n^{j+1} - B_n^j\right). \tag{8.16}$$

Therefore, in numerical form equation (8.12) becomes:

$$\frac{1}{\Delta t}\left(B_n^{j+1} - B_n^j\right) = \frac{1}{\chi}\left(P_m^B - L^B\right) B_n^j. \tag{8.17}$$

Such equations are typically rearranged to have biomass at the next time step B_n^{j+1} on the left hand side:

$$B_n^{j+1} = B_n^j + \frac{1}{\chi}\left(P_m^B - L^B\right) B_n^j \Delta t. \tag{8.18}$$

This is a prototypical form in which such numerical expressions are written in. The left hand side holds the quantity at time $t + \Delta t$ that is to be calculated from the quantities on the right hand side, which are all known at time t. Therefore, with a given initial condition for B at time $t = 0$ the equation can be used to calculate B at time $t + \Delta t$. Subsequently, the process can be repeated, now starting from $t + \Delta t$, to calculate B at time $t + 2\Delta t$. The procedure is often referred to as **time stepping**.

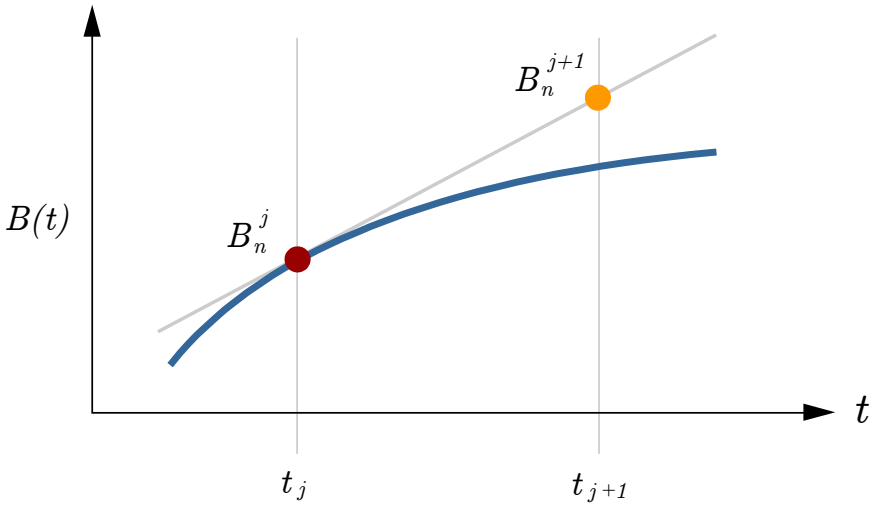

Figure 45: Graphical illustration of the Euler method. The value of B at depth z and time $t_{j+1} = (j+1)\Delta t$, marked B_n^{j+1} (orange point), is approximated with the first derivative of B at depth z and time $t_j = j\Delta t$, marked B_n^j (red point).

Therefore, time stepping of the numerical scheme (8.18) enables us to simulate the solution to equation (8.12), but comes at a cost in the form of an associated error, which we define as:

$$e_n^j = B(z_n, t_j) - B_n^j. \tag{8.19}$$

To demonstrate the origin of the error let us compare the Taylor series in (8.14) to its numerical counterpart (8.18). Both expressions predict biomass at depth z_n and time t_{j+1}. By equating the two expressions we obtain the following:

$$B_n^j + \left.\frac{\partial B}{\partial t}\right|_{(z_n,t_j)} \Delta t + \frac{1}{2}\left.\frac{\partial^2 B}{\partial t^2}\right|_{(z_n,t_j)} (\Delta t)^2 + \ldots = B_n^j + \frac{1}{\chi}\left(P_m^B - L^B\right) B_n^j \Delta t. \tag{8.20}$$

After cancelling B_n^j and rearranging we are left with:

$$\left.\frac{\partial B}{\partial t}\right|_{(z_n,t_j)} = \frac{1}{\chi}\left(P_m^B - L^B\right) B_n^j - \frac{1}{2}\left.\frac{\partial^2 B}{\partial t^2}\right|_{(z_n,t_j)} \Delta t + \ldots \tag{8.21}$$

Comparing this expression to the original equation we set out to solve (8.12), we observe the appearance of additional terms, which are not present in the numerical scheme (8.18). These terms form the **truncation error**. In case of (8.21) we observe that the leading term is of first order in Δt and the scheme is said to be first order accurate. In the limit of ever smaller Δt we recover the original equation (8.12) and therefore the scheme is consistent.

The stability of the scheme can be studied in the following manner. First, we rewrite (8.18) as:

$$B_n^{j+1} = \left[1 + \frac{1}{\chi}\left(P_m^B - L^B\right)\Delta t\right] B_n^j, \tag{8.22}$$

and observe that by induction the following holds:

$$B_n^j = \left[1 + \frac{1}{\chi}\left(P_m^B - L^B\right)\Delta t\right]^j B_n^0, \tag{8.23}$$

Whether or not this expression is stable is determined by the term in the square brackets. When it is greater than unity the scheme is unstable, whereas when it is less than unity the scheme is stable.

However, when production dominates, that is $P_m^B > L^B$, the analytical solution itself (8.13) is unstable in this sense. On the other hand, when the loss term dominates, that is $P_m^B < L^B$, the analytical solution (8.13) decays over time. For the numerical scheme to exhibit this same behaviour we require the error not to go to infinity. By looking at the error in time t_{j+1}, that is:

$$e_n^{j+1} = B(z_n, t_{j+1}) - B_n^{j+1}, \tag{8.24}$$

and inserting (8.14) and (8.22) we get, after some meticulous algebra, the following expression for the error:

$$e_n^{j+1} = \left[1 + \frac{1}{\chi}\left(P_m^B - L^B\right)\Delta t\right] e_n^j + \frac{1}{2}\frac{\partial^2 B}{\partial t^2}\bigg|_{(z_n, t_j)} (\Delta t)^2 + \ldots \tag{8.25}$$

If at initial time $B(z_n, t_j) = B_n^j$ the error is of second order. Upon disregarding second order terms we are left with:

$$e_n^{j+1} = \left[1 + \frac{1}{\chi}\left(P_m^B - L^B\right)\Delta t\right] e_n^j. \tag{8.26}$$

The factor in the square brackets in this expression determines the growth of the error over time. In order for the error to be bounded, the modulus of the term in the square brackets to be less than unity:

$$\left|1 + \frac{1}{\chi}\left(P_m^B - L^B\right)\Delta t\right| \leq 1, \tag{8.27}$$

implying the interval of stability for Euler's method is:

$$-2 < \frac{1}{\chi}\left(P_m^B - L^B\right)\Delta t < 0. \tag{8.28}$$

Choosing Δt such that the derived condition is met will render the Euler scheme stable. The simplifying assumption here is that the production term is constant and equal to the assimilation number, which does not hold in the ocean. Therefore, a proper numerical treatment of the production term is in order, which is done in the following section.

8.4 PRODUCTION TERM

Given light is the driver of production we proceed first to demonstrate how to calculate irradiance at depth. For surface irradiance we now write:

$$I_0^j = I_0(t_j). \tag{8.29}$$

Irradiance at depth I_n^j can be calculated by directly discretizing equation (8.2), as shown in Figure 46. We begin with the first level $z_1 = \Delta z/2$, where irradiance equals:

$$I_1^j = I_0(t_j) \exp\left(-\left(K_w + k_B B_1^j\right)\frac{\Delta z}{2}\right), \tag{8.30}$$

with water contributing to attenuation with the $K_w \Delta z/2$ term and biomass with the $k_B B_1^j \Delta z/2$ term. Having irradiance at the first model depth $z_1 = \Delta z/2$ now allows us to calculate irradiance at the second model depth, where $z_2 = 3\Delta z/2$:

$$I_2^j = I_1^j \exp\left(-K_w \Delta z + k_B B_1^j \frac{\Delta z}{2} - k_B B_2^j \frac{\Delta z}{2}\right), \tag{8.31}$$

where water contributes with the $K_w \Delta z$ term and biomass with two terms: $k_B B_1^j \Delta z/2$ corresponding to biomass from $\Delta z/2$ to Δz and $k_B B_2^j \Delta z/2$ corresponding to biomass from Δz to $3\Delta z/2$. By generalizing we can calculate I_n^j, where $n = 2, 3, ..., N$, level by level:

$$I_n^j = I_{n-1}^j \exp\Big(- K_w \Delta z + k_B B_{n-1}^j \frac{\Delta z}{2} - k_B B_n^j \frac{\Delta z}{2} \Big). \tag{8.32}$$

An alternative approach is to represent (8.2) directly as a sum for all the levels where $n = 2, 3, ..., N$:

$$I_n^j = I_0(t_j) \exp\left(- \sum_{i=1}^{n-1} \big(K_w + k_B B_i^j\big) \Delta z - \big(K_w + k_B B_n^j\big) \frac{\Delta z}{2} \right), \tag{8.33}$$

while still using (8.30) for the first level.

Having numerically calculated irradiance I_n^j we now proceed to calculate the production term numerically. Calculation of the production term is straightforward, with irradiance at depth I_n^j used in the $p^B(I)$ function to calculate $P^B(z_n, t_j)$:

$$P_n^j = B_n^j p^B(I_n^j). \tag{8.34}$$

This expression will give production at the model level z_n and we can regard it as representative of production taking place in the layer extending from $z_n - \Delta z/2$ up to $z_n + \Delta z/2$. With this in mind, an alternative approach for calculating $P^B(z_n, t_j)$ is to calculate irradiance at top of each level and use it to calculate average production in that layer (Figure 47). Irradiance at the top of each level is simply:

$$I_{n-1/2}^j = I_0(t_j) \exp\left(- \sum_{i=1}^{n-1} \big(K_w + k_B B_n^j\big) \Delta z \right), \tag{8.35}$$

where $n - 1/2$ is used to indicate the top of the layer and $n = 2, 3, ..., N$, with the understanding that $I_{1/2}^j = I_0(t_j)$. Having irradiance at the top of each layer, we can now use it to calculate average instantaneous production in that layer:

$$\langle P \rangle_n^j = \frac{1}{\Delta z} \int_{z_n - \Delta z/2}^{z_n + \Delta z/2} B_n^j p^B(I) \, \mathrm{d}z, \tag{8.36}$$

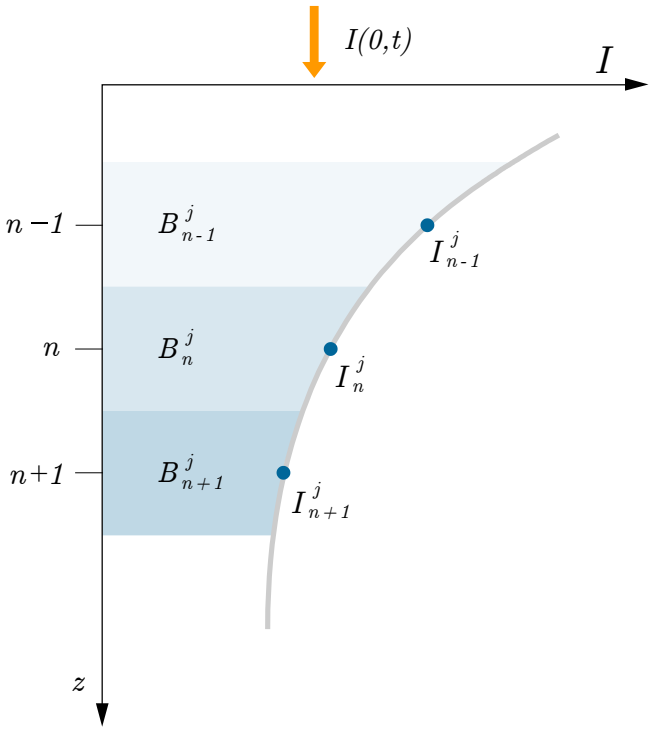

Figure 46: Numerical calculation of irradiance at model depths z_n (blue points), indexed with n. Irradiance at each model depth is attenuated due to the water and biomass above that depth and can be calculated from irradiance at the level above (8.32), or from an integral expression extending from the surface up to that depth (8.33).

where we introduce the notation $\langle P \rangle^j_n$ for average instantaneous production for the layer with index n. We can rewrite this expression as:

$$\langle P \rangle^j_n = \frac{B^j_n}{\Delta z} \left(\int_{z_n - \Delta z/2}^{\infty} p^B(I)\, \mathrm{d}z - \int_{z_n + \Delta z/2}^{\infty} p^B(I)\, \mathrm{d}z \right), \tag{8.37}$$

where biomass B^j_n comes out of the integral due to it being uniform in each layer. Therefore, solving (8.36) amounts to assuming uniform biomass below $z_n - \Delta z/2$ and subtracting the two integrals. This is

analogous to the approach used in (3.38). To find an exact solution we employ (1.18) for the photosynthesis irradiance function, turning (8.36) into:

$$\langle P\rangle_n^j = \frac{B_n^j P_m^B}{\Delta z} \int_{z_n-\Delta z/2}^{z_n+\Delta z/2} \left\{1 - \exp\left[-\frac{\alpha^B}{P_m^B} I_{n-1/2}^j \exp\Big(-(K_w + k_B B_n^j)z\Big)\right]\right\} \mathrm{d}z. \tag{8.38}$$

By a change of variables:

$$x = \frac{\alpha^B}{P_m^B} I_{n-1/2}^j \exp\Big(-(K_w + k_B B_n^j)z\Big) \tag{8.39}$$

the first integral on the right hand side of (8.37) becomes a table integral and its solution reads:

$$\int_{z_n-\Delta z/2}^{\infty} \left\{1 - \exp\left[-\frac{\alpha^B}{P_m^B} I_{n-1/2}^j \exp\Big(-(K_w + k_B B_n^j)z\Big)\right]\right\} \mathrm{d}z = \tag{8.40}$$

$$= \frac{1}{K_w + k_B B_n^j} \sum_{m=1}^{\infty} \frac{(-1)^{m+1}}{m \cdot m!} \left(\frac{\alpha^B}{P_m^B} I_{n-1/2}^j\right)^m.$$

The same holds for the second integral, but with a difference in index $n - 1/2$, becoming $n + 1/2$ instead, due to the depth changing from $z_n - \Delta z/2$ to $z_n + \Delta z/2$:

$$\int_{z_n+\Delta z/2}^{\infty} \left\{1 - \exp\left[-\frac{\alpha^B}{P_m^B} I_{n-1/2}^j \exp\Big(-(K_w + k_B B_n^j)z\Big)\right]\right\} \mathrm{d}z = \tag{8.41}$$

$$= \frac{1}{K_w + k_B B_n^j} \sum_{m=1}^{\infty} \frac{(-1)^{m+1}}{m \cdot m!} \left(\frac{\alpha^B}{P_m^B} I_{n+1/2}^j\right)^m.$$

This substitution was used prior in (3.10). Merging the two expressions gives the solution to (8.38):

$$\langle P\rangle_n^j = \frac{B_n^j P_m^B}{(K_w + k_B B_n^j)\Delta z} \sum_{m=1}^{\infty} \frac{(-1)^{m+1}}{m \cdot m!} \left[\left(\frac{\alpha^B}{P_m^B} I_{n-1/2}^j\right)^m - \left(\frac{\alpha^B}{P_m^B} I_{n+1/2\cdot}^j\right)^m\right] \tag{8.42}$$

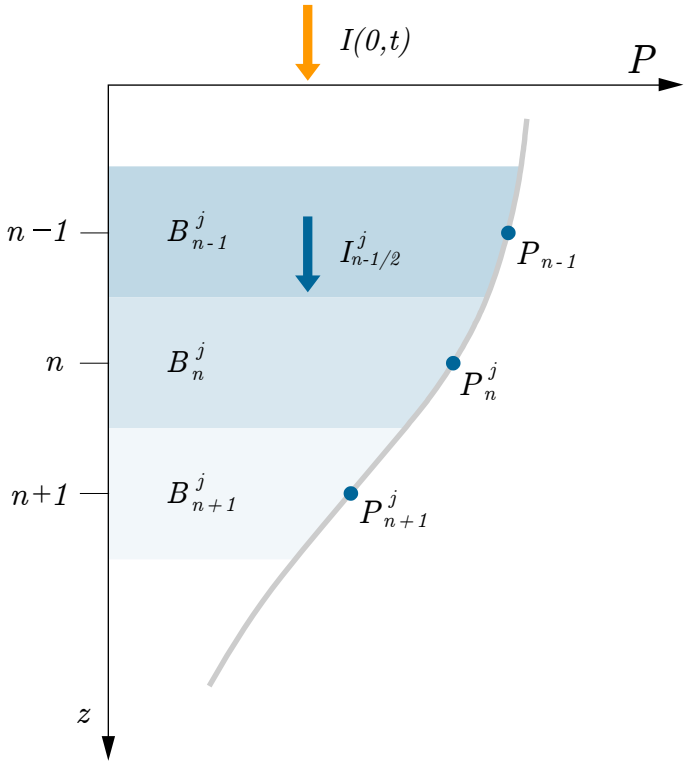

Figure 47: Numerical calculation of the production term at model depths z_n, indexed by n. Production at each model depth (blue points) can be calculated using irradiance at that depth (8.34), or from average production in the layer (8.42), which is calculated using irradiance at the top of the layer (blue arrow).

This expression provides the average production in the layer extending from $z_n - \Delta z/2$ to $z_n + \Delta z/2$. It takes into account the curvature in the production profile (blue area in Figure 47). In comparison, expression (8.34) does not take into account the curvature, but represents production of the total layer as the production in the middle point of the layer (blue dots in Figure 47). Consequently, expression (8.42) does not have this error associated with it. Naturally, how big this error will depends on the shape of the normalized production profile and the size of the separation between two layers Δz.

8.5 ADVECTIVE TERM

Having shown how to calculate the production term we now proceed to model sinking, which is represented with an advective term in equation (8.1). To elucidate the numerical procedure for discretizing the advective term in (8.1) we will first focus solely on the **advection equation** (7.19), restated here:

$$\frac{\partial B}{\partial t} + w\frac{\partial B}{\partial z} = 0, \tag{8.43}$$

along with its exact analytical solution in case of no flux boundary condition at the surface (7.20):

$$B(z,t) = B_0(z - wt), \tag{8.44}$$

where $B_0(z) = B(z,0)$ is the initial condition. The advection equation will here be translated into numerical form in order to later be incorporated into the larger model, which will take into account production and losses, along with mixing. Before proceeding to discretize the equation we will briefly state some of its properties, which are relevant for obtaining correct numerical representations of the equation and subsequently correct numerical solutions.

The advection equation in our case represents the effect of phytoplankton sinking under gravity, therefore $w > 0$ in our model. The sinking speed is assumed uniform throughout the water column $w \neq w(z)$, implying all phytoplankton cells sink at the same rate. Imagine now an observer starts at a depth z_0 and sinks at the same rate w (Figure 48), such that its vertical velocity is described by:

$$\frac{\mathrm{d}z_{obs}}{\mathrm{d}t} = w, \tag{8.45}$$

and the position of the the observer follows easily as:

$$z_{obs}(t) = z_0 + wt. \tag{8.46}$$

Consider now what such an observer would measure. The biomass concentration at $z_{obs}(t)$ would not change over time, since there is no

production nor losses taking place. Therefore biomass which the observer would measure at any time would correspond to the biomass concentration at initial time:

$$B_{obs}(z_{obs}(t)) = B_{obs}(z_{obs}(0)). \tag{8.47}$$

By setting $t = 0$ in (8.46) and inserting it in this expression, yields:

$$B_{obs}(z_{obs}(t)) = B_0(z_0). \tag{8.48}$$

We can now express z_0 from (8.46) as:

$$z_0 = z_{obs}(t) - wt, \tag{8.49}$$

and insert it in the prior expression to get:

$$B_{obs}(z_{obs}(t)) = B_0(z_{obs}(t) - wt). \tag{8.50}$$

Since z_0 is arbitrary the same holds for the entire water column, which allows us to drop the subscript on z_{obs} to write:

$$B(z,t) = B_0(z - wt), \tag{8.51}$$

and recover solution (8.44). A mathematically straightforward way to confirm this conclusion is to simply insert (8.46) in (8.44) and take the derivative with respect to time:

$$\frac{\mathrm{d}}{\mathrm{d}t}B(z_{obs}(t),t) = \frac{\partial B}{\partial z}w + \frac{\partial B}{\partial t}. \tag{8.52}$$

where the chain rule was used along with (8.45) to write $\mathrm{d}z_{obs}/\mathrm{d}t = w$. On the right hand side of this expression we recognize the advection equation (8.43), allowing us to write:

$$\frac{\mathrm{d}}{\mathrm{d}t}B(z_{obs}(t),t) = 0. \tag{8.53}$$

With this procedure we have effectively reduced a partial differential equation (8.43) to an ordinary differential equation stating that $B(z_{obs}(t))$ is constant along a trajectory given by (8.46).

Mathematically, the procedure of finding curves along which a partial differential equation becomes an ordinary differential equation is called **method of characteristics** and curves such as:

$$z(t) = z_0 + wt, \tag{8.54}$$

are called **characteristic curves**. Physically, for an observer moving with the speed w there is no change of biomass in the observer's reference frame. The significance of the characteristic curves becomes evident when constructing numerical schemes for solving the advection equation.

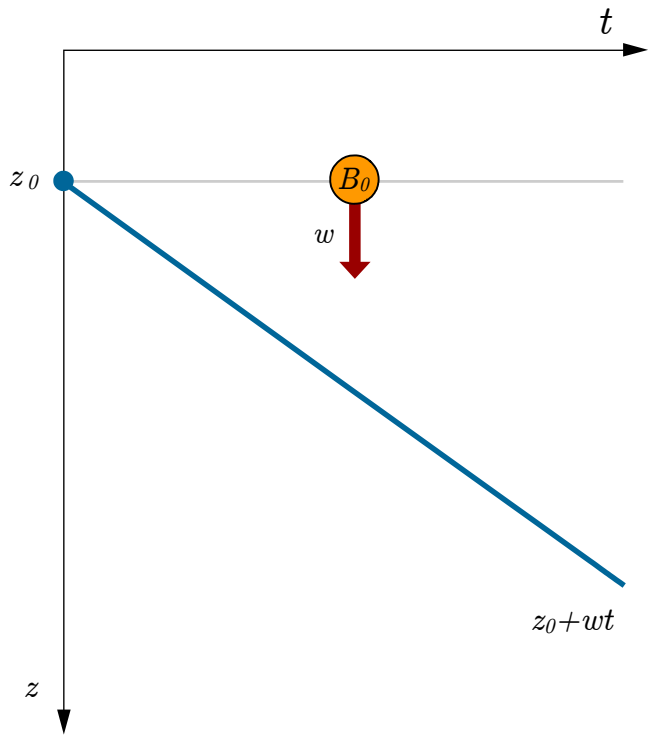

Figure 48: Characteristic curve (blue line) of the advection equation (8.43). The value of biomass on the characteristic curve does not change over time, such that on the characteristic curve biomass is constant and equal to $B_0(z_0)$. An observer sinking with speed w (8.45) would move on the characteristic curve and would measure no change in biomass.

The numerical scheme should ideally carry physically accurate information from time t_j to time t_{j+1}. This implies that we can look from where in the model domain should information on biomass B_n^{j+1} come from. The information should lie on the characteristic curve passing through B_n^{j+1} (Figure 49). Knowing this, we can move backwards in time on the characteristic curve to arrive at the point where the information would come from physically. By looking at the numerical grid the characteristic curve passes through the point B^*, which can be approximated from nearby points B_{n-1}^j and B_n^j. The vertical distance between B^* and B_n^j is equal to $w\Delta t$ and the vertical distance between B^* and B_{n-1}^j is equal to $\Delta z - w\Delta t$. We can leverage this information to approximate B^* as:

$$B^* = \frac{\Delta z - w\Delta t}{\Delta z} B_n^j + \frac{w\Delta t}{\Delta z} B_{n-1}^j. \tag{8.55}$$

By requiring that $B_n^{j+1} = B^*$ and after some algebra, we obtain:

$$B_n^{j+1} = B_n^j - w\frac{\Delta t}{\Delta x}\left(B_n^j - B_{n-1}^j\right). \tag{8.56}$$

This numerical scheme is referred to as the **upwind scheme**. Its main advantage to simulate the problem at hand is its asymmetry with respect to the direction of information propagation. It only propagates information from the physically correct direction, which for sinking phytoplankton is from the top of the water column downwards. However, for the scheme to yield physically realistic solutions it has to be able to grasp B^*, which may not always be the case, as we now proceed to demonstrate.

Consider the scenario in which the sinking speed is such that the characteristic curve lies outside the line connecting B_{n-1}^j and B_n^j (Figure 49). In this case the numerical grid would not be able to get at B^*. To see why this holds we simply go two steps back in time. The point B_n^j gets formation from points B_n^{j-1} and B_{n-1}^{j-1}, whereas the point B_{n-1}^j gets formation from points B_{n-1}^{j-1} and B_{n-2}^{j-1}. All those points do not grasp the information propagating along the red characteristic curve in Figure 49. Going back three time steps the same holds. Subsequently, going to the initial time the same reasoning applies. The numerical scheme therefore carries incorrect information.

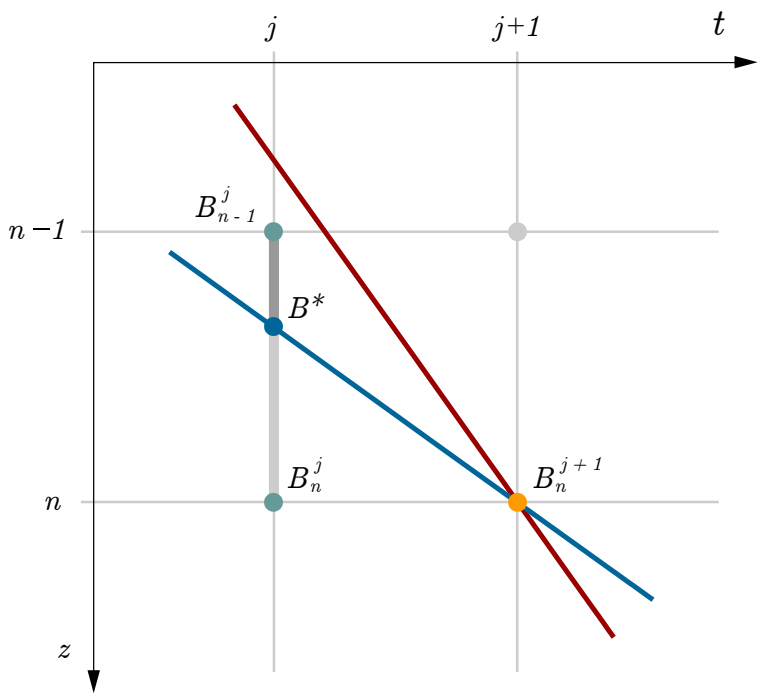

Figure 49: Graphical depiction of the upwind scheme for solving the advection equation. Information at the point B_n^{j+1} (orange curve) physically arrives along the characteristic curve (blue line) from the point B^* (blue circle). By approximating B^* from nearby points B^j_{n-1} and B^j_n (green circles) the upwind scheme emerges. In case the characteristic curve falls outside the grasp of the numerical scheme (red line) the scheme carries physically unrealistic information.

To remedy the problem we require that the point from which information propagates lies within the region the numerical grid can grasp. That will occur when the grid is able to propagate information faster then the information propagates along the characteristic curve. The rate at which information propagates along the grid is given by the ratio of $\Delta z/\Delta t$, whereas the rate at which the information propagates along the characteristic curve is simply w. Therefore, the following condition has to be met:

$$w\Delta t \leq \Delta z. \tag{8.57}$$

This is the **Courant Friedrichs Lewy** stability condition [49], often stated as:

$$w\frac{\Delta t}{\Delta z} \leq 1. \tag{8.58}$$

For a given w it sets a restriction on the ratio $\Delta t/\Delta z$ in order for the upwind scheme (8.56) to be stable. Therefore, by appropriately selecting $\Delta t/\Delta x$ the advection equation can be solved numerically using the upwind scheme (8.56). The upwind scheme does so in a physically consistent manner by receiving information from the direction of sinking phytoplankton cells, that is from above in the water column.

To gain further insight into the workings of the advection equation and the type of solutions we expect from the upwind scheme, let us rewrite (8.43) in the following form:

$$\frac{\partial B}{\partial t} = -w\frac{\partial B}{\partial z}. \tag{8.59}$$

It is now easy to observe that the time derivative of biomass on the left hand side is dictated by its spatial derivative on the right hand side. Consider now an arbitrary depth z_0 and observe the slope of the biomass profile at that depth (Figure 50). When the spatial derivative is positive the time derivative is negative and vice versa. Therefore, for each depth where the spatial derivative is positive the value of biomass will decline over time and for each depth where the spatial derivative is negative the value of biomass will increase over time, as shown in Figure 50. In such a manner, and for positive sinking speed $w > 0$, the biomass profile propagates towards greater depth without changing its shape, in accordance with (8.44).

The numerical scheme may not be able to preserve the shape of the analytical solution perfectly, which is referred to as **numerical dispersion**. Due to numerical dispersion the numerical solution departs from the analytical. How strong this effect will be depends on the selection of the numerical scheme and naturally on the ratio $w\Delta t/\Delta z$. There have been many schemes developed for handling numerical dispersion, the details of which are beyond the scope of this book, but the interested reader may learn more about numerical dispersion in [10] and [49].

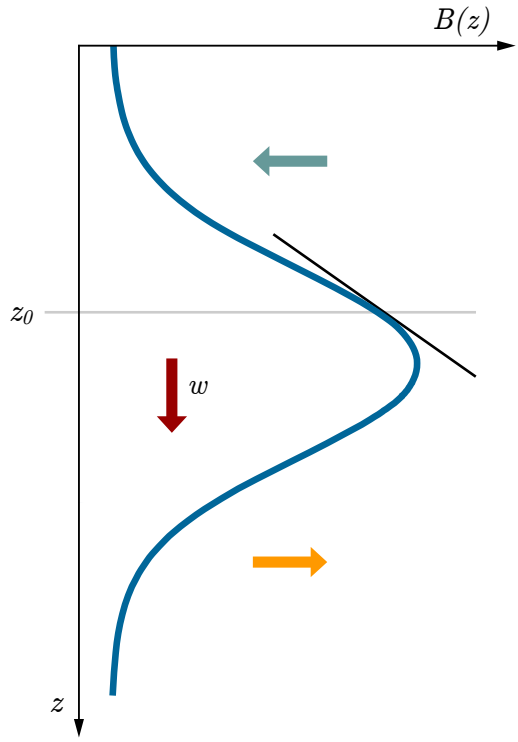

Figure 50: At a given depth z_0 (grey line) the advection equation (8.59) states that the change over time in biomass at that depth is dictated by the first spatial derivative of biomass (black line). Where the spatial derivative is positive biomass declines (green arrow), due to the negative sign in (8.59), and where it is negative biomass increases (orange arrow).

Finally, by combining advection with production and losses we arrive at the following numerical scheme:

$$B_n^{j+1} = B_n^j + \frac{1}{\chi}\Big(P^B(z_n, t_j) - L^B\Big)B_n^j \Delta t - w\frac{\Delta t}{\Delta z}\Big(B_n^j - B_{n-1}^j\Big). \tag{8.60}$$

To complete the numerical version of equation (8.1) mixing needs to be added to this numerical model, which we now proceed to do. We first analyse the diffusion equation and how to solve it numerically, in order to highlight some important aspects of the numerical approach.

8.6 MIXING TERM

To demonstrate how to construct the numerical version of the mixing term in equation (8.1) we start with the **diffusion equation**:

$$\frac{\partial B}{\partial t} = M\frac{\partial^2 B}{\partial z^2}, \tag{8.61}$$

where the mixing coefficient M is held constant. This equation is of first order in time, therefore it requires an initial condition on biomass:

$$B(z, 0) = B_0(z). \tag{8.62}$$

It is second order in space, implying it requires two boundary conditions, which can be set as fluxes, or as biomass values at the ends of the model domain, or a combination of both. In case of the ocean it is natural to set these boundary conditions at the ocean surface and at great depth, $z = \infty$, or at the mixed layer base, $z = Z_m$. The flux boundary conditions, with say $z = \infty$, are set as:

$$M\frac{\partial B}{\partial z}\bigg|_0 = F_0, \qquad M\frac{\partial B}{\partial z}\bigg|_\infty = F_\infty, \tag{8.63}$$

where F_0 and F_∞ are prescribed values of the fluxes, which can also be time dependent. Setting biomass values as boundary conditions is done simply as:

$$B(0, t) = B_0, \qquad B(\infty, t) = B_\infty, \tag{8.64}$$

where B_0 and B_∞ are also known. A natural combination of both boundary conditions, best suited for modelling biomass profiles, would be to set a no flux boundary condition at the surface and zero biomass at infinite depth:

$$M\frac{\partial B}{\partial z}\bigg|_0 = 0, \qquad B(\infty, t) = 0. \tag{8.65}$$

To analyse the behaviour of the diffusion equation (8.61), relevant for the construction of the numerical scheme for solving it, we will now consider a special case which will lead us to an analytical solution. Although not realistic for an oceanographic application the example is illustrative from a modelling standpoint as it helps to elucidate how diffusion proceeds.

We look at an infinite domain and set the following boundary conditions:

$$B(-\infty, t) = 0, \qquad B(\infty, t) = 0. \tag{8.66}$$

Under such boundary conditions the ends of the domain never experience a change in biomass. Physically, this situation would correspond to an ocean which is weekly mixed, such that biomass at some depth never reaches the surface, nor great depth.

For the initial condition we take a finite amount of biomass B_0 located at depth z_0 at initial time. Mathematically, we set this initial condition using a Dirac delta function:

$$B(z, 0) = \delta(z_0) B_0, \tag{8.67}$$

which is zero everywhere except at z_0 and whose integral over the entire domain is equal to unity:

$$\int_{-\infty}^{\infty} \delta(z_0)\, \mathrm{d}z = 1. \tag{8.68}$$

The exact solution to the diffusion equation under these conditions is:

$$B_e(z, t) = \frac{B_0}{\sqrt{4\pi M t}} \exp\left(-\frac{(z - z_0)^2}{4Mt}\right). \tag{8.69}$$

This is the well known **elementary solution** of the diffusion equation, labelled here as B_e (Figure 51). It has two important properties. First, the centre of biomass does not change over time and stays at z_0, which is shown simply by calculating the following integral:

$$\frac{1}{B_0} \int_{-\infty}^{\infty} z B_e(z, t)\, \mathrm{d}z = z_0. \tag{8.70}$$

The spatial variance of biomass, a measure of the spread of biomass around z_0, is time dependent and given as:

$$\sigma^2 = 2Mt, \tag{8.71}$$

implying that stronger mixing causes biomass to spread out more quickly. Following (8.71) at great time variance tends to infinity and biomass concentration tends to zero throughout the domain (8.69).

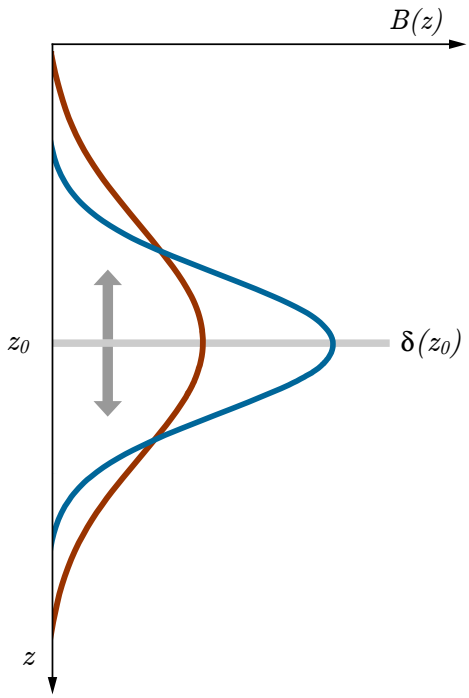

Figure 51: Elementary solution of the diffusion equation (8.69) at different times (blue and red curves) with the Dirac delta as the initial condition (light grey line). The initially concentrated biomass at depth z_0 gets spread out with time due to mixing (grey arrows), but the centre of biomass stays at z_0.

The utility of the elementary solution comes from the fact that it can be used to solve the diffusion equation for an arbitrary initial condition:

$$B(z, 0) = B_0(z), \tag{8.72}$$

where $B_0(z)$ is assumed known. In this case the analytical solution for biomass at any time is given by the convolution of the elementary solution and the initial condition:

$$B(z, t) = \int_{-\infty}^{+\infty} \frac{B_0(z')}{\sqrt{4\pi M t}} \exp\left(-\frac{(z - z')^2}{4Mt}\right) \mathrm{d}z', \tag{8.73}$$

where z' is a dummy variable for integration.

Having an exact solution allows us to use it as a test case for numerical schemes. We now proceed to demonstrate how to construct one such scheme in a simple straightforward manner. To discretize the mixing term the second derivative of biomass has to be approximated. To this end we first expand $B(z+\Delta z,t)$ around $B(z,t)$:

$$B(z+\Delta z,t) = B(z,t) + \frac{\partial B}{\partial z}\bigg|_{(z,t)} \Delta z + \frac{1}{2}\frac{\partial^2 B}{\partial z^2}\bigg|_{(z,t)} (\Delta z)^2 + ..., \tag{8.74}$$

and $B(z-\Delta z,t)$ around $B(z,t)$:

$$B(z-\Delta z,t) = B(z,t) - \frac{\partial B}{\partial z}\bigg|_{(z,t)} \Delta z + \frac{1}{2}\frac{\partial^2 B}{\partial z^2}\bigg|_{(z,t)} (\Delta z)^2 + ..., \tag{8.75}$$

where Δz is positive and the minus sign in the second expression comes because we are expanding B at depth $z-\Delta z$ around z. By adding (8.74) to (8.75) and disregarding terms higher than the second derivative, we obtain the following approximation of the second derivative:

$$\frac{\partial^2 B}{\partial z^2}\bigg|_{(z,t)} \approx \frac{1}{(\Delta z)^2}\Big(B(z+\Delta z,t) - 2B(z,t) + B(z-\Delta z,t)\Big). \tag{8.76}$$

This scheme is called **centred in space** and using it the discrete version of the mixing term becomes:

$$M\frac{\partial^2 B}{\partial z^2}\bigg|_{(z_n,t_j)} \to \frac{M}{(\Delta z)^2}\Big(B^j_{n+1} - 2B^j_n + B^j_{n-1}\Big). \tag{8.77}$$

By combining it with the Euler scheme for time stepping (8.15) the descritezied version of the diffusion equation reads:

$$B^{j+1}_n = B^j_n + \frac{M\Delta t}{(\Delta z)^2}\Big(B^j_{n+1} - 2B^j_n + B^j_{n-1}\Big), \tag{8.78}$$

referred to in the literature as the **forward time centred space** scheme (Figure 52). It is arguably the most simple numerical scheme for solving the diffusion equation. Numerous other schemes are found in the literature and the interested reader is referred to [10], [61] and [49] for an in depth analysis. Here we proceed to analyse some properties of the derived scheme.

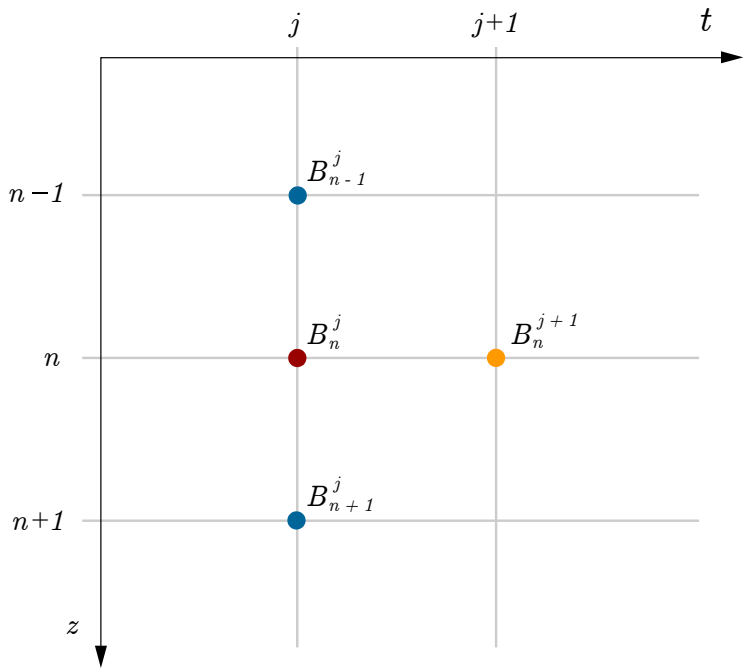

Figure 52: Graphical representation of the forward time centred space scheme for solving the diffusion equation. Calculating B_n^{j+1} (orange circle) requires information not only from B_n^j (red circle) but also from neighbouring points B_{n-1}^j and B_{n+1}^j (blue circles).

By rearranging (8.78) into the following form:

$$\frac{B_n^{j+1} - B_n^j}{\Delta t} = M\frac{B_{n+1}^j - 2B_n^j + B_{n-1}^j}{(\Delta z)^2}, \tag{8.79}$$

allows us to utilize (8.14) in the left hand side and (8.74) and (8.75) in the right hand side. After doing so we arrive at:

$$\left.\frac{\partial B}{\partial t}\right|_{(z,t)} + \frac{1}{2}\left.\frac{\partial^2 B}{\partial t^2}\right|_{(z,t)}\Delta t + \ldots = M\left.\frac{\partial^2 B}{\partial z^2}\right|_{(z,t)} + M\frac{1}{12}\left.\frac{\partial^4 B}{\partial z^4}\right|_{(z,t)}(\Delta z)^2 + \ldots, \tag{8.80}$$

which in the limit of small Δt and Δz goes to the original equation (8.61), implying the scheme is consistent.

To test the stability of the above scheme we insert the following elementary function as a trial solution:

$$B_n^j = A^j e^{ikn\Delta z}, \tag{8.81}$$

where A is a complex number, i the imaginary unit and k the wavenumber. The key idea in using an elementary function such as (8.81) lies in the fact that an arbitrary function can be represented as a sum of many elementary functions. If the total solution is to be stable, each and every one of those has to be bounded over time. Therefore, once inserted into a stable scheme the elementary function should not blow up over time. Upon inserting (8.81) into (8.78) and after some algebra, we arrive at:

$$\frac{A^{j+1}}{A^j} = 1 - \frac{4M\Delta t}{(\Delta z)^2} \sin^2\left(\frac{k\Delta z}{2}\right). \tag{8.82}$$

On the left hand side we have a ratio of the amplitude of the elementary function at time step $j+1$ to the amplitude at the time step j. For a stable scheme the ratio of the amplitudes should be less or equal to unity:

$$\frac{A^{j+1}}{A^j} \leq 1, \tag{8.83}$$

which will be the case when:

$$\frac{4M\Delta t}{(\Delta z)^2} \leq 2, \tag{8.84}$$

given that the square of the sine function is always less than unity. This condition finally translates to a constraint on the time step:

$$\Delta t \leq \frac{\Delta z}{2M}. \tag{8.85}$$

When this criterion is met the scheme is stable. However, requiring the amplitude ratio (8.83) to remain below unity implies the solution will have a lower amplitude with each time step. This behaviour is referred to as **numerical dissipation**. The smaller the ratio (8.83) the larger numerical dissipation is.

Additional complication comes from the fact that dissipation is the expected behaviour of the diffusion equation. To correctly capture dissipation due to diffusion it is preferable to minimize numerical dissipation. Ideally, there should be no numerical dissipation, in order for the scheme to produce correct solutions. In practice, this is achieved by keeping (8.83) as close to unity as possible, by altering the values of Δt and Δz, whilst simultaneously satisfying (8.85), therefore keeping the scheme stable.

To finalize the numerical approach for solving (8.1) we have to stitch together the production and loss terms, along with the advection and diffusion terms. This is achieved by combining (8.15) for the time derivative, (8.56) for the advection term and (8.76) for the diffusion term, in a single numerical scheme, such that the numerical version of equation (8.1) becomes:

$$\begin{aligned} B_n^{j+1} =& B_n^j + \frac{1}{\chi}\left(P^B(z_n, t_j) - L^B\right) B_n^j \Delta t - \frac{w\Delta t}{\Delta z}\left(B_n^j - B_{n-1}^j\right) \\ &+ \frac{M\Delta t}{(\Delta z)^2}\left(B_{n+1}^j - 2B_n^j + B_{n-1}^j\right). \end{aligned} \tag{8.86}$$

We can visually interpret the obtained numerical expression by observing Figure 53. The scheme calculates B_n^{j+1} from information on B_{n-1}^j and B_n^j using the upwind scheme for advection, and from B_{n-1}^j, B_n^j and B_{n+1}^j using the centred scheme for mixing. The production term can be calculated by using the relatively complicated, but exact expression (8.42), or by simply calculating production by directly applying the photosynthesis irradiance function on the irradiance value at the model level, as in (8.34). In both cases irradiance is calculated by using (8.32), or its integral version (8.33).

At this stage we stress again that there are various other numerical schemes for solving equation (8.1). Making such schemes amounts to the same procedure as highlighted here: discretization of each term in the equation and merger of all terms to form a numerical scheme. However, there is one final part of the story that needs to be addressed prior to actually solving (8.86) and that is the implementation of boundary conditions, which we now demonstrate how to do.

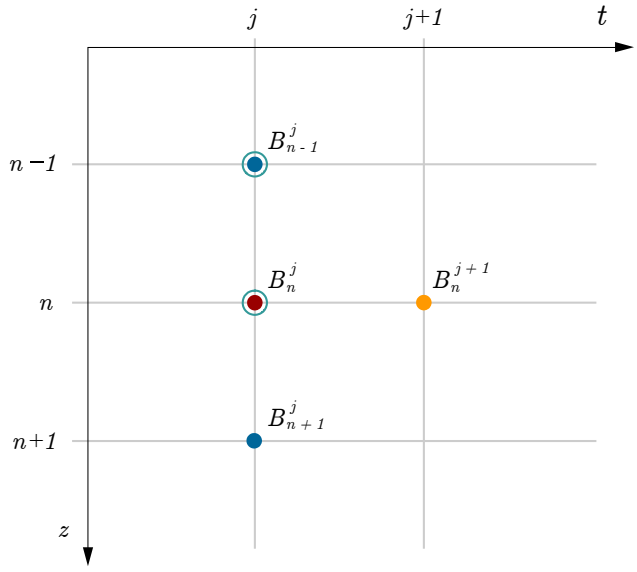

Figure 53: Grid for solving equation (8.1) numerically. Calculating B_n^{j+1} (orange circle) requires information from B_n^j (red circle) but also from neighbouring points B_{n-1}^j and B_{n+1}^j (blue circles) to account for diffusion and B_n^j and B_{n-1}^j to account for advection (green circumference).

8.7 IMPLEMENTATION OF BOUNDARY CONDITIONS

In order to specify what boundary conditions are needed, one first has to acknowledge what the relevant model variables are that require boundary conditions to be specified in the first place. In the system of equations we are solving, namely (8.1) and (8.2), two variables require boundary conditions: irradiance $I(z,t)$ and biomass $B(z,t)$. The irradiance equation in its differential form (7.4) is of first order in space and requires one boundary condition, which comes in the form of surface irradiance (8.29) and is straightforward to implement in (8.30), (8.32) and (8.33). Therefore, we now turn our attention to the numerical implementation of boundary conditions for biomass. Equation (8.1) is of second order in space and therefore requires two boundary conditions: one at the surface and one at depth.

Mathematically, the sinking term of equation (8.86) requires one boundary condition, whereas the mixing term requires two boundary conditions. For the sinking term it is natural to impose the boundary condition at the surface, given that information comes from above. That leaves us with the imposition of the second boundary condition at the bottom, which for an infinite water column is best specified at great depth, as was discussed prior. Numerical implementation of these boundary conditions is not unique and here we describe one manner in which they can be implemented.

First, we describe the implementation of a no flux surface boundary condition, as stated in (7.59). For numerical purposes we consider a more general scenario in which an arbitrary flux F_0 is set at the surface. Now the boundary condition reads:

$$wB(0) - M\frac{\partial B}{\partial z}\bigg|_0 = F_0, \tag{8.87}$$

with the flux F_0 specified at $z = 0$. To implement it we add an additional model level above the surface (Figure 54):

$$z_0 = -\frac{\Delta z}{2}. \tag{8.88}$$

The purpose of this level is to enable the discretization of the flux boundary condition (8.87). By writing (8.87) using finite difference we have:

$$w\left(\frac{B_1^j - B_0^j}{2}\right) - M\left(\frac{B_1^j - B_0^j}{\Delta z}\right) = F_0, \tag{8.89}$$

where biomass at the surface is approximated as an average of B_1^j and B_0^j and the first derivative of biomass at the surface is approximated as the difference between B_1^j and B_0^j, divided by Δz. From this expression biomass value at B_0^j is easily expressed as:

$$B_0^j = \left[F_0 + B_1^j\left(\frac{M}{\Delta z} - \frac{w}{2}\right)\right]\left(\frac{M}{\Delta z} - \frac{w}{2}\right)^{-1}. \tag{8.90}$$

A specific F_0 can then be inserted into (8.86) to obtain the equation for the time evolution of biomass at the first level $n = 1$.

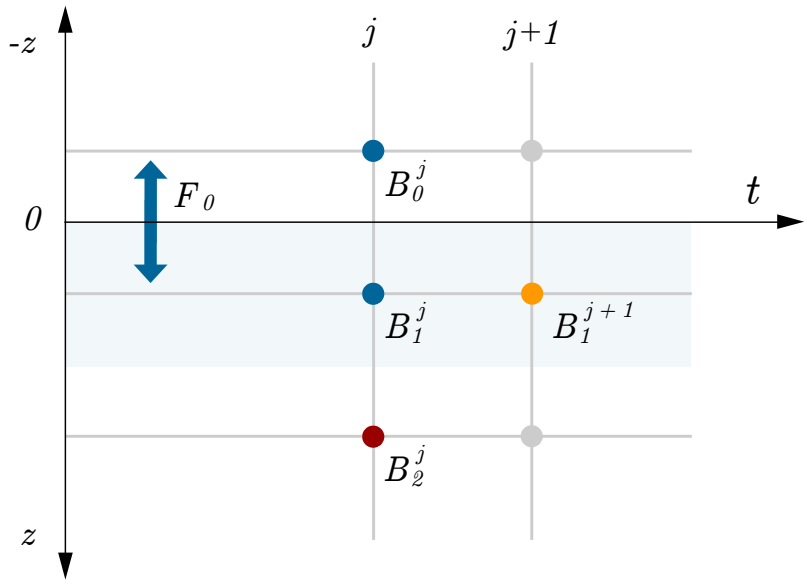

Figure 54: Sketch for implementation of the surface boundary condition in a form of a flux F_0 (blue arrow). The boundary condition is implemented by adding an additional model layer outside the domain at $z_0 = -\Delta z/2$. Using this additional layer the value of B_0^j can be calculated and inserted into the finite difference scheme (8.86) to obtain (8.92).

Given that we impose a no flux boundary condition at the surface $F_0 = 0$ (8.4), expression (8.90) becomes:

$$B_0^j = B_1^j, \tag{8.91}$$

turning (8.86) for the first level into:

$$B_1^{j+1} = B_1^j + \frac{1}{\chi}\left(P^B(z_1, t_j) - L^B\right)B_1^j\Delta t + \frac{M\Delta t}{(\Delta z)^2}\left(B_2^j - B_1^j\right). \tag{8.92}$$

The obtained expression is then used to calculate the evolution over time of biomass at the first level, whilst all the other levels, apart from the final one, are calculated using (8.86).

To calculate how biomass changes at the bottom most level we need to implement the bottom boundary condition (7.47) numerically. This can be done in a similar fashion as with the surface boundary condition, which resulted in (8.92). First we set the final layer N to be at great depth:

$$z_N = (N - 1/2)\Delta z, \tag{8.93}$$

as shown in Figure 55. For computational reasons this depth will obviously not be infinity, as in (7.47), but should nonetheless be deep enough that biomass goes to zero in that depth range naturally. A reasonable assumption for this depth would be that light levels are low, so as to keep production low and subsequently have the loss term dominate.

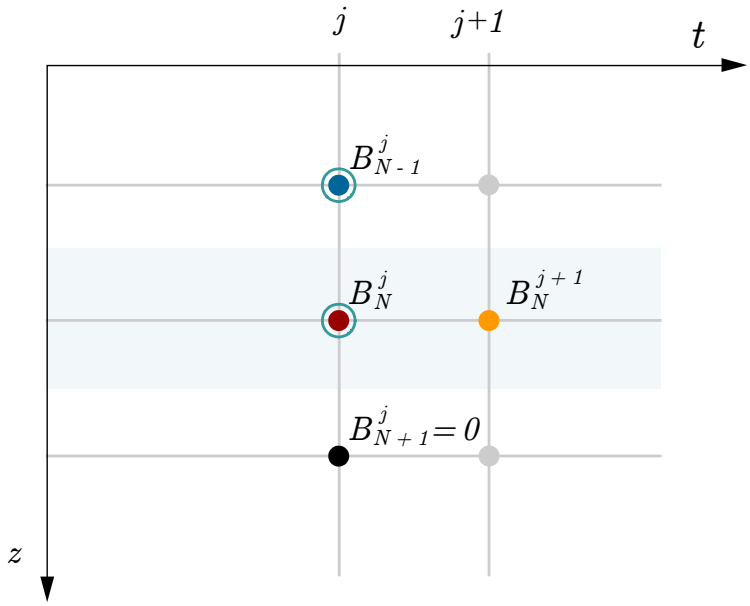

Figure 55: Sketch for implementation of bottom boundary condition $B(\infty, t) = 0$ by setting biomass at great depth equal to zero (black circle). The boundary condition is implemented by adding an additional model layer outside the domain at $z_{N+1} = (N + 1/2)\Delta z$. Using this additional layer the value of B^j_N can be calculated and inserted into the finite difference scheme (8.86) to obtain (8.96).

By placing an additional model level below the final level N, at depth z_{N+1} equal to:

$$z_{N+1} = (N+1)\Delta z, \tag{8.94}$$

enables us to set biomass as zero there:

$$B^j_{N+1} = 0, \tag{8.95}$$

further enabling us to write equation (8.86) for the final level N as:

$$\begin{aligned} B^{j+1}_N =& B^j_N + \frac{\Delta t}{\chi}\left(P^B(z_N, t_j) - L^B\right)B^j_N - \frac{w\Delta t}{\Delta z}(B^j_N - B^j_{N-1}) \\ &+ \frac{M\Delta t}{(\Delta z)^2}\left(B^j_{N-1} - 2B^j_N\right). \end{aligned} \tag{8.96}$$

This effectively makes biomass just below the final layer equal to zero, while the biomass in the final layer may be distinct from zero. Due to the attenuation of light with depth, if the final layer is selected sufficiently deep, approximately zero biomass may be reached even prior to the deepest layer, that is above it. In such a way the bottom boundary condition of zero biomass is satisfied.

8.8 PROBLEMS

1. Use different photosynthesis irradiance functions (1.27, 1.28, 1.29, 1.30, 1.31) to numerically solve equation (8.12), with a simple forward in time numerical scheme (8.18):

$$B_n^{j+1} = B_n^j + \frac{1}{\chi}\left(P_m^B - L^B\right)B_n^j \Delta t. \tag{8.97}$$

Observe how the biomass profile changes with time and if a steady state is reached. Compare the numerical with the analytical solution (8.13) and calculate the error using (8.24). Observe how the error changes by altering the time step Δt.

2. Set the biomass profile to be given by the shifted Gaussian and calculate irradiance by applying (8.30), (8.32) and (8.33). Compare the results and see how well they match. Subsequently, calculate production first by using (8.34) and then by using (8.42). Compare the results for production and see how well they match.

3. Assume a patch of phytoplankton cells sinks with uniform speed w starting from z_0, such that the position of the patch at any time is given by $z_0 + wt$. Calculate the irradiance $I(z_0 + wt)$ the cells in the patch experience as they sink trough the water column. From the information on irradiance calculate instantaneous production along the trajectory.

4. Build a Lagrangian model which numerically solves equation (7.25) using the forward in time numerical scheme:

$$B^{j+1} = B^j + \frac{1}{\chi}\left(P^B(z_0 + wt, j\Delta t) - L^B\right)B^j \Delta t. \tag{8.98}$$

where $B^j = B(z_0 + wj\Delta t, j\Delta t)$ is the biomass which is located at depth $z_0 + wj\Delta t$ at time $j\Delta t$, therefore its production is given as $P^B(z_0 + wt, t)$. Run the model with various initial conditions on z_0 and sinking speeds w. Does biomass at infinite time depend on initial conditions?

5. Solve equation (8.56) with the initial condition set by the shifted Gaussian. Extend this equation to include the production and loss terms, like in equation (8.60). Compare the two numerical solutions obtained by using (8.56) and (8.60), and observe the effect production and losses have on the solutions. Also, observe how the solution changes over time for varying values of w. Is a steady state reached?

6. Numerically solve equation (7.45) by using the centred in space scheme for diffusion:

$$B_n^{j+1} = B_n^j + \frac{\Delta t}{\chi}\left(P_n^j - L^B\right)B_n^j + \frac{M\Delta t}{(\Delta z)^2}\left(B_{n+1}^j - 2B_n^j + B_{n-1}^j\right). \tag{8.99}$$

Set a uniform biomass profile $B(z,0) = B_0$ for the initial condition. Observe how the solution changes over time for varying values of M. Is a steady state reached? Do the obtained solutions resemble those depicted in Figure 42?

7. Solve the full equation (8.86). Use uniform biomass for the initial condition $B(z,0) = B_0$. Observe how the solution changes over time for varying values of w and M. Is a steady state reached? Do the obtained solutions resemble those depicted in Figure 43?

8. Implement the numerical scheme given in (8.86) for a finite depth water column. Vary the mixing coefficient M from 10^{-7} to 10^{-1} $\mathrm{m^2\,s^{-}1}$ and observe at which range of M the solutions become vertically uniform in biomass.

BIBLIOGRAPHY

[1] E. C. C. Baly. The kinetics of photosynthesis. *Proceedings of the Royal Society of London*, 117B:218–239, 1935.

[2] A. Beckman and I. Hense. Beneath the surface: Characteristics of oceanic ecosystems under weak mixing conditions - A theoretical investigation. *Progress in Oceanography*, 75:771–796, 2007.

[3] M. J. Behrenfeld and P. G. Falkowski. Photosynthetic rates derived from satellite-based chlorophyll concentration. *Limnology and Oceanography*, 42:1–20, 1997.

[4] M. J. Behrenfeld, O. Prasil, M. Babin, and F. Bruyant. In search of a physiological basis for covariations in light-limited and light-saturated photosynthesis. *Journal of Phycology*, 40:4–25, 2004.

[5] F. F. Blackman. Optimal and limiting factors. *Annals of Botany*, 19:281–295, 1905.

[6] Dall'Olmo G. Brewin, R. J. W., J. Gittings, X. Sun, P. K. Lange, D. E. Raitsos, H. A. Bouman, I. Hoteit, J. Aiken, and S. Sythyendranath. A conceptual approach to partitioning a vertical profile of phytoplankton biomass into contributions from two bcommunities. *Journal of Geophysical Ressearch: Oceans*, 127:e2021JC018195, 2022.

[7] B. E. Chalker. Modelling light saturation curves for photosynthesis: An exponential function. *Journal of Theoretical Biology*, 84:205–215, 1980.

[8] R. M. Corless, G. H. Gonnet, D. E. G. Hare, D. J. Jeffrey, and D. E. Knuth. On the lambert w function. *Advances in Computational Mathematics*, 5(1):329–359, 1996.

[9] J. J. Cullen. The deep chlorophyll maximum: Comparing certical profiles of chlorophyll *a*. *Canadian Journal of Fisheries and Aquatic Sciences*, 39:791–803, 1982.

[10] B. Cushman-Roisin and J. M. Beckers. *Introduction to geophysical fluid dynamics: Physical and numerical aspects*. Academic Press, 2nd edition, 2011.

[11] Mobley Cutris D. *The Oceanic Optics Book*. International Ocean Colour Coordinating Group, 1.0 edition, 2022.

[12] P. G. Falkowski. Molecular ecology of phytoplankton photosynthesis. In *Primary productivity and biogoechemical cycles in the sea*, pages 47–68. Plenum Press, New York, 1992.

[13] P. G. Falkowski and J. A. Raven. *Aquatic Photosynthesis*. Princeton University Press, 2nd edition, 2007.

[14] P. J. S. Franks. NPZ models of plankton dynamics: Their construction, coupling to physics, and application. *Journal of Oceanography*, 58:379–387, 2002.

[15] P. J. S. Franks. Has sverdrup's critical depth hypothesis been tested? mixed layers vs. turbulent layers. *ICES Journal of Marine Science*, 72:1897–1907, 2015.

[16] J. Frenette, S. Demers, and L. Legendre. Lack of agreement among models for estimating the photosynthetic parameters. *Limnology and Oceanography*, 38:679–687, 1993.

[17] A. Gargett and J. Marra. Effects of upper ocean physical processes (turbulence, advection and air-sea interaction) on oceanic primary production. In *The sea*, pages 19–49. John Wiley & Sons, New York, 2002.

[18] W. Gautschi. The lambert w-functions and some of their integrals: a case study of high-precision computation. *Numerical Algorithms*, 57:27–34, 2011.

[19] W. Gentleman. A chronology of plankton dynamics in silico: How computer models have been used to study marine ecosystems. *Hydrobiologia*, 480:69–85, 2002.

[20] M. Golicnik. On the lambert w function and its utility in biochemical kinetics. *Biochemical Engineering Journal*, 63:116–123, 2012.

[21] S. Hayking. *Neural networks: A comprehensive foundation*. Pearson Education, 2nd edition, 2005.

[22] B. A. Hodges and D. L. Rudnick. Simple models of steady deep maxima in chlorophyll and biomass. *Deep Sea Research Part I: Oceanographic Research Papers*, 51:999–1015, 2004.

[23] A. Houari. Additional application of the lambert w function in physics. *European journal of physics*, 34:695–702, 2013.

[24] J. Huisman and B. Sommeijer. Population dynamics of sinking phytoplankton in light-limited environments: simulation techniques and critical parameters. *Journal of sea research*, 48:83–96, 2002.

[25] J. Huisman and F. J. Weissing. Light-limited growth and competition for light in well-mixed aquatic environments: An elementary model. *Ecology*, 75:507–520, 1994.

[26] A. Huppert, B. Blasius, and L. Stone. A model of phytoplankton blooms. *The American Naturalist*, 159:156–171, 2002.

[27] M. Iqbal. *Introduction to solar radiation*. Academic Press, 1st edition, 1984.

[28] A. D. Jassby and T. Platt. Mathematical formulation of the relationship between photosynthesis and light for phytoplankton. *Limnology and Oceanography*, 21:540–547, 1976.

[29] C. T. Jones, S. E. Craig, A. B. Barnett, H. L. MacIntyre, and J. J. Cullen. Curvature in models of the photosynthesis-irradiance response. *Journal of Phycology*, 50:341–355, 2014.

[30] J. T. O. Kirk. *Light and photosynthesis in quatic ecosystems*. Cambridge University Press, 3rd edition, 2011.

[31] Z. Kovač, T. Platt, S. Antunović, S. Sathyendranath, M. Morović, and C. Gallegos. Extended formulations and analytic solutions for watercolumn production integrals. *Frontiers in Marine Science*, 4:163, 2017.

[32] Z. Kovač, T. Platt, Shubha S., and M. Morović. Analytical solution for the vertical profile of daily production in the ocean. *Journal of Geophysical Research: Oceans*, 121, 2016.

[33] Z Kovač, T. Platt, and S Sathyendranath. Sverdrup meets lambert: analytical solution for sverdrup's critical depth. *ICES Journal of Marine Science*, fsab013, 2021.

[34] M. Kyewalyanga, T. Platt, and S. Sathyendranath. Ocean primary production calculated by spectral and broad-band models. *Marine Ecology Progress Series*, 85:171–185, 1992.

[35] A. R. Longhurst and W. G. Harrison. The biological pump: Profiles of plankton production and consumption in the upper ocean. *Progress in Oceanography*, 22:47–123, 1989.

[36] J. L. Monteith and M. H. Unsworth. *Principles of environmental physics*. Academic Press, Elsevier, 4th edition, 2008.

[37] D. H. Peterson, M. J. Perry, K. E. Bencala, and M. C. Talbot. Phytoplankton productivity in relation to light intensity: A simple equation. *Estuarine, Coastal and Shelf Science*, 24:813–832, 1987.

[38] T. Platt, D. F. Bird, and S. Sathyendranath. Critical depth and marine primary production. *Proceeding of the Royal Society B*, 246:205–217, 1991.

[39] T. Platt, D. S. Broomhead, S. Sathyendranath, A. M. Edwards, and E. J. Murphy. Phytoplankton biomass and residual nitrate in the pelagic ecosystem. *Proceeding of the Royal Society A*, 459:1063–1073, 2003.

[40] T. Platt, C. Caverhill, and S. Sathyendranath. Basin-scale estimates of oceanic primary production by remote sensing: The North Atlantic. *Journal of Geophysical Research*, 96:15147–15159, 1991.

[41] T. Platt, K. L. Denman, and A. D. Jassby. Modelling the productivity of phytoplankton. In *The sea: ideas and observations on progress in the study of the seas*, pages 807–856. Wiley, New York, 1977.

[42] T. Platt, C. L. Gallegos, and W. G. Harrison. Photoinsmihibition of photosynthesis in natural assemblages of marine phytoplankton. *Journal of Marine Research*, 38:687–701, 1980.

[43] T. Platt and S. Sathyendranath. Oceanic primary production: Estimation by remote sensing at local and regional scales. *Science*, 241:1613–1620, 1988.

[44] T. Platt and S. Sathyendranath. Biological production models as elements of coupled, atmosphere-ocean models for climate research. *Journal of Geophysical Research*, 96:2585–2592, 1991.

[45] T. Platt, S. Sathyendranath, C. M. Caverhill, and M. R. Lewis. Ocean primary production and available light: Further algorithms for remote sensing. *Deep-Sea Research*, 35:855–879, 1988.

[46] T. Platt, S. Sathyendranath, A. M. Edwards, D. S. Broomhead, and Ulloa. Nitrate supply and demand in the mixed layer of the ocean. *Marine Ecology Progress Series*, 254:3–9, 2003.

[47] T. Platt, S. Sathyendranath, and P. Ravindran. Primary production by phytoplankton: Analytic solutions for daily rates per unit area of water surface. *Proceeding of the Royal Society B*, 241:101–111, 1990.

[48] T. Platt, J. D. Woods, Sathyendranath, and W. Barkmann. Net primary production and stratification in the ocean. *Geophysical Monograph*, 85:247–254, 1994.

[49] L. R. Roed. *Atmospheres and Oceans on Computers: Fundamental Numerical Methods for Geophysical Fluid Dynamics*. Springer, 1st edition, 2019.

[50] A. B. Ryabov and B. Blasius. Population growth and persistence in a heterogeneous environment: The role of diffusion and advection. *Mathematical Modelling of Natural Phenomena*, 3:42–86, 2008.

[51] S. Sathyendranath, G. Cota, V. Stuart, H. Maass, and T. Platt. Remote sensing of phytoplankton pigments: A comparison of empirical and theoretical approaches. *International Journal of Remote Sensing*, 22:249–273, 2001.

[52] S. Sathyendranath, R. Ji, and H. I. Browman. Revisiting Sverdrup's critical depth hypothesis. *ICES Journal of Marine Science*, 72:1892–1896, 2015.

[53] S. Sathyendranath and T. Platt. Computation of aquatic primary production: Extended formalism to include the effect of angular and spectral distribution of light. *Limnology and Oceanography*, 34:188–198, 1989.

[54] S. Sathyendranath, V. Stuart, A. Nair, K. Oka, T. Nakane, H. Bouman, M. Forget, H. Maass, and T. Platt. Carbon-to-chlorophyll ratio and growth rate of phytoplankton in the sea. *Marine Ecology Progress Series*, 383:73–84, 2009.

[55] E. L. Smith. Photosynthesis in relation to light and carbon dioxide. *Proceedings of the National Academy of Science of the United States*, 22:504–511, 1936.

[56] E. Steemann Nielsen. The use of radioactive carbon (^{14}C) for measuring organic production in the sea. *Journal du Conseil International pour l'Exploration de la Mer*, 18:117–140, 1952.

[57] S. M. Stewart. Wien peaks and the lambert w function. *Revista Brsileira de Ensino de Fisica*, 33:3308–1–3308–6, 2011.

[58] H. U. Sverdrup. On conditions for the vernal blooming of phytoplankton. *Journal du Conseil International pour l'Exploration de la Mer*, 18:287–295, 1953.

[59] J. F. Talling. The phytoplankton population as a compound photosynthetic system. *New Phytologist*, 56:133–149, 1957.

[60] W. L. Webb, M. Newton, and D. Starr. Carbon dioxide exchange of Alnus Rubra: A mathematical model. *Oecologia (Berl.)*, 17:281–291, 1974.

[61] B. J. Williams. *Hydrobiological Modelling*. University of Newcastle, NSW, Australia, 1st edition, 2006.

[62] L. Zhai, T. Platt, C. Tang, C. Sythyendranath, S. Fuentes-Yaco, E. Devred, and Y. Wu. Seasonal and geographic variations in phytoplankton losses from the mixed layer on the northwest atlantic shelf. *Journal of Marine Systems*, 80:36–46, 2010.